VOLUME 33 NOVEMBER 1955 NUMBER 6

UNIVERSITY OF MICHIGAN

Canadian Journal of Technology

Editor: G. A. LEDINGHAM

Published by THE NATIONAL RESEARCH COUNCIL
OTTAWA CANADA

CANADIAN JOURNAL OF TECHNOLOGY

(Formerly Section F, Canadian Journal of Research)

Under the authority of the Chairman of the Committee of the Privy Council on Scientific and Industrial Research, the National Research Council issues THE CANADIAN JOURNAL OF TECHNOLOGY and six other journals devoted to the publication, in English or French, of the results of original scientific research. Matters of general policy concerning these journals are the responsibility of a joint Editorial Board consisting of: members representing the National Research Council of Canada; the Editors of the Journals; and members representing the Royal Society of Canada and four other scientific societies.

The Chemical Institute of Canada has chosen the Canadian Journal of Technology and the Canadian Journal of Chemistry as its medium of publication for scientific papers.

EDITORIAL BOARD

Representatives of the National Research Council

A. N. Campbell, *University of Manitoba*
G. E. Hall, *University of Western Ontario*
E. G. D. Murray, *McGill University*
D. L. Thomson, *McGill University*
W. H. Watson (Chairman), *University of Toronto*

Editors of the Journals

D. L. Bailey, *University of Toronto*
T. W. M. Cameron, *Macdonald College*
J. B. Collip, *University of Western Ontario*
G. A. Ledingham, *National Research Council*
Léo Marion, *National Research Council*
R. G. E. Murray, *University of Western Ontario*
G. M. Volkoff, *University of British Columbia*

Representatives of Societies

D. L. Bailey, *University of Toronto*
Royal Society of Canada
T. W. M. Cameron, *Macdonald College*
Royal Society of Canada
J. B. Collip, *University of Western Ontario*
Canadian Physiological Society
R. G. E. Murray, *University of Western Ontario*
Canadian Society of Microbiologists
H. G. Thode, *McMaster University*
Chemical Institute of Canada
T. Thorvaldson, *University of Saskatchewan*
Royal Society of Canada
G. M. Volkoff, *University of British Columbia*
Royal Society of Canada; Canadian Association of Physicists

Ex officio

Léo Marion (Editor-in-Chief), *National Research Council*

Manuscripts for publication should be submitted to Dr. Léo Marion, Editor-in-Chief, Canadian Journal of Technology, National Research Council, Ottawa 2, Canada.
(For instructions on preparation of copy, see **Notes to Contributors** (inside back cover).)

Proof, correspondence concerning proof, and orders for reprints should be sent to the Manager, Editorial Office (Research Journals), Division of Administration, National Research Council, Ottawa 2, Canada.

Subscriptions, renewals, requests for single or back numbers, and all remittances should be sent to Division of Administration, National Research Council, Ottawa 2, Canada. Remittances should be made payable to the Receiver General of Canada, credit National Research Council.

The journals published, frequency of publication, and prices are:

Canadian Journal of Biochemistry and Physiology	Bimonthly	$3.00 a year
Canadian Journal of Botany	Bimonthly	$4.00 a year
Canadian Journal of Chemistry	Monthly	$5.00 a year
Canadian Journal of Microbiology*	Bimonthly	$3.00 a year
Canadian Journal of Physics	Monthly	$4.00 a year
Canadian Journal of Technology	Bimonthly	$3.00 a year
Canadian Journal of Zoology	Bimonthly	$3.00 a year

The price of single numbers of all journals is 75 cents.

*Volume 1 will combine three numbers published in 1954 with six published in 1955 and will be available at the regular annual subscription rate of $3.00.

Contents

	Page
Nomographs for Evaluation of Tensile Data of Rubber—*Shigeo Kase*	409
A Frequency Stable Transistor Audio Oscillator of Very Simple Design—*W. D. Edwards*	413
Estimation of the Heat Capacities of Organic Liquids—*A. I. Johnson and Chen-Jung Huang*	421
The Chemical Bleaching of Hydrocarbon Oils—*J. R. Farnand, A. E. McIlhinney, W. S. Peterson, P. E. Gishler, and I. E. Puddington*	426
Statistical Factors in Tower Packing—*A. I. Johnson and J. M. L. Beeckmans*	434
The Oxidation, Decomposition, Ignition, and Detonation of Fuel Vapors and Gases. XXVII. The Hydrogen Engine—*R. O. King and Mogens Rand*	445
Fluid Turbulence and Suspended Sediment—*A. W. Marris*	470
Contents of Volume 33	494

Printed in Canada by University of Toronto Press

CANADIAN JOURNAL OF TECHNOLOGY

Notes to Contributors

Manuscripts

(i) ***General.*** Manuscripts, in English or French, should be typewritten, double spaced, on paper 8½×11 in. **The original and one copy are to be submitted.** Tables and captions for the figures should be placed at the end of the manuscript. Every sheet of the manuscript should be numbered.

Style, arrangement, spelling, and abbreviations should conform to the usage of this journal. Names of all simple compounds, rather than their formulas, should be used in the text. Greek letters or unusual signs should be written plainly or explained by marginal notes. Superscripts and subscripts must be legible and carefully placed.

Manuscripts and illustrations should be carefully checked before they are submitted. Authors will be charged for unnecessary deviations from the usual format and for changes made in the proof that are considered excessive or unnecessary.

(ii) ***Abstract.*** An abstract of not more than about 200 words, indicating the scope of the work and the principal findings, is required, except in Notes.

(iii) ***References.*** References should be listed **alphabetically by authors' names,** numbered, and typed after the text. The form of the citations should be that used in this journal; in references to papers in periodicals, inclusive page numbers should be given but titles should not. All citations should be checked with the original articles and each one referred to in the text by the key number.

(iv) ***Tables.*** Tables should be numbered in roman numerals and each table referred to in the text. Titles should always be given but should be brief; column headings should be brief and descriptive matter in the tables confined to a minimum. Vertical rules should be used only when they are essential. Numerous small tables should be avoided.

Illustrations

(i) ***General.*** All figures (including each figure of the plates) should be numbered consecutively from 1 up, in arabic numerals, and each figure referred to in the text. The author's name, title of the paper, and figure number should be written in the lower left corner of the sheets on which the illustrations appear. Captions should not be written on the illustrations (see Manuscripts (i)).

(ii) ***Line Drawings.*** Drawings should be carefully made with India ink on white drawing paper, blue tracing linen, or co-ordinate paper ruled in blue only; any co-ordinate lines that are to appear in the reproduction should be ruled in black ink. Paper ruled in green, yellow, or red should not be used unless it is desired to have all the co-ordinate lines show. All lines should be of sufficient thickness to reproduce well. Decimal points, periods, and stippled dots should be solid black circles large enough to be reduced if necessary. Letters and numerals should be neatly made, preferably with a stencil (**do NOT use typewriting**) and be of such size that the smallest lettering will be not less than 1 mm. high when reproduced in a cut 3 in. wide.

Many drawings are made too large; originals should not be more than 2 or 3 times the size of the desired reproduction. In large drawings or groups of drawings the ratio of height to width should conform to that of a journal page but the height should be adjusted to make allowance for the caption.

The original drawings and one set of clear copies (e.g. small photographs) are to be submitted.

(iii) ***Photographs.*** Prints should be made on glossy paper, with strong contrasts. They should be trimmed so that essential features only are shown and mounted carefully, with rubber cement, on white cardboard with no space or only a very small space (less than 1 mm.) between them. In mounting, full use of the space available should be made (to reduce the number of cuts required) and the ratio of height to width should correspond to that of a Journal page (4½×7½ in.); however, allowance must be made for the captions. Photographs or groups of photographs should not be more than 2 or 3 times the size of the desired reproduction.

Photographs are to be submitted in duplicate; if they are to be reproduced in groups one set should be mounted, the duplicate set unmounted.

Reprints

A total of 50 reprints of each paper, without covers, are supplied free. Additional reprints, with or without covers, may be purchased.

Charges for reprints are based on the number of printed pages, which may be calculated approximately by multiplying by 0.6 the number of manuscript pages (double-spaced typewritten sheets, 8½×11 in.) and including the space occupied by illustrations. An additional charge is made for illustrations that appear as coated inserts. The cost per page is given on the reprint requisition which accompanies the galley.

Any reprints required in addition to those requested on the author's reprint requisition form must be ordered officially as soon as the paper has been accepted for publication.

CORRECTION

Vol. 33, p. 353. In the first line of Item 4 under Procedure (Reagents) "0.75 gm. salicylic acid" should read "0.075 gm. salicylic acid".

Canadian Journal of Technology

Issued by THE NATIONAL RESEARCH COUNCIL OF CANADA

VOLUME 33 NOVEMBER 1955 NUMBER 6

NOMOGRAPHS FOR EVALUATION OF TENSILE DATA OF RUBBER[1]

BY SHIGEO KASE

ABSTRACT

Nomographs for the evaluation of tensile strength of rubber vulcanizates are described. The use of such nomographs is illustrated. The calculations necessary for preparing the nomographs for use with five samples are tabulated.

Use of a nomograph to evaluate tensile data quickly is desirable when results of measurements of tensile strength of rubber are distributed doubly exponentially (1) since this is complicated for routine work. Nomographs for this purpose are described here with exclusion of detailed discussions. They will be valuable for purchasing, production, quality-control, and research staffs.

The minimum-variance and unbiased estimation of averages from at least five or six observations is recommended in presenting data of tensile strength of rubber (2). This estimation is based on the method of least squares and is performed by calculation. If there is no computer available, as is often the case with routine work, the calculation is troublesome. The nomographs which will be explained in what follows are constructed in order to reduce this work without the uncertainty or uneasiness which there may be in graphical analysis (3).

CONSTRUCTION OF THE NOMOGRAPH

If the tensile strengths are ranked from S_i to S_n in order of decreasing magnitude, the minimum-variance and unbiased estimators for averages are given by (average equals sum of products of individual values and the respective weights)

$$[1] \qquad \hat{S} = \sum_{i=1}^{i=n} w_i S_i.$$

For n equal to 5 the values of w_i are in Table I (2). The nomograph for estimation of the mode, the most pertinent average for evaluating tensile data of rubber (2), is constructed from the relation:

$$S = 0.4189S_1 + 0.2463S_2 + 0.1676S_3 + 0.1088S_4 + 0.0584S_5.$$

[1]*Manuscript received July 18, 1955.*
Contribution from Togawa Rubber Manufactory, Sumiyoshi, Osaka, Japan.

TABLE I

WEIGHTS WHEN n IS 5 IN EQ. [1]

Average	w_1	w_2	w_3	w_4	w_5
Mode	0.4189	0.2463	0.1676	0.1088	0.0584
Median	0.2345	0.2487	0.2154	0.1754	0.1260
Mean	0.1285	0.2500	0.2429	0.2137	0.1648

All nomographs are constructed in the same way and have n plotting lines for tensile strength S_i ($i = 1, 2, \ldots, n$), $n - 2$ auxiliary lines t_j ($j = 1, 2, \ldots, n - 2$), and one estimation line $\hat{S}$ for the average tensile strength. In Figs. 1–3 which may be used to estimate the averages from five measurements, the plotting lines are light solid, the auxiliary lines are dotted, and the estimation line is heavy solid. Since the nomographs in Figs. 1–3 are specially constructed, each line has the same ordinate. The graduation on each line is arbitrary but linear. In general the auxiliary lines need not be graduated.

This gives advantages to the nomographs. When the range of observations (or the difference between the greatest and the smallest values among the tensile strength) is small, accurate estimation can be performed by graduating the ordinate widely so that the range may cover the scale. When the range is large the estimation becomes possible by compressing the scale. If the abscissas corresponding to all lines whose distances are equal or proportional to those in Figs. 1–3 are transferred to vertically long section paper, the nomograph will be capable of repeated application by moving the ordinate slightly upwards or downwards. For convenience of reproduction of these nomographs, the abscissas of all lines are in Table II.

From Table II, the abscissas of three auxiliary lines (t_1–t_3) and estimation line ($\hat{S}$) are equal on the nomographs for mode, median, and mean. Nomo-

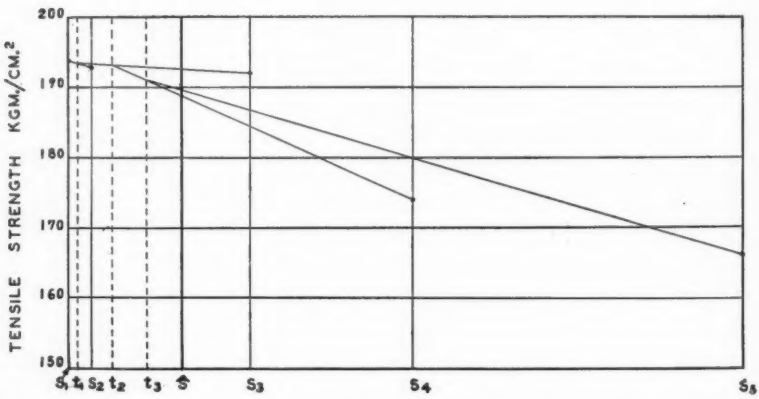

FIG. 1. Nomograph for estimating the mode from five measurements of tensile strength of rubber.

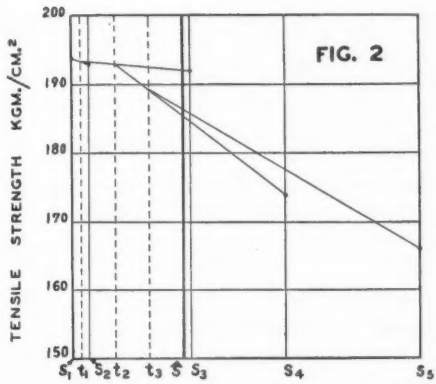

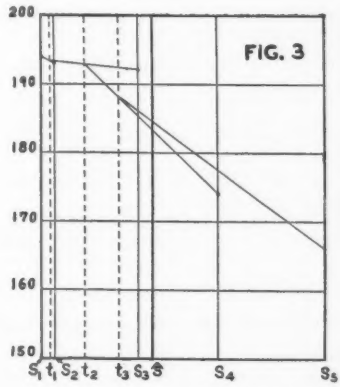

FIG. 2. Nomograph for estimating the median from five measurements of tensile strength of rubber.
FIG. 3. Nomograph for estimating the mean from five measurements of tensile strength of rubber.

graphs can be overlapped on one sheet of section paper, if one allows for the complication and possible confusion caused by the scatter of the lines except the S_i line.

TABLE II

EXACT ABSCISSAS OF ALL LINES IN THE NOMOGRAPHS FOR ESTIMATING AVERAGES FROM FIVE MEASUREMENTS

Average	S_1	S_2	S_3	S_4	S_5	t_1	t_2	t_3	$\hat{S}$
Mode	0	0.68	5.22	9.90	19.39	0.25	1.25	2.25	3.25
Median	0	0.49	3.49	6.23	10.19	0.25	1.25	2.25	3.25
Mean	0	0.38	2.81	5.16	8.32	0.25	1.25	2.25	3.25

PROCEDURE FOR USING THE NOMOGRAPHS

A summary of the method of using the nomographs is as follows:

1. Arrange the five measurements of tensile strength in order of decreasing size, and then rank them from S_1 to S_5.

2. Plot these values as ordinates on the corresponding plotting lines located on a linear scale at abscissas shown in Table II.

3. Draw a line connecting points S_1 and S_2, and settle the point of intersection between this line and the first auxiliary line t_1.

4. Determine the intersection between the line connecting the point chosen on the auxiliary line t_1 and point S_3 and the second auxiliary line t_2.

5. Obtain the intersection on the third auxiliary line t_3 by connecting the point on the second auxiliary line t_2 and S_4.

6. Read the ordinate of the intersection on the $\hat{S}$-scale, which is fixed by connecting the point chosen on the third auxiliary line t_3 and S_5. The final

ordinates are the averages by the minimum-variance and unbiased estimators relationship, Eq. [1].

The use of the nomographs is illustrated by an example. The observations are the same as in the previous paper (3), that is, the tensile strengths are:

$$S_1 = 194,\ S_2 = 193,\ S_3 = 192,\ S_4 = 174, \text{ and } S_5 = 166 \text{ kgm./cm}^2.$$

The estimation of averages of these observations is shown in Figs. 1–3. Estimated values of averages agree extremely well with the values calculated from Eq. [1] and the coefficients in Table I.

Appreciation is expressed to Dr. H. L. Williams, Polymer Corporation Limited, for assistance with the preparation of the manuscript.

REFERENCES

1. KASE, S. J. Polymer Sci. 11: 425–431. 1953.
2. KASE, S. J. Polymer Sci. 14: 579–582. 1954.
3. KASE, S. Rubber World, 131: 504–506. 1955.

A FREQUENCY STABLE TRANSISTOR AUDIO OSCILLATOR OF VERY SIMPLE DESIGN[1]

By W. D. Edwards

ABSTRACT

Attention is called to the excellent frequency stability of a very simple transistor oscillator. The frequency stability with respect to supply voltage, temperature, load, and transistor interchange has been investigated.

Transistor audio oscillators are simple to construct but their frequency stability often leaves much to be desired. The inherent stability of a number of simple oscillators has been determined. Point contact and junction transistors have been used. The most stable circuit tested in the range 200–1300 cycles per second is described in the following paragraphs.

Presently available transistors are low impedance devices and their use at low audio frequencies with parallel resonant circuits appreciably reduces the Q of the circuit unless the L/C ratio is kept small. However, the large physical size of suitably valued mica condensers used for stability is not always desirable. The series resonant circuit with its low impedance at resonance is more suited to this type of oscillator.

The most stable series resonant oscillator of simple design which has been built uses a point contact transistor and is shown in Fig. 1. Without the inductor, L, it is seen that the circuit of Fig. 1(a) is that of a relaxation oscillator. Even with L in the circuit, relaxation oscillations take place at low frequencies for which $2\pi\sqrt{LC} \sim CR_e$. The diode shown in Fig. 1(b) together with the emitter forward characteristics maintains the emitter potential close to base potential. Emitter voltages far beyond the cutoff point which are associated with relaxation oscillators are eliminated. The sinusoidal mode of operation is extended to lower frequencies and a great increase in the stability of the circuit results. The transistor maintains oscillations by supplying current pulses to the series LC circuit during the conduction half cycle. These current pulses are represented by the major voltage peaks shown in Fig. 2. The minor peaks show the voltage which exists across the series tuned circuit during the period in which the emitter is effectively non-conducting. The magnitude ratio of the two peaks depends on the Q of the series resonant circuit and to a lesser extent on the collector load resistor R_c. The maximum frequency stability obtainable from a simple circuit was the prime interest and no attempt was made to regulate the oscillation amplitude.

The variation of frequency with collector supply voltage has been investigated using the circuits shown in Figs. 1(a) and 1(b). The results are shown in Figs. 3, 4, and 5. Without diode stabilization, Fig. 1(a), the circuit is most

[1]*Manuscript received July 21, 1955.*
Contribution from the Division of Radio and Electrical Engineering, National Research Council, Ottawa, Canada. Issued as N.R.C. No. 3726.

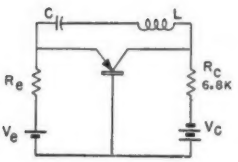

FIG. 1a

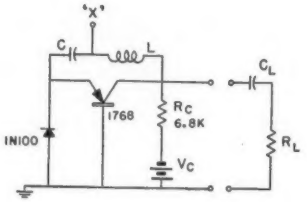

FIG. 1b

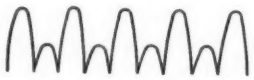

FIG. 2

FIG. 1. Series resonant audio oscillator circuits: *a*. Conventional emitter current bias. *b*. Diode stabilization of oscillator frequency.

FIG. 2. The voltage wave form observed at the collector with respect to ground. Circuit of Fig. 1*b*. $L = 7$ henries.

stable when large emitter bias currents are used. However, as expected and as seen from Figs. 3, 4, and 5, the circuit now operates only over a reduced range of collector supply voltage. The increase in frequency stability which occurs when the emitter bias source is replaced by a diode is clearly seen. With diode stabilization and a frequency of 1036 cycles per second a supply voltage change from 5 to 45 shifts the frequency by barely 0.5%. Similar results were obtained with a second Type 1768 transistor. From Table I it is seen that the oscillation frequency is reasonably independent of the transistor

TABLE I

A TABLE TO SHOW THE EFFECT OF TRANSISTOR INTERCHANGE ON THE OSCILLATOR FREQUENCY. CIRCUIT AS SHOWN IN FIG. 1*b*

Transistor		Frequency 1 in c.p.s.	Frequency 2 in c.p.s.
1768	T15	257.8	1036.4
1768	T13	257.1	1036.0
1768	T42	257.7	1036.1
1768	T55	258.7	1036.2
1768	T61	258.1	1036.0
1768	T72	257.5	1037.7
1768	T89	257.1	1035.9
1768	T97	257.7	1036.0
1729	No. 2	259.7	1037.7
1729	No. 3	259.1	1036.7
1729	No. 4	257.7	1035.8
1729	No. 5	258.0	1036.3
1729	No. 6	257.9	1036.5
1729	No. 7	258.3	1035.9
1729	No. 8	258.2	1036.0
1729	No. 10	259.8	1036.4

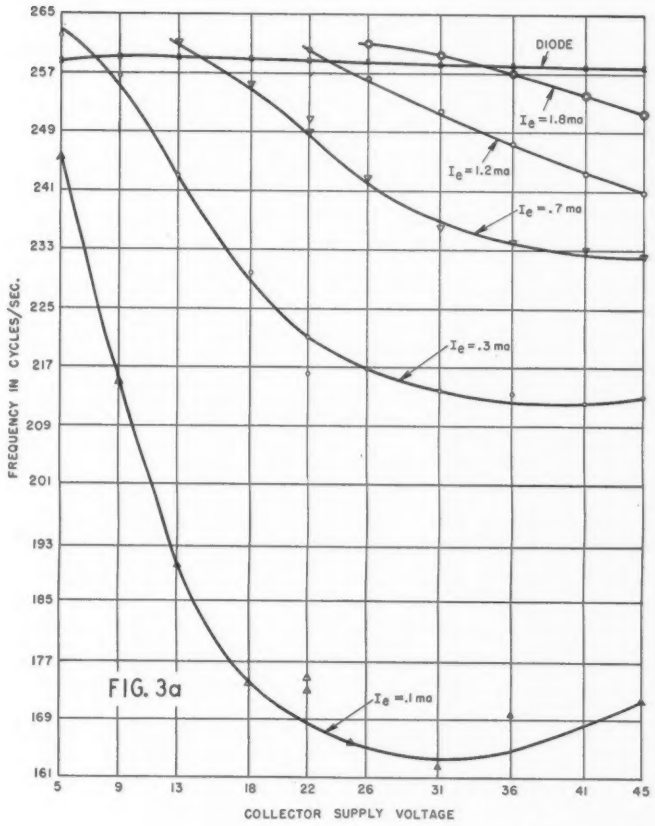

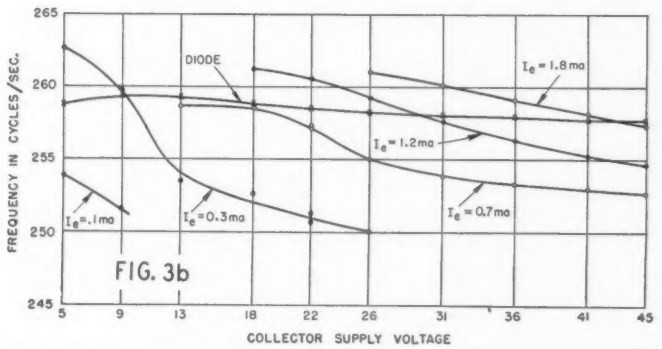

FIGS. 3*a* and 3*b*. Frequency versus collector supply voltage curves to illustrate the effectiveness of diode frequency stabilization. Nominal frequency: 250 c.p.s. Transistor T61.
3*a*, R_s = 33 K. 3*b*, R_s = 3.3 K.

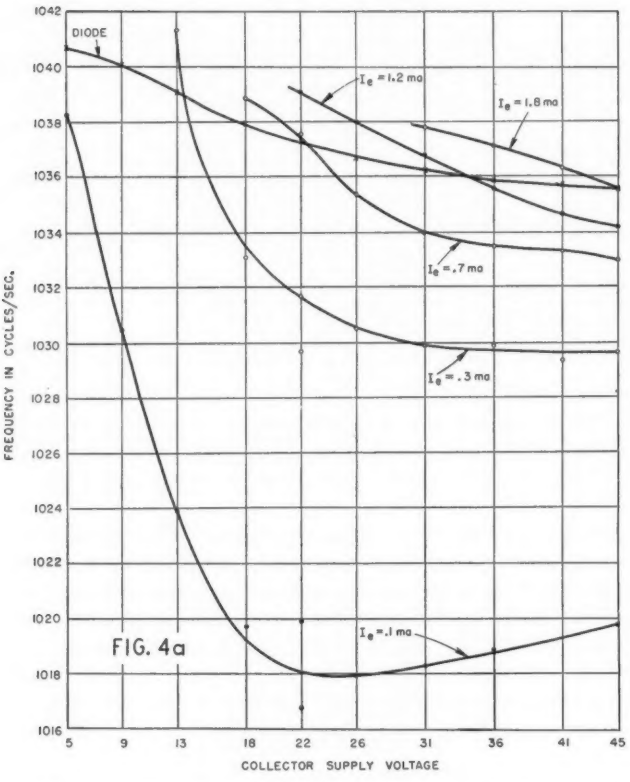

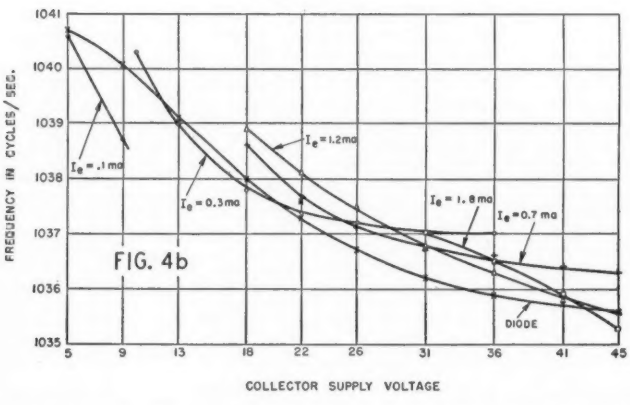

FIGS. 4*a* and 4*b*. Frequency versus collector supply voltage curves to illustrate the effectiveness of diode frequency stabilization. Nominal frequency: 1000 c.p.s. Transistor T61.
4*a*, R_s = 33 K. 4*b*, R_s = 3.3 K.

used. The maximum frequency shifts observed, and these with two types of transistor, are 0.2% and 1% at 1036 and 257 cycles per second respectively. Except where otherwise stated a collector supply voltage of 22.5, a load resistance of 6.8 K, and an inductance of 7 henries was used, both for these and for later results.

In the initial determination of the frequency versus temperature relationship the temperature of the transistor alone was varied with the rest of the circuit remaining at room temperature. At a frequency of 235 cycles per second a change in frequency of approximately one per cent occurred as the temperature changed from 5° to 35° C. This variation was traced to the inductor L, a

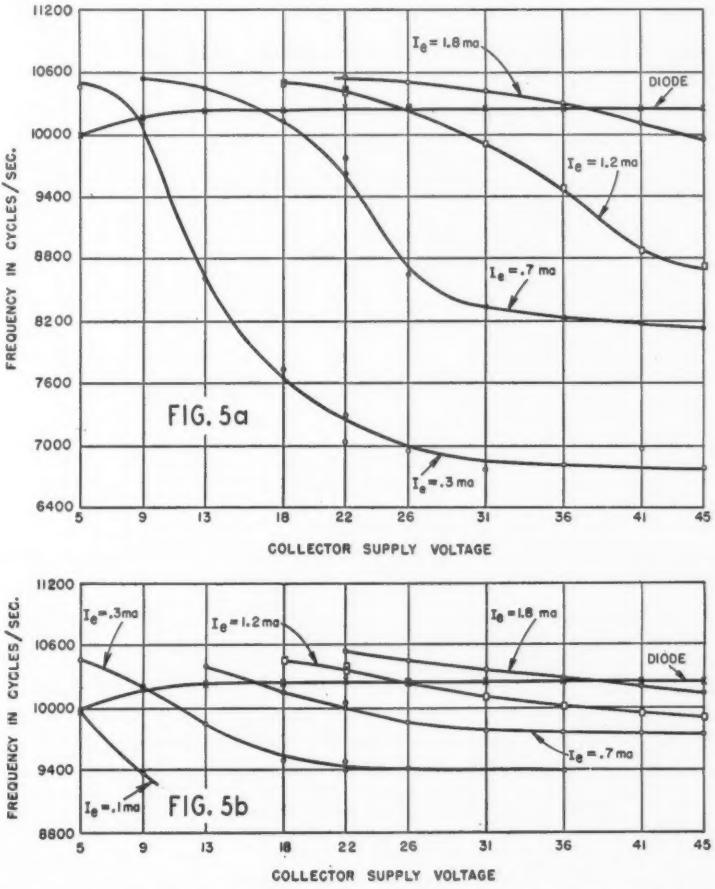

FIGS. 5*a* and 5*b*. Frequency versus collector supply voltage curves to illustrate the effectiveness of diode frequency stabilization. Nominal frequency: 10,000 c.p.s., L = 0.1 henry. Transistor T61.

5*a*, R_e = 33 K. 5*b*, R_e = 3.3 K.

10-henry filter choke having silicon–steel laminations. The transistor gain varied appreciably with temperature and this changed the current fed back through L from the collector to the emitter circuit. Because of the non-linear permeability, load current relationship of the inductor, this current variation changed the effective L and so the resonant frequency. This 10-henry inductor was replaced by a variable inductor (General Radio Type 1490B) which had much more linear characteristics. The 1490B is physically large and was not subjected to the temperature tests described below as was the rest of the circuit. The transistor was immersed in a silicone oil temperature bath and the results shown in Figs. 6(*a*) and 6(*b*) were obtained. In these figures the stabilization achieved by the diode is emphasized by comparing the results

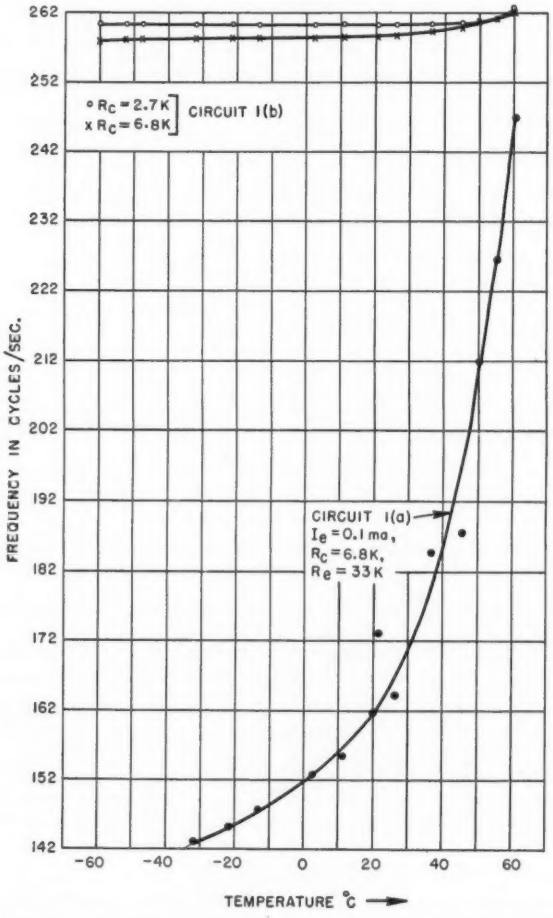

FIG. 6*a*. Variation of oscillator frequency with temperature, with and without stabilizing diode. Transistor T55. Nominal frequency = 250 c.p.s.

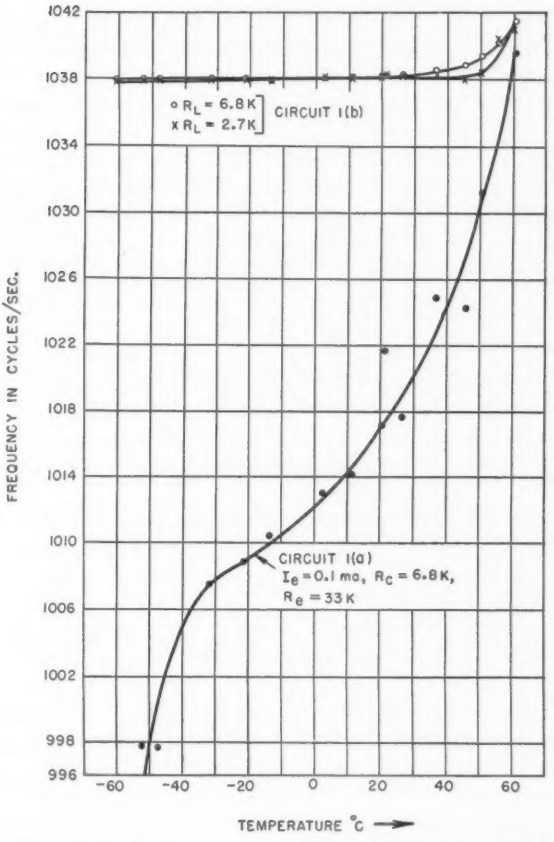

FIG. 6*b*. Variation of oscillator frequency with temperature, with and without stabilizing diode. Transistor T55. Nominal frequency = 1000 c.p.s.

with those obtained for an emitter bias current of 0.1 milliampere. Between $-60°$ C. and $+45°$ C. the frequency is stable to within 0.1% at 1038 cycles per second, and to within 0.7% at 258 cycles per second. The latter figure may be reduced to 0.15% at 260 cycles per second by reducing the collector load from 6.8 K to 2.7 K. However, this increases the battery drain and reduces the starting reliability of the oscillator at the high frequencies, of the order of 1300 cycles per second (L = 7 h.). The temperature coefficient of the inductor will normally give rise to frequency variations in excess of these figures, and recognized methods may be used to compensate for these changes. The oscillation amplitude is approximately constant below 35° C. but decreases rapidly as the temperature rises above this point, and at 61° C. was about 10 per cent of the amplitude at 20° C. The oscillator ceases to function within a few degrees of the highest temperature recorded. Very similar results were obtained with a second transistor, T97, Type 1768.

The long term stability of the oscillator appears to be excellent. At a frequency of 1038 cycles per second, and with a collector supply of 22 volts, the frequency did not change more than ± 1.5 parts in 20,000 over a 14-day period.

The voltage wave form at the collector with respect to ground, obtained with the circuit of Fig. 1(*b*), is of the form shown in Fig. 2. This wave form is suitable for many purposes and the oscillator frequency is reasonably independent of loading at this point. A *CR* load in which C_L and R_L were varied over the range 0.01 μf. to 1 μf. and 5 K to 1 meg, respectively, was applied to the collector as indicated in Fig. 1(*b*). The maximum load condition of $R = 5$ K and $C_L = 1$ μf. caused maximum frequency shifts with respect to the unloaded circuit frequency of 0.6% and 0.15% for 250-cycle and 1000-cycle signals respectively. A large amplitude sine wave is available at point *X*, Fig. 1(*b*), owing to the resonant rise across the condenser. However, this places the load in parallel with the reactive elements of the resonant circuit and will render the oscillator frequency dependent on the load. By restricting the loop gain, the oscillator (Type 1*a*) may be operated to give a low audio-frequency sine wave output at the collector, but the circuit adjustment is critical and this leads to instability.

The measurements made on this oscillator are given in detail, for it is felt that the degree of stability obtainable with such a simple transistor circuit is not generally recognized. A very simple laboratory oscillator may be built around the circuit of Fig. 1(*b*), and will be quite stable enough for most test purposes. By sacrificing frequency stability the collector signal amplitude for a given supply voltage may be considerably increased by replacing the load resistor R_c with an inductor or with a transformer if desired. The circuit described is most suited to frequencies of less than about 1300 cycles per second. If greater frequency stability is desired the circuit will necessarily be more complicated, the first step being to stabilize the oscillator amplitude.

ESTIMATION OF THE HEAT CAPACITIES OF ORGANIC LIQUIDS[1]

By A. I. Johnson and Chen-Jung Huang

ABSTRACT

A method of estimating heat capacities of organic liquids at 20°C. based on the addition of group heat capacities is suggested. The group contributions were estimated for the most part from the data summarized by Chow and Bright. The method compares favorably with the correlation of Chow and Bright, being easier to apply and only slightly less accurate. The accuracy of the proposed method is much greater than that possible by assuming the atomic heat capacities suggested by Wenner.

In recent years chemical engineers have become more aware of the need for rapid methods of estimating physical properties of substances for design calculations. Liquid heat capacity is one of these properties for which experimental data on new compounds is often lacking.

Recently Chow and Bright summarized the existing methods of estimating liquid heat capacity (1); they suggested a new correlation involving the parachor and molar refraction. Although their correlation works well (usually within 5%), the calculations are rather lengthy and the strain constants require some experience for proper use. A greater difficulty with the correlation is that the proposed equation involves two constants which apply to a particular type of compound. If the functional groups of an organic compound would place it in several groups at the same time, the heat capacities should be calculated using the several constants and presumably an average taken.

Chow and Bright refer to attempts to calculate liquid heat capacity by statistical mechanical methods. Recently (4) Sakiadis and Coates reported success in using velocity of sound and infrared and Raman spectra data. These data may be difficult to obtain for many compounds, particularly for new compounds.

A MODIFIED KOPP'S RULE

Hougen and Watson (3) recommend the use of Kopp's rule with Wenner's atomic heat capacities (5). Chow and Bright point out that this ignores the constitutive properties of a molecule. The purpose of this paper is to report on an attempt to calculate group heat capacities which are additive and which reflect the constitution of the molecule. The authors have not been able to find any report of such a method, other than that of Wenner, in the literature.

Molar heat capacities at 20°C. were calculated from the data summarized by Chow and Bright.

Using homologous series of hydrocarbons, alcohols, acids, and esters, the contribution of the —CH_2— group was found to be 6.32 cal./°C. (average of 23 values).

[1]*Manuscript received July 8, 1955.*
Contribution from the Department of Chemical Engineering, University of Toronto, Toronto, Ontario.

From the homologous series of normal hydrocarbons (seven values) the contribution of the CH_3— group was found to be 9.87 cal./°C.

These values were then used to estimate the contributions of other groups shown in Table I. It should be emphasized that experimental values at 20°C. are scarce and that some of these values should be revised as more data become available. The values of —CN, —S—, and Br— were based on specific heat data taken from the Handbook of Chemistry and Physics (2). The list of benzene compounds of Chow and Bright was supplemented by five handbook values, resulting in a slightly higher group contribution for C_6H_5— than calculated from the data of Chow and Bright only.

TABLE I

GROUP HEAT CAPACITIES

CH_3—	9.9	—OH	11.0
—CH_2—	6.3	—NH_2 (amines)	15.2
—C(=O)OH	19.1	—CH<	5.4
—C(=O)O— (esters)	14.5	—Cl	8.6
		—NO_2	15.3
		—O— (ethers)	8.4
		—S—	10.6
—C(=O)— (ketones)	14.7	—Br	3.7
—CN	13.9	C_6H_5—	30.5

USE OF THE SUGGESTED GROUP CONTRIBUTIONS

The group contributions of Table I are used in the same manner as atomic contributions are used by Kopp's rule, as illustrated by the following sample calculations:

Isobutyl acetate

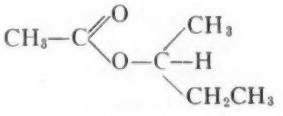

3 CH_3—	3 × 9.87	29.61
—C(=O)—O—		14.52
—CH_2—		6.32
—CH<		5.42
		55.87

The observed value is 53.27 cal./°C. per mole.

Anisole

	$C_6H_5—O—CH_3$
C_6H_5—	30.51
—O— (ether)	8.37
CH_3—	9.87
	48.75

The observed value is 52.23 cal./°C. per mole.

TABLE II

COMPARISON OF CALCULATED AND OBSERVED HEAT CAPACITIES (20°C.)

Compound	Heat capacity, gm-cal. / (°C.) (gm.)	Mol. wt.	Molal heat capacity, gm-cal. / (°C.)(gm. mole) Obs.	Calc.	Deviation, %	Molal heat capacity calculated Chow and Bright
Normal hydrocarbons						
n-Butane	0.549	58.12	32.2	32.5	0.8	32.7
n-Pentane	0.558	72.15	40.3	38.8	3.5	39.2
n-Hexane	0.527	86.17	45.4	45.2	0.6	44.8
n-Heptane	0.491	100.20	49.2	51.5	4.6	51.5
n-Octane	0.505	114.23	57.7	57.8	0.2	58.7
n-Nonane	0.503	128.25	64.5	64.1	0.6	65.3
n-Decane	0.493	142.25	70.1	70.4	0.4	71.8
Acids						
Formic acid	0.512	46.03	23.6	22.7	3.6	24.0
Acetic acid	0.488	60.05	29.3	29.0	1.0	29.6
Propionic acid	0.473	74.08	35.0	35.3	0.9	35.6
n-Butyric acid	0.473	88.10	41.7	41.7	0.0	41.7
Alcohols						
Methanol	0.600	32.04	19.2	20.9	8.6	19.3
Ethanol	0.569	46.07	26.2	27.2	3.4	26.8
n-Propanol	0.571	60.09	34.3	33.5	2.6	34.3
n-Butanol	0.563	74.12	41.7	39.8	4.6	42.0
Isopropanol	0.602	60.09	36.2	36.2	0.0	37.9
Isobutanol	0.603	74.11	44.7	42.5	4.9	43.2
Isoamyl alcohol	0.549	88.11	48.4	48.8	0.9	48.8
Esters						
Methyl formate	0.519	60.05	36.2	27.9	10.3	30.4
Ethyl formate	0.508	74.08	37.6	34.3	9.0	36.0
n-Propyl formate	0.459	88.10	40.4	40.6	0.4	41.8
n-Butyl formate	0.459	102.13	46.9	46.9	0.0	47.6
Methyl acetate	0.468	74.08	34.7	34.3	1.2	36.1
Ethyl acetate	0.457	88.10	40.3	40.6	0.8	41.8
n-Propyl acetate	0.459	102.13	46.9	46.9	0.0	47.6
Methyl propionate	0.459	88.10	40.4	40.6	0.3	41.8
Ethyl propionate	0.457	102.13	46.7	46.9	0.5	47.6
n-Propyl propionate	0.459	116.16	53.3	53.2	0.2	53.4
n-Butyl propionate	0.459	130.18	59.8	59.5	0.4	59.4
Methyl butyrate	0.459	102.13	46.9	46.9	0.1	47.6
Ethyl butyrate	0.457	116.16	53.1	53.2	0.3	53.4
n-Propyl butyrate	0.459	130.18	59.8	59.5	0.4	59.4
n-Butyl butyrate	0.459	144.21	66.2	65.9	0.5	65.3
Ketones						
Dimethyl ketone	0.514	58.08	29.9	34.4	15.4	28.3
Methyl ethyl ketone	0.549	72.10	39.6	40.8	3.0	39.9
Methyl butyl ketone	0.553	100.16	55.4	53.4	3.6	55.5
Diethyl ketone	0.555	86.13	47.8	47.1	1.5	47.6
Dipropyl ketone	0.550	114.18	62.8	59.7	4.9	62.9

TABLE II (*Concl'd*)

COMPARISON OF CALCULATED AND OBSERVED HEAT CAPACITIES (20°C.) (*Concl'd*)

Compound	Heat capacity, gm-cal. / (°C.) (gm.)	Mol. wt.	Molal heat capacity, gm-cal. / (°C.) (gm. mole)		Deviation, %	Molal heat capacity calculated Chow and Bright
			Obs.	Calc.		
Nitriles						
Acetonitrile	0.542	41.05	22.2	23.8	6.9	22.1
Propionitrile	0.538	55.08	29.6	30.1	1.6	29.5
Butyronitrile	0.548	69.10	37.9	36.4	3.8	36.8
Valeronitrile	0.521	83.13	43.3	42.7	1.3	44.1
Amines						
Methylamine	0.765	31.06	23.8	25.1	5.4	24.3
Ethylamine	0.691	45.08	31.2	31.4	0.7	31.2
Propylamine	0.663	59.11	39.2	37.7	3.8	40.1
Chlorides						
Methyl chloride	0.371	50.49	18.7	18.4	1.5	18.1
Ethyl chloride	0.369	64.52	23.8	24.8	4.0	25.6
Propyl chloride	0.404	78.54	31.7	31.1	2.0	32.9
Butyl chloride	0.452	92.57	41.8	37.4	10.6	40.1
Methylene dichloride	0.287	84.94	24.4	23.5	3.7	24.8
Chloroform	0.226	119.39	27.0	31.1	15.4	26.3
Esters of chloroacetic acids						
Methyl chloroacetate	0.383	108.53	41.6	39.3	5.5	41.5
Ethyl chloroacetate	0.399	122.55	48.9	45.6	6.7	48.9
Propyl chloroacetate	0.415	136.55	56.7	51.9	8.4	56.3
Methyl dichloroacetate	0.311	143.00	44.5	47.0	5.6	45.5
Ethyl dichloroacetate	0.330	157.00	51.8	53.3	2.8	52.6
Propyl dichloroacetate	0.342	171.00	58.5	59.6	1.9	57.6
Methyl trichloroacetate	0.268	177.45	47.6	52.9	11.2	46.7
Ethyl trichloroacetate	0.286	191.45	54.8	59.2	8.1	53.4
Propyl trichloroacetate	0.298	205.45	61.2	65.5	7.0	59.8
Benzene compounds and others						
Toluene	0.364	92.13	33.5	40.4	20.4	33.8
Ethyl benzene	0.402	106.15	42.7	46.7	9.4	40.8
Propyl benzene	0.400	120.17	48.1	53.0	10.3	49.0
Butyl benzene	0.428	134.19	57.4	59.3	3.3	56.1
Benzyl alcohol* (20–100°)	0.511	108.13	55.3	47.8	13.4	
Benzonitrile (22–186°)	0.441	103.12	45.5	44.4	2.3	
Benzyl chloride (0°)	0.323	126.58	40.9	45.4	11.0	
Phenol (14–26°)	0.561	94.11	52.8	41.5	21.3	
Benzophenone	0.383	182.1	69.7	82.5	18.2	
Aniline	0.50	93.1	46.5	49.1	5.5	
Allyl benzoate	0.388	162.1	62.9	67.1	6.6	
Allyl butyrate	0.451	128.17	57.8	57.7	0.1	
Allyl propionate	0.451	114.2	51.5	51.4	0.2	
Isoamyl propionate	0.459	144.2	66.2	68.5	3.5	
Isobutyl acetate	0.459	116.06	53.3	55.9	4.9	
Diethyl malonate	0.433	160.08	69.3	61.4	11.4	
Anisole	0.483	108.13	52.2	48.8	6.7	
Diethyl ether	0.531	74.12	39.4	40.8	3.5	
Diethyl sulphide	0.477	90.18	43.0	43.0		
Bromobenzene	0.231	157.02	36.3	34.2	5.8	
Nitromethane	0.412	61.04	25.2	25.1		
Nitrobenzene	0.339	123.11	41.7	45.8	9.7	
Cyclohexanol	0.42	100.16	42.1	48.0	14.2	
Benzene	0.406	78.11	31.7	32.5	2.5	

**The heat capacities of benzyl alcohol and following compounds are from the Handbook of Chemistry and Physics.*

Table II compares calculated and observed molal heat capacities at 20°C. for 84 organic liquid compounds. The average deviation was 5% with greatest deviations observed with benzene derivatives and esters of the chloroacetic acids. The values obtained by Chow and Bright are listed for comparison. Values calculated using the atomic contributions suggested by Wenner did not agree well with the observed heat capacities and are not shown.

It is interesting to note fairly close agreement in the calculated value for benzene, based on six $\rangle$CH groups.

It should be noted that in formic acid and in the formates the contribution of hydrogen was taken as 3.55 (9.87 for CH_3— minus 6.32 for CH_2).

CONCLUSIONS

This paper proposes group heat capacities which may be used to estimate liquid heat capacities at 20°C. The method appears to be as useful as that of Chow and Bright in that it may be applied much more rapidly yet with sufficient accuracy for design purposes.

Although comparison values are not shown in Table II, the suggested group contributions are more accurate than the atomic heat capacities of Wenner.

No attempt was made to consider the temperature dependence of liquid heat capacity; Chow and Bright propose a method for extrapolating heat capacities to other temperatures which is probably satisfactory for design purposes.

REFERENCES

1. Chow, W. M. and Bright, J. A. Chem. Eng. Progr. 49: 175. 1953.
2. Hodgman, C. D. *Editor*. Handbook of chemistry and physics. 27th ed. Chemical Rubber Publishing Co., Cleveland, Ohio. 1943.
3. Hougen, O. A. and Watson, K. M. Chemical process principles. John Wiley & Sons, Inc., New York. 1950.
4. Sakiadis, B. C. and Coates, J. Prediction of specific heat of organic liquids. Paper presented before the Houston meeting of the American Institute of Chemical Engineers. May, 1955.
5. Wenner, R. R. Thermochemical calculations. McGraw-Hill Book Company, Inc., New York. 1941.

THE CHEMICAL BLEACHING OF HYDROCARBON OILS[1]

By J. R. Farnand, A. E. McIlhinney, W. S. Peterson, P. E. Gishler, and I. E. Puddington

ABSTRACT

A method of bleaching hydrocarbon oils is described wherein the colored portions are selectively oxidized. In its most convenient form, air is blown through the oil at temperatures of 150–200°C. in the presence of metallic sodium. After a suitable period, the sludge formed is coagulated with water and is separated from the bleached oil by gravity settling or by centrifuging. The recovered oil has good oxidation stability and possesses detergent properties.

INTRODUCTION

The transparency of oleaginous materials is frequently improved by contacting them, at elevated temperatures, with adsorbents such as silica gel, alumina, fuller's earth, bentonite, and bog iron. As an alternative procedure, a chemical method that is applicable to hydrocarbon oils has been examined recently and the results presented here indicate its possible utility.

Under suitable conditions, it is possible to oxidize the colored components in oils selectively, and after removal of the oxidation products a material with a considerably improved color remains. Hydrogen peroxide, air, and oxygen at temperatures of 100–200°C. are suitable oxidizing agents while a number of alkali metals, their alloys or their salts, when added in small quantities improve the selectivity of the oxidation to a satisfactory degree. In some instances oils approaching medicinal oils in color, with only a slight bluish tint remaining, may be produced from either new unbleached raw material or from certain used crankcase oils. The chemical treatment, used in conjunction with adsorption, either prior to or after contacting with active clay, sometimes produces better results than can be obtained with successive applications of either procedure alone, thus indicating that the new and the conventional processes may be partially complimentary.

LABORATORY—EXPERIMENTAL AND RESULTS

Of the various possible selective agents, metallic sodium appeared to be the most effective and convenient, and the following procedure was eventually adopted. The oil was heated to about 120°C., sodium that had been emulsified previously in an additional portion of oil by mechanical agitation, at a temperature slightly above its melting point, was then added in quantities of 0.2 to 5% by weight, and the dispersion heated to 150–200°C. Air, dispersed in the form of fine bubbles by a porous glass disk, was then passed through the emulsion for periods of time ranging from 15 min. to several hours. During this treatment any light ends remaining in the oil may distil from the batch and

[1]*Manuscript received June 13, 1955.*
Contribution from the Division of Applied Chemistry, National Research Laboratories, Ottawa, Canada. Issued as N.R.C. No. 3735.

some sludge will form. The amount of sludge produced varies from sample to sample, the smallest quantities being formed in new oils and a much larger amount in the case of used oils.

The sodium is consumed in the process apparently owing to the formation of a complex with some of the constituents of the oil. The rate of bleaching is materially affected by the state of subdivision of the sodium, the rate increasing with decreasing particle size. The oxidation products are dispersed in the oil in a rather stable fashion and their removal is facilitated if coagulation can be induced. The most suitable method found for doing this was the dispersion into the system of from 1 to 25% of an oil-insoluble polar liquid such as water, glycerol, or alcohol. These liquids apparently wet the dispersed particles of sludge preferentially, causing them to collect at the oil–water interfaces. Either gravity settling or centrifuging then gave a satisfactory separation. These operations were usually performed at about 70°C. to take advantage of the reduced oil viscosity to promote more rapid sedimentation of the sludge.

The oils from which the sludge has been separated appear to have a much improved resistance to further oxidation when compared to the unbleached oil. This may be due, in part, to a small amount of residual sodium complex that remains in solution in the oil. The presence of residual complex is indicated by the small increase in ash value found in the treated oil. If the oxidation is carried out for an extended period of time the color of the oil is found to pass through a minimum after which it increases again. The time required to reach the minimum in color is temperature dependent. With treatment temperatures up to 200°C., no increase in color was observed, however, as long as free sodium remained in the mixture. The rate of bleaching is markedly increased at higher temperatures and an increased amount of bleaching is usually obtained by using larger amounts of sodium and longer times. The treatment caused no substantial change in viscosity of the oils except where the optimum time was exceeded by a large margin. While the effect on viscosity index was usually small, one sample of oil with viscosity index 40 improved 10 points during the bleaching process. A surface active material which behaved like soap when titrated with acid could be recovered from the sludge.

If the detergent properties of the oils are assessed in the manner suggested by Garner (2) it is found that dispersions of standard micronex (Binney and Smith Co. New York) are stable after some months when prepared with the oxidatively bleached new oil, whereas coagulation and sedimentation of the carbon black occur within a few days when the same oil either untreated or bleached with clay is used.

Table I gives typical results of some of the laboratory tests where about 200 cc. portions of an unbleached test oil SAE #30 were treated as described above, using 1% of metallic sodium. The colors are reported as percentage light transmission as determined by a Lumitron colorimeter (Photovolt Corp. New York). The instrument was adjusted to give a transmission of 100% with a white medicinal oil. The colors of several commercial lubricating oils, obtained in sealed cans on the open market, are shown for comparison as A–G.

TABLE I

THE EFFECT OF TEMPERATURE AND TIME ON THE OXIDATIVE BLEACHING OF A LUBRICATING OIL

Treatment		% Transmission	
Temp., °C.	Time of oxidation (min.)	Red filter*	Green filter*
—	None	66	28
130	30	89	59
130	120	94	72
130	240	99	86
130	720	99	87
160	15	89	62
160	30	99	87
180	15	97	84
200	5	94	72
A	—	54	16
B	—	74	41
C	—	71	30
D	—	50	13
E	—	64	26
F	—	68	34
G	—	76	36

**Red:* $\lambda = 6200$ Å.
Green: $\lambda = 5200$ Å.

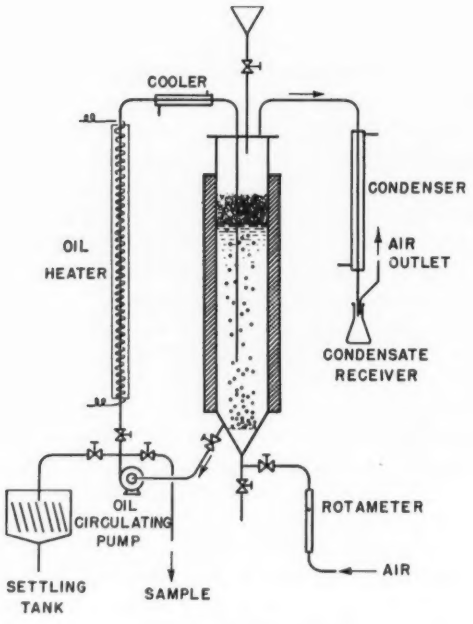

FIG. 1. Pilot unit.

PILOT PLANT—EXPERIMENTAL AND RESULTS

In order to secure data on the behavior of larger quantities of oil, a pilot unit was set up that would handle four gallon batches. This is shown in Fig. 1 and Fig. 2. The reactor was a 6 in. diameter flanged glass vertical column, 6 ft. long. At the base was a metal cone in which was inserted a 2 in. diameter sintered

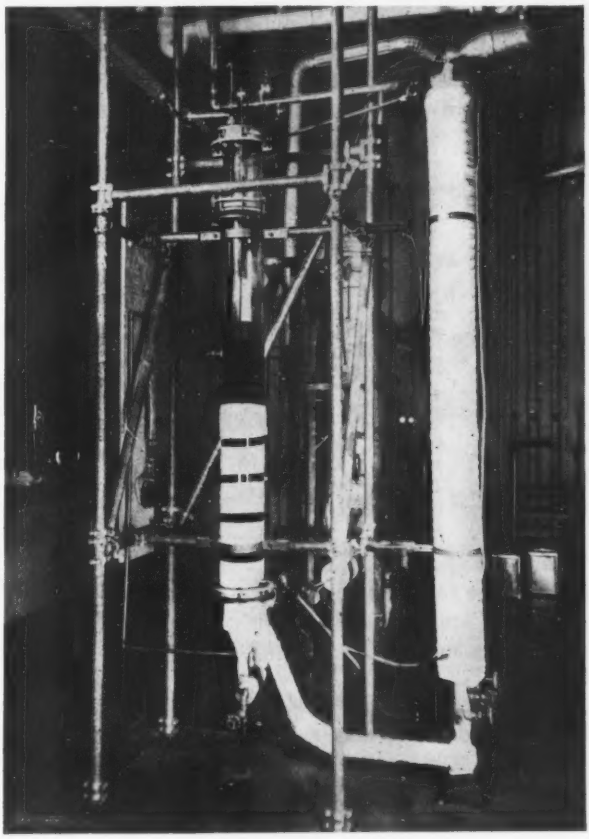

FIG. 2. Pilot unit.

stainless steel diffuser plate. The desired temperature was obtained by circulating the oil through a heated pipe. Possible overheating caused by any exothermicity in the reaction could be controlled by means of a cooler in the oil circulating line. This cooler was never required in actual practice, however. Light ends or water vapor that were distilled from the reacting mixture during a run were recovered by a condenser on the air outlet line.

The experimental procedure was essentially the same as described for the laboratory work. A weighed portion of sodium emulsified in oil at 125°C. by

means of a Waring Blendor was dispersed in a known quantity of oil at a similar temperature in the reactor. The mixture was heated to the desired reaction temperature while air at the rate of about one cubic foot per minute was bubbled through the column. Oil samples were withdrawn periodically, the sludge coagulated with water, and the oil recovered by centrifuging at 70°C. In order to establish the optimum time of treatment, the reaction was frequently taken beyond the point of minimum oil color. Overtreatment normally had an adverse effect on the rate of settling and on the sharpness of separation. This effect is reflected in some of the recovery data presented, and is illustrated in Table II where no gravitational settling was possible in runs Nos. 1 and 6.

TABLE II

BLEACHING RESULTS ON NEW TEST OIL

Run No.	1	2	3	4	5	6
Oil weight, lb.	31.55	31.13	32.78	32.85	32.12	30.76
Feed						
Sodium, %	0.25	0.5	0.5	1.0	1.0	2.0
Reaction temp., °C.	200	200	200	200	200	200
Reaction time, min.	70	25	5	60	10	180
Yield clear oil, %						
Settled	—	95.2	87.0	97.3	96.5	—
Centrifuged	—	2.9	11.6	2.2	1.9	—
Total	—	98.1	98.6	99.5	98.4	—
Light transmission						
Optimum red, %	86	88	86	94	92	97
Optimum green, %	43	53	51	72	69	75
Time to optimum, min.	20	10	5	15	5	30
Light transmission of original oil, %	Red 40					
	Green 10					

In these runs the time to optimum color was greatly exceeded. The optimum was usually indicated approximately by the color of the oil–water emulsion in the sludge coagulation step and by the appearance of a small amount of water in the condensate.

About 15% of water gently emulsified into the oil after it was removed from the reactor coagulated the sludge sufficiently to give satisfactory gravity settling. The clear oil was recovered by decantation. Oil that was missed by this method of separation or that was retained in the sludge was estimated by centrifuging an aliquot of the material remaining in the settler after it had been homogenized.

The results from the pilot unit are presented in Tables II and III. In Table II the oil treated was a new test oil normally used for evaluating decolorizing adsorbents. This oil contained no constituents volatile under the conditions of the procedure and it was used as received. In Table III the material described was a used crankcase oil obtained in 45 gal. lots from a local service station on two separate occasions. This oil was allowed to settle until it was reasonably free of sludge before treatment, and on one occasion the four gallon sample was washed with a 5% solution of NaOH, prior to use. About 20% of light ends contained in this oil, probably as the result of crankcase dilution, was recovered during the treatment.

TABLE III

BLEACHING RESULTS ON USED CRANKCASE OIL

	Series I			Series II			Series III				
Run No.	1	2	3	4	5	6	7	8	9	10	11
Variable	Temp.	Temp.	Temp.	% Na	Alkali prewash	Temp.	Sample	Sample	Sample	Sample	Sample
Feed											
Type	1	2	2	1	1	1	1	2	2 (Topped)	3	4
Wt., lb.	30.24	30.53	31.55	32.09	25.34	30.17	31.98	31.55	31.83	31.39	31.11
Sodium, %	2	2	2	1	1	1	2	2	2	2	2
Reaction temp., °C.	150	175	200	200	200	175	200	200	200	200	200
Reaction time, min.	320	180	60	110	80	240	55	60	60	65	75
Yield clear oil, %											
Condensed	14.2	13.4	13.9	16.5	15.3	16.1	14.6	13.9	0.9	8.2	6.5
Settled	65.2	71.0	62.6	44.7	76.4	62.4	67.3	62.6	88.9	75.0	61.7
Centrifuged	9.4	9.2	16.4	29.7	3.9	12.1	10.8	16.4	6.1	8.9	19.7
Total	88.8	93.6	92.9	90.9	95.6	90.6	92.7	92.9	95.9	92.1	87.9
Light transmission											
Optimum red, %	62	72	84	35	73	58	79	84	81	90	80
Optimum green, %	16	25	40	3	20	8	32	40	32	54	34
Time to optimum, min.	40	60	60	—*	50	—*	50	60	60	35	60
Light transmission of original oil, %	Red <5 Green 0										

Optimum not reached.

A series of runs designed to show the effect of air flow on the bleach indicated that the rate of decolorizing increased as the air flow increased and as the pressure at which the reaction was carried out was increased. Treatment of samples from two other service stations (Feed Types Nos. 3 and 4 in Table III) indicated that the behavior reported is probably fairly representative. Removal of the volatiles prior to treatment with air and sodium had virtually no effect on the subsequent bleaching process. This is indicated in run No. 9 in Table III.

DISCUSSION

A comparison of Table I with Tables II and III shows that colors normally found in commercial oils may be obtained quite easily from used crankcase oils, while from the new unbleached oil tested, considerably lighter oil could be produced with similar treatments. Recoveries from the treated new oil were excellent and only a small amount of sludge was formed. In the case of the used oils the sludge formation and sodium requirements were higher than for new oil. Considerable reduction in the sodium requirement was effected, however, with a caustic prewash and the smaller quantity of sludge formed is reflected in the amount of oil recovered by gravity settling. The most convenient temperature at which to work appears to be 200°C.

For the new test oil treated with 1% of sodium at 200°C. the optimum contact time was in the vicinity of 20 min. For a single treatment 1% of sodium appears to be the optimum quantity. These points are illustrated in Figs. 3 and 4. Longer periods of treatment seem desirable in the case of used oils. In this case too an alkali prewash appears to be useful.

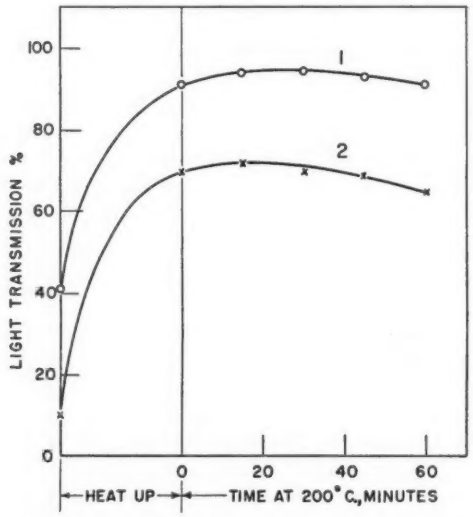

FIG. 3. Effect of time on the decolorizing of test oil at 200°C. using 1% sodium. Curve 1, using red filter; curve 2, using green filter.

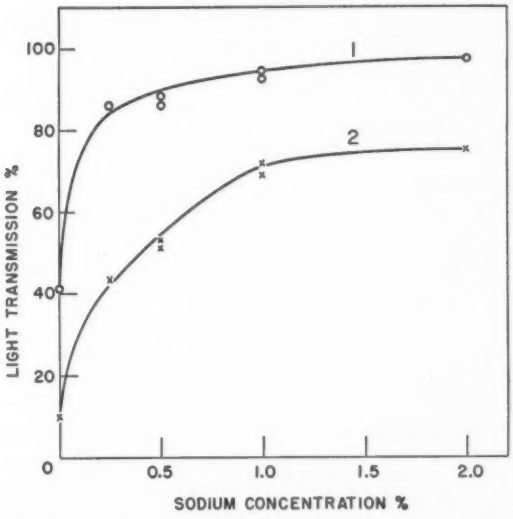

FIG. 4. Effect of sodium concentration on the optimum color obtained from test oil at 200°C. Curve 1, using red filter; curve 2, using green filter.

The chemical reactions involved in the process remain obscure. Hydrocarbon oxidations are generally considered to proceed by a free radical mechanism (1) and it would appear that in the case of the colorless species the sodium retards the reaction in the early stages, possibly by reacting with hydroperoxides. In any case the colored molecules are more susceptible to attack during the oxidation in the presence of sodium.

ACKNOWLEDGMENT

The authors wish to record their indebtedness to Imperial Oil Limited for a generous supply of oil samples.

REFERENCES

1. FRANK, C. E. Chem. Revs. 46: 155. 1950.
2. GARNER, F. H., MOHTADI, M. F., and NUTT, C. W. J. Inst. Petroleum, 38: 974. 1952.

STATISTICAL FACTORS IN TOWER PACKING[1]

By A. I. Johnson and J. M. L. Beeckmans

ABSTRACT

This investigation was made to determine to what extent flooding rates in packed extraction towers could be affected by random factors in the arrangement of the packing. It was found that such an effect does exist, and that the data could be correlated. The forms of the equations were predicted by an analysis based on certain simplifying assumptions. It was concluded that no exact prediction of flooding rates is possible, but the accuracy improves with the height of the packing.

INTRODUCTION

A knowledge of flooding rates is required for the economic design of packed liquid–liquid extraction columns, and a number of correlations have appeared in the literature. Although many refinements have been introduced, a fairly considerable spread of the data about the correlation equation could not be avoided. All these equations show that the flooding rate is independent of the height of the column, and that the throughput for a given ratio of disperse phase rate to continuous phase rate is strictly proportional to the cross-sectional area of the column. Nevertheless, doubts have been expressed as to the accuracy of the equations because of the possibility of random bottle-necking in the packing. Dell and Pratt (1) demonstrated that the flooding rate could be appreciably altered by the method used in dumping the packing. If air is bubbled through the column whilst it is being loaded, the flooding rates are reduced.

A straight line results if the square roots of the respective phase rates are plotted against each other. Dell and Pratt (1) report that when a set of runs was repeated after redumping the packing, the straight line obtained was parallel to that plotted from the first set of runs, but slightly displaced. This is a very significant result because it can only mean that a random variable is present, assuming of course that the physical properties of the phases have remained constant.

THEORETICAL DISCUSSION

A randomly packed column is a highly complex geometrical system which defies rigorous mathematical description. The following treatment is based on an idealized model. It is by no means the only method of attack, but it has the advantage of simplicity combined with a fair degree of approximation to reality.

Consider a plane section through a column, at right angles to its axis. Part of the area of the section will be taken by the packing, the remainder being available for the flow of the phases. Corresponding to this free area

[1]*Manuscript received June 27, 1955.*
Contribution from the Department of Chemical Engineering, University of Toronto, Toronto, Ontario.

there will be a maximum throughput which we will assume to be proportional to it, and independent of conditions above or below it. If the continuous phase rate is constant, there will be a maximum disperse phase rate which we will designate by v. This is the observed flooding rate in a column of infinitely small height which has in theory been sectioned out of a column of normal height. All other variables being constant, v will be a function of the free area of that section only. Hence v will vary statistically along the length of the column, and we may postulate that a distribution function of the v's exists. However, owing to the finite size of the packing, v cannot vary infinitely quickly with the height, which we will call z. We will assume that $dv/dz = 0$ over a small but definite element of height a. This does not occur in practice, but it will serve as an approximation to actual conditions. Fig. 1 shows the nature of the approximation.

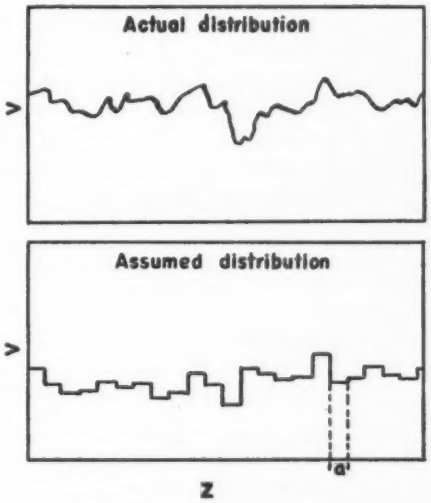

FIG. 1. Typical section velocity distribution in a column.

Let the column be divided into n such segments of width a. The distribution function of the v's will be denoted by $p(v)$. The cumulative distribution function is

$$P(v) = \int_{-\infty}^{v} p(v)\, dv.$$

For any one segment, $P(0 \leqslant V \leqslant v) = P(v)$, V representing the value of an observation and v the value in the function.

Since $P(0 < V < \infty) = 1$, it follows that $P(v < V < \infty) = 1 - P(v)$. We now make the assumption that all the v's are stochastically independent. In other words the probability of getting a particular v in any segment is not influenced by the v's in the adjacent segments. Under these conditions the

probability that V should be greater than a specified value of v in n segments of a column simultaneously is given by the following equation: $P(v < V < \infty) = [1-P(v)]^n$. This is essentially a restriction on the minimum value of V in a column of height na. Thus the right-hand side gives the cumulative distribution function of the minimum flooding velocities as a function of the number of segments and of the distribution function of the flooding velocities in the individual segments. If it is assumed that the flooding velocity in a column is equal to the flooding velocity of that section which has the minimum area somewhere in the column, then the above function must also be the cumulative distribution function of the observed flooding rates.

Differentiation of the above equation gives the distribution function of the flooding rates

$$p^*(v) = n[1-P(v)]^{n-1}p(v). \qquad [1]$$

The next step is to determine whether the elemental height a is an inherent property of the packing, or whether it is possible to derive an equation between it and the parameters of the distribution function of the elemental segments, in such a way that an equation may be found between z, $p^*(v)$, and v. If such an equation exists, then $p^*(v)$ must be independent of a, for fixed values of v and z, since a may then be eliminated. If z/a is substituted for n in equation [1] and the equation is differentiated partially with respect to a, there results

$$\frac{\partial p^*(v)}{\partial a} = -\frac{z}{a^2}p(v)[1-P(v)]^{(z-a)/a} + \frac{z}{a}[1-P(v)]^{(z-a)/a}\frac{\partial p(v)}{\partial a} - \frac{z^2}{a^3}p(v)[1-P(v)]^{(z-a)/a}\log_e[1-P(v)] + \frac{z(z-a)}{a^2}p(v)\frac{\partial P(v)}{\partial a}[1-P(v)]^{(z-a)/a}.$$

The terms in z do not drop out when this expression is equated to zero; hence there is no relation between a and the functions $p(v)$ and $P(v)$ which is independent of the height.

The fundamental equation [1] is not suitable for analysis of the data in its present form, because nothing is known about the form of $p(v)$. It would doubtless be possible to calculate the $p(v)$ curve from values of $p^*(v)$ if sufficient data were available. However, the mathematical difficulties are considerable, principally because equation [1] is a differential equation. An exact solution would involve the measurement of slopes, and when one remembers that one is dealing with an empirical distribution function, one soon realizes that a solution with a relatively small number of readings with which to construct a distribution curve is out of the question.

A better approach consists in assuming a form for $p(v)$, with a number of parameters which can then be evaluated from the data. The form of $p^*(v)$ will depend chiefly on the form of $p(v)$ in the small range of v. This is because the larger n, the greater the chances that a small value of V will occur in a

given column. Since one is measuring the smallest V which occurs, it is evident that the form of the curve $p(v)$ at its lower end will almost entirely determine the whole of the $p^*(v)$ curve. This allows one to select a simple function to represent $p(v)$, since the exact shape or form is important in only a relatively small range of the curve. The function selected is:

$$p(v) = C(v-v_0)^\theta. \tag{2}$$

Here v_0 is included because $p(v)$ must be zero at some finite value of v, since it is not possible to block up completely a smooth circular section with irregularly shaped areas of finite size.

If this expression is integrated and the boundary condition that $P(v) = 0$ when $v = v_0$ is inserted, the following equation results:

$$P(v) = \frac{C}{\theta+1}(v-v_0)^{\theta+1}. \tag{3}$$

Then $p^*(v)$ can be obtained by substituting [2] and [3] in [1]:

$$p^*(v) = Cn\left[1-\frac{C}{\theta+1}(v-v_0)^{\theta+1}\right]^{n-1}(v-v_0)^\theta. \tag{4}$$

The next step is to determine the mean of this distribution. As it stands, however, this is impossible, because it is only valid in the low range of v. Strictly the integral of the above distribution functions should tend to 1 as v tends to infinity. This is not so as can be seen by inspection, since the integrands themselves tend to infinity. Most distribution functions which are not too pronouncedly skew have a mode which is close to the mean. The mode is defined as that value of the independent variable for which the value of the function is a maximum. Furthermore the present distribution tends to get thinner and higher as n gets larger. This will tend to make the mode and the mean coincide. Fig. 2 shows the trend of $p^*(v)$ as n gets larger.

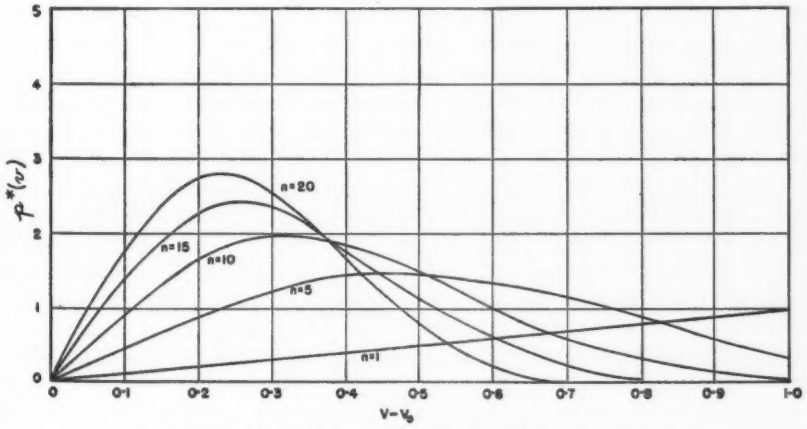

FIG. 2. Distribution of the minimum velocities. $\theta = 1$, $C = 1$.

The mode is given by the equation $dp^*(v)/dv = 0$,

$$dp^*(v)/dv = Cn(n-1)(v-v_0)^\theta\left[1-\frac{C}{\theta+1}(v-v_0)^\theta\right]^{n-2}(-C)(v-v_0)^\theta + \left[1-\frac{C}{\theta+1}(v-v_0)^{\theta+1}\right]^{n-1}\theta(v-v_0)^{\theta-1} = 0.$$

The solution $1-[C/(\theta+1)](v-v_0)^{\theta+1} = 0$ is trivial, since it is equivalent to $P(v) = 1$. The remaining solution is:

$$(v-v_0)^{\theta+1} = \frac{\theta}{C[n-1+\theta/(\theta+1)]}.$$

If one assumes that $n \gg 1/(\theta+1)$, this reduces to

[5] $$v-v_0 = \left(\frac{\theta}{Cn}\right)^{1/(\theta+1)}.$$

Or, calling $1/(\theta+1) = s$,

$$v-v_0 = \left(\frac{a.\theta}{C.z}\right)^s.$$

Thus the mean and the height of the packing are related by an equation of the form:

[6] $$\bar{x}-v_0 = K/z^s.$$

The same difficulties are encountered in trying to evaluate the variance of the distribution as were encountered in estimating the mean. It is not possible to attack the problem directly because the appropriate integrals do not tend to finite values as v tends to infinity. Again this is because $p(v)$, in the form assumed here, is only valid in its lower range. A qualitative estimate of the variance may be made by noticing that since the integral of any distribution function over its entire range must always be equal to 1, tall distribution functions will always be thin, and low ones will tend to be broad. For the normal distribution function there is a nice relationship between the value of the maximum ordinate and the standard deviation, viz., maximum $p(v) = 1/\sqrt{2\pi}\,\sigma$.

A relationship of this form will be assumed here. First the value of the maximum $p^*(v)$ must be calculated. This is done by substituting equation [5] into equation [1].

Thus $$p^*(v) = Cn\left[1-\frac{\theta}{n(\theta+1)}\right]^n\left(\frac{\theta}{C.n}\right)^{\theta/(\theta+1)}.$$

If it is assumed that n is large, the following approximation may be made:

$$\left[1-\frac{\theta}{n(\theta+1)}\right]^{n(\theta+1)/\theta} = e,$$

where e is the base of the natural logarithms. Substituting and simplifying, one obtains

$$p^*(v)_m = Cn\left(\frac{e\theta}{Cn}\right)^{\theta/(\theta+1)}. \quad [7]$$

If one makes the assumption that this value is inversely proportional to the variance, as in the normal distribution, then the standard deviation and the height must be related by an equation of the form

$$\sigma = K'z^t. \quad [8]$$

The exponent t is related to the exponent s of equation [6] by the following equations:

$$t = -\left(1-\frac{\theta}{\theta+1}\right) = \frac{-1}{\theta+1} \text{ and } s = \frac{1}{\theta+1}.$$

Hence

$$t = -s. \quad [9]$$

A small correction may be brought in at this stage. The observed standard deviations are due to two causes, one being that of the random elements in the packing, the other being the error in making the measurements. The theory of probability states that the standard deviation of a variable which is the sum of two independent variables is related to the standard deviation of these variables by the equation:

$$\sigma^2 = \sigma_1^2+\sigma_2^2. \quad [10]$$

If one postulates a distribution function of the experimental errors, with standard deviation σ_e, then the following equation gives the relation between the observed standard deviation $\bar{s}$ and that due to random factors in the packing: $\bar{s}^2 = \sigma^2+\sigma_e^2$. The relation between $\bar{s}$ and z then assumes the form $\bar{s}^2-\sigma_e^2 = K'z^{-s}$. This concludes the derivation of the correlating equations.

APPARATUS AND PROCEDURE

The arrangement of the apparatus is shown schematically in Fig. 3. The column had an internal diameter of 6 in. All conduits were of $1\frac{1}{2}$ in. copper tubing. The method of supporting the packing and the connections between the column and the end-pieces are shown in Fig. 4. The packing consisted of $\frac{1}{2}$ in. ceramic Raschig rings.

The solvent used was a mixture of carbon tetrachloride and gasoline, the proportions being such that the mixture had a density of 1.340.

In operation the procedure was to drop in packing to a certain height, determine the flooding rate, then add more packing, etc. The flooding rate was taken to be that rate which caused a layer of solvent about 6 in. wide above the packing neither to increase nor to decrease with time. Flooding was observed at packing heights of 3 in., 6 in., 1 ft., 1 ft. 6 in., 2 ft., 2 ft. 6 in., 3 ft., and 4 ft. At the end of a series of runs the column was repacked and so on. A total of 19 series were made. A close check was held on the density by means

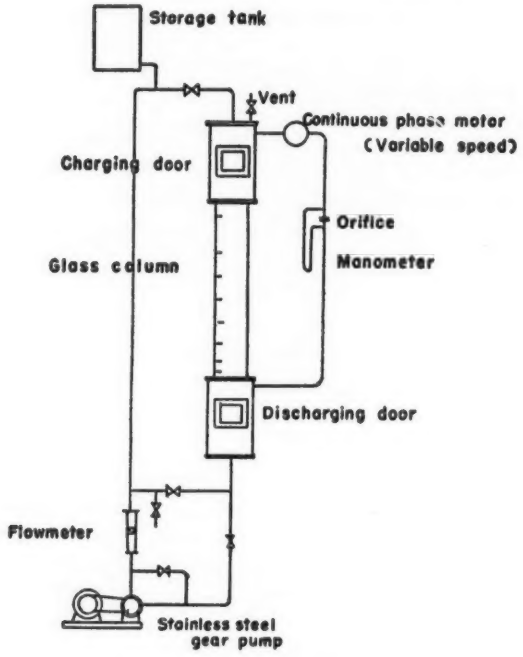

FIG. 3. Schematic flow diagram.

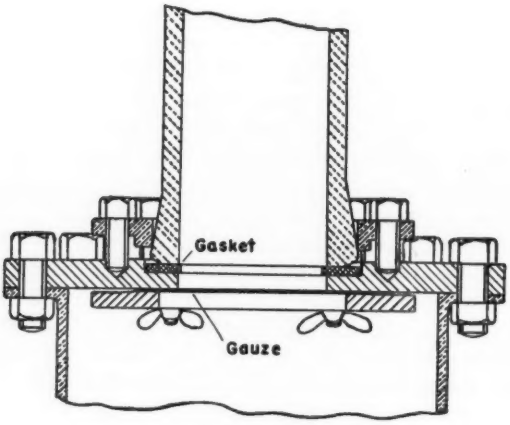

FIG. 4. Section through base of column.

of a hydrometer. The permissible limits of variation were 0.010 about a mean of 1.340.

It should be noticed that the readings in a series (Table I) are not independent of each other, since the column is not entirely repacked at each reading. However, in a fairly large sample such as this, this could not be of importance.

Unfortunately, parts of the column corroded during the experiments, and corrosion products contaminated the phases. In particular, it is thought that the interfacial tension was affected. As a result, the readings at any given value of the height tended to rise as the investigation proceeded.

Fig. 6 shows that the data can be correlated by an equation of the type predicted, equation [6]. The value of the exponent s is 1.284, and v has a value 16.5 lb./min.

TABLE I

FLOODING RATES, LB./MIN.

Series number	Height of packing, in.							
	3	6	12	18	24	30	36	48
A			22.2	21.4	21.4	20.6	20.6	18.3
B	25.6	23.2	20.6	18.3	18.9	18.9	18.3	18.3
C	21.4	15.1	16.5	15.1	15.1	15.1	16.5	16.5
D	24.2	21.4	20.6	20.6	20.6	18.3	17.5	17.5
E	26.5	24.2	18.3	16.5	16.5	15.1	16.5	15.1
F	26.5	22.2	18.9	17.5	17.5	16.5	16.5	16.5
G	24.2	19.8	18.9	17.5	17.5	16.5	16.5	16.5
H	29.1	22.2	18.9	17.5	17.5	16.5	16.5	16.5
I	24.2	18.9	17.5	16.5	17.5	16.5	17.5	17.5
J	32.4	25.6	20.6	18.3	18.3	16.5	15.1	16.5
K	31.7	24.2	20.6	17.5	17.5	17.5	16.5	16.5
L	27.4	24.2	19.8	16.5	16.5	15.1	15.1	15.1
M	34.1	30.9	25.0	19.8	17.5	18.3	18.3	18.3
N	32.4	29.1	23.2	19.8	17.5	17.5	17.5	17.5
O	34.7	32.4	20.6	19.8	17.5	17.5	17.5	17.5
P	27.4	23.2	21.4	18.9	18.9	18.9	18.9	18.3
Q	38.0	29.1	20.6	19.8	18.3	18.3	16.5	17.5
R	31.7	27.4	21.4	19.8	19.8	19.8	18.9	18.3
S	42.6	34.1	25.0	23.2	22.2	21.4	19.8	19.8

TABLE II

CALCULATED VALUES OF THE MEAN AND STANDARD DEVIATION

Height, in.	Σx	$\bar{x}$	Σx^2	$\bar{x}\Sigma x$	σ^2	σ
3	534.1	29.67	16266.8	15846.7	24.64	4.97
6	448.2	24.90	11429.1	11160.2	15.81	3.98
12	390.6	20.55	8120.3	8026.8	5.022	2.24
18	356.8	18.77	6772.9	6697.1	4.033	2.01
24	345.5	18.18	6339.4	6281.2	3.150	1.77
30	335.8	17.67	5991.1	5933.6	3.127	1.76
36	330.5	17.39	5786.8	5747.4	2.100	1.45
48	326.6	17.18	5642.5	5617.5	1.583	1.26

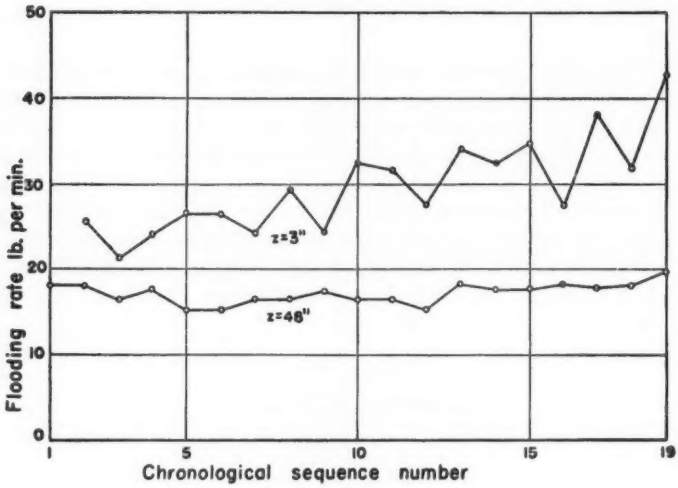
Flooding rate lb. per min.
Chronological sequence number
z=3"
z=48"
0
10
20
30
40
50
1
5
10
15
19

FIG. 5.

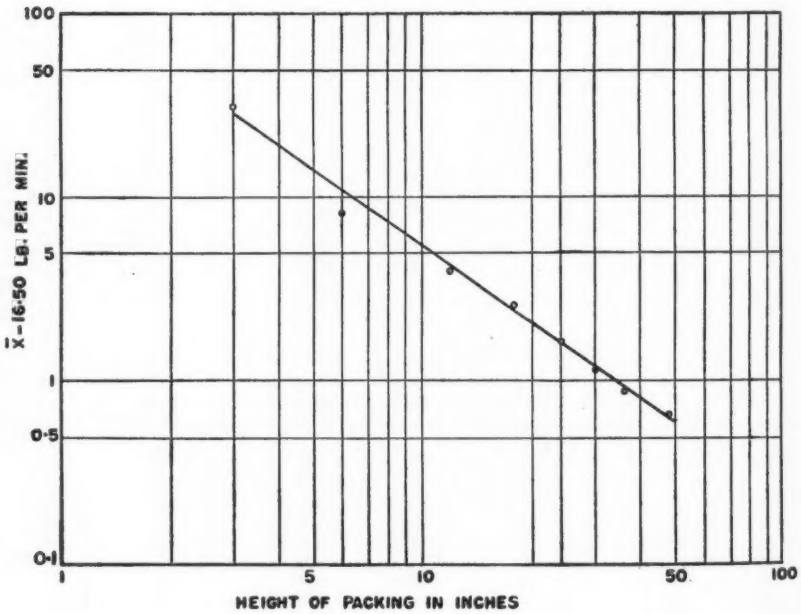
$\bar{X}$ - 16·50 LB. PER MIN.
HEIGHT OF PACKING IN INCHES
100
50
10
5
1
0·5
0·1
1
5
10
50
100

FIG. 6.

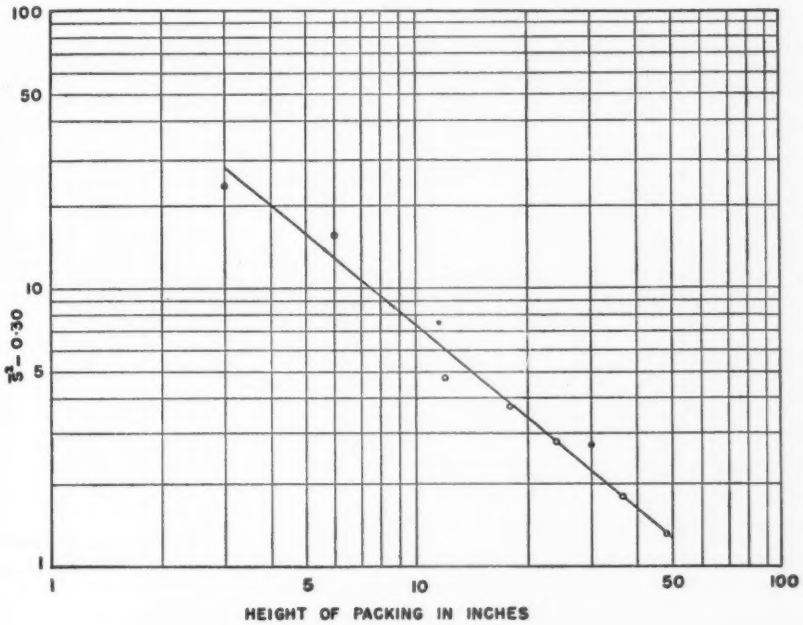

FIG. 7.

The same can be said of the correlation of the variances, shown in Fig. 7, corresponding to equation [8]. The parameters are $\sigma_\epsilon^2 = 0.3$ and $s = 0.532$. The agreement between the two values of s is not good, but this is to be expected in view of the approximations made and the experimental error. Fig. 5 shows plots of the flooding rate versus chronological sequence of the readings for packing heights of 3 in. and 4 ft. The trend is obvious, even allowing for legitimate fluctuations. It is interesting to notice that the drift is much more pronounced at low heights of packing. Although the equations developed are now no longer strictly applicable, the qualitative predictions remain true nevertheless.

CONCLUSIONS

The agreement between theory and experiment is as good as could be expected, and it is reasonable to conclude that a mechanism such as that postulated is operative. The percentage deviation at 4 ft. of packing, 7.3%, is quite small considering that it is inflated owing to the experimental error.

It can therefore be concluded that statistical factors are not very important in affecting the flooding rate in a column of this kind, using $\frac{1}{2}$ in. Raschig rings, with a packing depth of 4 ft. or more. This conclusion cannot be extended to other cases without further experimental work. It is expected that the ratio

of packing size to column diameter would be an important parameter affecting the statistical effect, as well as the ratio of packing size to depth of packing, and the type of packing used. It is recommended that no experimental work be done on columns for which the above ratios are greater than in the present case.

NOTATION

a Height of an elemental segment, ft.
C A constant defined by equation [2].
s Exponent defined by equation [5].
$\bar{s}$ Standard deviation of the flooding rates at constant height of packing, lb./min.
t Exponent defined by equation [8].
v Theoretical flooding rate in the elemental segment, lb./min.
v_0 Smallest possible flooding rate, lb./min.
V Observed flooding rate, lb./min.
θ Exponent defined by equation [2].
σ Theoretical standard deviation, lb./min.
$\bar{x}$ Mean flow rate at a given height, lb./min.

REFERENCE

1. DELL, F. R. and PRATT, H. R. C. Trans. Inst. Chem. Engrs. 29: 89. 1951.

THE OXIDATION, DECOMPOSITION, IGNITION, AND DETONATION OF FUEL VAPORS AND GASES

XXVII. THE HYDROGEN ENGINE[1]

By R. O. King[2] and Mogens Rand[3]

ABSTRACT

Experiments made with hydrogen as the fuel for an Otto cycle engine show that optimum performance in terms of power and economy is limited only by preignition arising from the temperatures attained by the ceramic core of the spark plug or by the exhaust valve, or from nuclei formed by pyrolysis of lubricating oil vapor. On reduction of the magnitude of these igniting effects it became possible to operate the engine with speeds rising to 1800 r.p.m. and the compression ratio fixed at 12:1. A value of 146 p.s.i. for I.M.E.P. with an indicated thermal efficiency of 37% was obtained when the maximum power mixture strength was used. A value of 90 p.s.i. was obtained for I.M.E.P. with an indicated thermal efficiency of 47% with a mixture 55% weak. These values exceed, by a wide margin, any recorded in the literature of the subject.

INTRODUCTION

Results in conformity with the nuclear theory of ignition, as stated in Part IV (7), were obtained when hydrogen was used as the fuel for experiments with a C.F.R. knock rating engine (Part V (12)). These experiments were carried out at the standard knock rating speed of 900 r.p.m. and with compression ratios rising to 10:1. Ignition otherwise than by the electric spark did not occur unless finely divided carbon had been allowed to accumulate in the combustion chamber. It was found later that the carbon was a product of the pyrolysis of lubricating oil *vapor*. A similar igniting effect occurred when charcoal dust was added to the hydrogen–air mixture before it entered the combustion chamber and when in subsequent experiments the laboratory atmosphere was impregnated to an unusual degree with concrete dust (11). This was of especial interest in that the nuclei were not combustible. A significant feature of the experiments was the occurrence of some degree of preignition on increase of the temperature of the jacket coolant from 140° to 212°F. This effect according to the nuclear theory of ignition would be due to a surface in the combustion chamber having attained an igniting temperature or to nuclear ignition arising from an increase in the rate of vaporization of lubricating oil. The surfaces that would be expected to attain an igniting temperature were those of the exhaust valve, and the ceramic core of the spark plug or of its central electrode. The most effective way of raising the temperature of these indirectly cooled surfaces would have been to increase the heat load by increasing engine speed but the unbalanced C.F.R. knock rating engine

[1]*Manuscript received May 31, 1955.*
Contribution from Defence Research Board, Ottawa, Canada, in association with the Department of Mechanical Engineering, University of Toronto, Toronto, Ontario.
[2]*Scientific Officer-in-Charge, Combustion Research, Defence Research Board, Ottawa, Canada, and Special Lecturer, Department of Mechanical Engineering, University of Toronto.*
[3]*Principal Scientific Officer, Defence Research Board.*

was not suitable for operation at speeds higher than 900 r.p.m. The engine experiments were therefore discontinued until a C.F.R.-F4 engine, balanced for high speed operation, became available for the new series of experiments described in this Part.

Experiments with combustion tubes of materials similar to those in the combustion chamber of the engine were however initiated in order to determine the wall temperature required for the ignition of hydrogen–air mixtures passing through them and are described in Part XXVI (10).

EXPERIMENTAL ARRANGEMENTS AND METHODS, PRESENTATION OF RESULTS

The Engine

The C.F.R.-F4 engine, bore $3\frac{1}{4}$ in. stroke $4\frac{1}{2}$ in., is fitted with balancing pistons in the crank case, as required for high speed running. The cast iron piston is fitted with an oil scraper ring and three pressure rings. The engine was direct connected to a d-c. generator arranged as a swinging field dynamometer for the measurement of B.H.P. directly and of I.H.P. by the motoring method. Provision was made for the measurement of compression ratios varying from 4 to 20:1.

Camshafts which provided suitable valve timing for speed ranges of 900 to 1200 r.p.m. and 1200 to 1500 r.p.m. were available. They will be described respectively as low and high speed camshafts. The valve timing and lift are given in the appendix to this Part.

Cylinders with holes for three spark plugs in the wall and one in the head were available. One was fitted with a sodium cooled exhaust valve, and others with the C.F.R. standard uncooled valve of silchrome steel. The types of the cooled and uncooled valves are illustrated by Fig. 15 of the appendix. A plain or a shrouded inlet valve could be used in either cylinder.

Exhaust Valve Surface State

The surface state of the face of the exhaust valve varies with time of use and this was found to have an appreciable effect on the temperature required for the ignition of other than weak hydrogen–air mixtures. Exhaust valves with two varieties of surface state were used, namely *clean* and *aged*.

A valve cleaned with abrasive material and then washed with alcohol before a set of experiments was begun is described as *clean* although it ceases to remain in that condition to an extent depending on the time required to complete a set. A running time of from three to four hours is generally required.

An *aged* valve is one that has been used for many sets of experiments and cleaned only by washing with alcohol, before a set of experiments is begun.

The Ignition System

The designs of spark plugs used for the experiments are illustrated by Fig. 14 of the appendix. Champion C.F.R.-8 was until recently the standard spark plug for use with the A.S.T.M.-C.F.R. method of knock rating. It is a "hot" variety, near the top of the commercial heat scale. Spark plugs K.L.G. 100 and Champion R 2-S were used as cool varieties.

The coil ignition supplied as standard had been found to be ineffective with hydrogen–air mixtures at a C.R. of 10.0, unless the spark gap were reduced to 0.012 in. A special Auto-Lite ignition system was used for experiments made subsequently with hydrogen and other gases and it was then possible to increase the spark gap to 0.025 in. if necessary. The system is described in the appendix to Part XIII (9).

Temperature Control

It was found in the course of preliminary experiments that as the heat load carried by the engine was raised, by increasing speed for example, it became necessary to control the temperatures of the air and hydrogen supplied to the engine if repeatable results were to be obtained. The temperature of the air drawn from the laboratory atmosphere was subject to variations of approximately 40°F. The method used for maintaining the supply of air and hydrogen at a nearly constant temperature of 65°F. is described in the appendix to this Part.

Water was used as the jacket coolant and temperatures lower than 212°F. were controlled automatically by the thermostatic method described in Part XIII (9, pp. 152–153). The flow of water through the cylinder jacket could be controlled by this method to ensure that the temperature at the outlet was never more than 5°F. higher than that at the inlet.

The lubricating oil in the crank case sump was maintained at 140°F. by an exterior electric heater with manual control. Oil pressures maintained at speeds of 900, 1200, 1500, and 1800 r.p.m. were 18, 21, 23, and 25 p.s.i. respectively.

The Hydrogen Supply

Electrolytic hydrogen as supplied by the Canadian Liquid Air Company, Toronto, compressed to 2000 p.s.i. in steel cylinders was used for the experiments. The hydrogen was reputed to be 99.95% pure and as compressed was nearly dry, the dew point being below minus 100°F. The lower calorific value as used for calculations of thermal efficiency was taken as 274.5 B.T.U. per cu. ft., at 60°F. and 30 in. Hg. The method used for the measurement of the rate of hydrogen supply to the engine is described in the appendix to this Part.

The Lubricating Oil

A separate series of experiments with lubricating oils indicated that the least amount of residue remained in the combustion chamber after Ucon had been used. This is a synthetic lubricant made by the Carbide and Chemicals Corporation with a base composed of polyalkylene glycols and derivatives. The grade selected for the experiments is described as L.G. 300 X, which indicates that it is water insoluble, has a viscosity of 300 Saybolt universal seconds, and is oxidation inhibited but without additives. According to A.S.T.M. tests, the viscosity index is 142, ash less than 0.01%, carbon residue also less than 0.01%, and water less than 0.25%. The viscosity is close to S.A.E. 30 at 210°F. and the same as S.A.E. 20 at 130°F.

Methods of Experiment

The engine was always prepared for a particular set of experiments by being dismantled for a top overhaul. The cylinder, piston, and rings were then washed with acetone and alcohol. The valves were inspected and hand lapped into their seats if signs of leakage were detected. On conclusion of the set it was verified, by measurement of compression pressure before the engine had cooled, that piston sealing had not deteriorated.

The lubricating oil and the jacket cooling water were heated electrically to working temperatures before a set of experiments was begun. The engine was then started on a hydrogen–air mixture 50% weak and run for at least 30 min. The mixture was then reduced to the leanest on which the speed selected for the first experiment could be maintained. This was always the lowest of the speeds to be used for a set of experiments. The engine was then run for 15 min. before a determination of the optimum spark timing.

Hydrogen burns with high velocity in mixtures with air approaching and exceeding the correct value and relatively slowly when in small concentration in air, and the ignition timing required for maximum power output when a particular mixture strength and engine speed was used can be determined with accuracy, solely by a series of lower measurements. Brake horsepower was measured accordingly for a series of ignition timings giving rising and falling values for power output and the optimum timing was then obtained from a plot of results, as described in Part XII (8, pp. 438–439).

Presentation of Experimental Results

Experiments were carried out at engine speeds rising to 1800 r.p.m. and with compression ratios of 10 and 12:1. Comprehensive performance data are given by graphs plotted on a mixture strength base as used for experiments with liquid fuels. A "correct" mixture is 100% stoichiometric. The percentage stoichiometric diminishes or increases as the mixture is weakened or enriched. Thus for example a mixture 20% weak is 80% of stoichiometric and one 20% rich is 120% of stoichiometric.

The terms Compression Ratio, Mixture Strength, Indicated Thermal Efficiency, and Indicated Mean Effective Pressure are, when convenient, abbreviated to C.R., M.S., I.T.E., and I.M.E.P. respectively. Values of C.R. are given as single numbers. A stoichiometric mixture is described as "correct" in the text; the abbreviation C.C.M. is used on the graphs. It is to be understood that numerical values given on graphs for I.M.E.P. and Engine Speed are in pounds per square inch (p.s.i.) and revolutions per minute (r.p.m.) respectively.

I. THE IGNITING EFFECT OF THE CERAMIC CORE OF A SPARK PLUG

Preliminary Experiments

The operating conditions were similar to those in which some degree of preignition occurred in the course of the experiments described in Part V (12) when a correct hydrogen–air mixture was used at a C.R. of 10, with the

jacket coolant at 212°F. and the mixture supplied at room temperature. A C.F.R.-8 spark plug which is a "hot" variety was used, the exhaust valve was of silchrome steel, uncooled, and the inlet valve was of the shrouded type which provided a swirl in the entering mixture. Thus the conditions were essentially those used for the knock rating of fuels by the C.F.R.-A.S.T.M. motor method.

The experiments were carried out with the C.R. fixed at 10, with engine speeds of 600, 900, 1200, and 1500 r.p.m. while mixtures were varied from very weak to extremely rich. The results obtained for the relation between I.H.P. and M.S. are given by the graphs of Fig. 1.

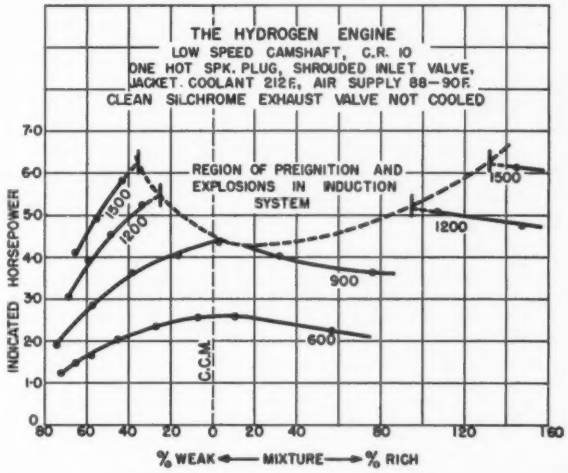

FIG. 1. Mixture strengths over which premature ignition occurs when engines speeds exceed 900 r.p.m. and a C.F.R.-8 spark plug, a hot variety, is used in the standard position.

It will be seen by reference to the graphs that at 600 r.p.m. a maximum value of 2.6 was obtained for I.H.P. when the mixture was 10% rich. There was no preignition. When however the heat load was increased by raising the speed to 900 r.p.m. and I.H.P. attained a maximum of 4.3, there was some degree of preignition but not enough to interrupt the experiment. This result was similar to that obtained in similar conditions as described in Part V (12). Then when the heat load was further increased by raising the speed to 1200 and then to 1500 r.p.m. the range of M.S. over which running was impossible, because of backfiring into the induction system, increased as shown by the relevant graphs. Thus at 1500 r.p.m. backfiring occurred over the mixture range 40% weak to 140% rich.

Ignition by a Hot Spark Plug without a Central Electrode

Preignition is frequently attributed to the central electrode of the spark plug becoming overheated. Pye (15, p. 91), for example, mentions only the

central electrode and scraps of incandescent carbon; Hundere and Bert (6, p. 553), fragments *detached* from the ceramic core. The experiments described in Part XXVI (10) indicated that preignition would preferably be initiated by the surface of the ceramic core of the spark plug even if its temperature were not higher than that of other surfaces in the combustion chamber.

Experiments were carried out accordingly in the operating conditions used for the preliminary experiments but with the mixture fired by a cool variety of spark plug, a K.L.G.-100, in the standard position while a standard but unfired hot variety, a C.F.R.-8, was in the No. 2 position. The central electrode of this plug had been cut off. The standard and the No. 2 positions are shown by Fig. 2. It will be seen by reference to the figure that the swirl due to the

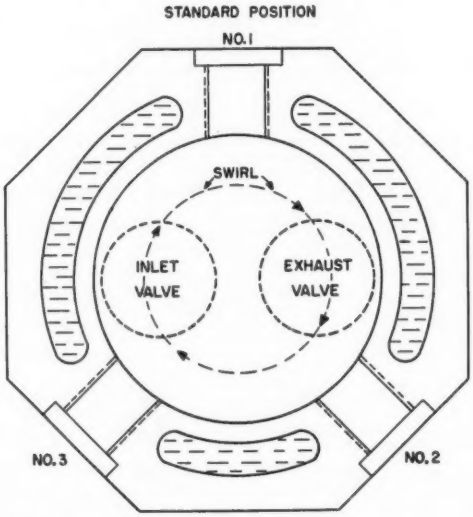

FIG. 2. Location of spark plug holes in wall of the combustion chamber and the mixture swirl due to the use of the C.F.R. shrouded inlet valve.

shrouded inlet valve directs the relatively cool entering mixture over the spark plug in the standard position and that it then passes over the hot exhaust valve before arriving at the unfired plug in the No. 2 position.

The experimental results obtained for the relation between I.H.P. and M.S. with speeds of 600, 900, 1200, and 1500 r.p.m. are given by the graphs of Fig. 3. It was just possible to use the maximum power mixture strength without the occurrence of preignition at the low speed of 600 r.p.m., the corresponding maximum I.H.P. being 2.6. Then on raising the speed to 900 r.p.m. preignition accompanied by backfiring occurred with mixtures ranging from 16% weak to 67% rich and the range of mixture strength over which running was impossible increased as speed and the corresponding heat load were further increased, as illustrated by the graphs of the figure.

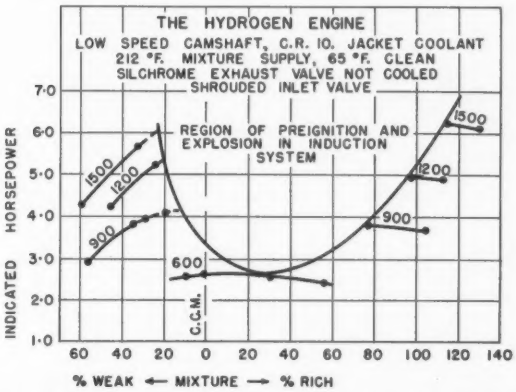

FIG. 3. Mixture strengths over which premature ignition occurs at engine speeds exceeding 600 r.p.m. when an unfired hot spark plug without projecting central electrode is in No. 2 position and ignition is by a cool spark plug in the standard position.

II. THE LIMITATION OF POWER AND ECONOMY BY THE ONSET OF PREIGNITION DUE TO THE ATTAINMENT OF AN IGNITING TEMPERATURE BY THE CERAMIC CORE OF THE SPARK PLUG

The experiments described in Section I were carried out at a C.R. of 10 and in the absence of an accumulation of finely divided carbon in the combustion chamber. The maximum power attainable was limited by preignition arising from the ceramic core of the C.F.R.-8 spark plug having attained an igniting temperature in respect of the hydrogen–air mixture. Moreover it was shown by the experiments with combustion tubes (Part XXVI (10)) that a correct mixture would be ignited by the exhaust valve if it attained a temperature of approximately 1100°F. It was decided accordingly to use a sodium cooled valve for further experiments and to maintain the jacket coolant at 100°F. and the entering mixture at 65°F. The shrouded inlet valve was replaced by a plain type although this led to an increase in volumetric efficiency and consequently to an increase in heat load. The volumetric efficiency at high speeds was however restricted to some extent by the continued use of the low speed camshaft. The object of the changes mentioned was to ensure that preignition, when it occurred, was due solely to the temperature attained by the ceramic core of the spark plug. Experiments were carried out at a C.R. of 10 and with speeds of 900, 1200, 1500, and 1800 r.p.m. when a hot spark plug was used and repeated after a change to a cool variety of spark plug.

Hot Spark Plug Experiments

A Champion C.F.R.-8 was used as a hot plug. The relation between I.H.P. and the values of M.S. that could be used before the experiment was interrupted by the occurrence of preignition and backfiring is given by the *A* graphs of Fig. 4, for the four engine speeds. Backfiring began on increasing M.S. to the values shown by the short vertical lines of the graphs. The mixture was then 42% weak at speeds of 1500 and 1800 and 38% weak at 900 and 1200. A value

of 40% weak, taken irrespective of engine speed, would be within experimental accuracy. Preignition and backfiring did not occur when extremely rich mixtures were used. The values then obtained for I.H.P. are not given by the graphs. The small ranges of M.S. usable in the conditions of the experiments included the weak value for which indicated thermal efficiency was a maximum. Relevant data are tabulated below.

TABLE I

MIXTURE STRENGTH FOR MAXIMUM I.T.E., 60% WEAK
ONE HOT SPARK PLUG, LOW SPEED CAMSHAFT, C.R. 10.0

Speed	Opt. spk. Advance	I.M.E.P.	I.T.E.%
1800	30°	80	43.0
1500	32°	81	43.5
1200	32°	81	43.0
900	32°	80	41.5

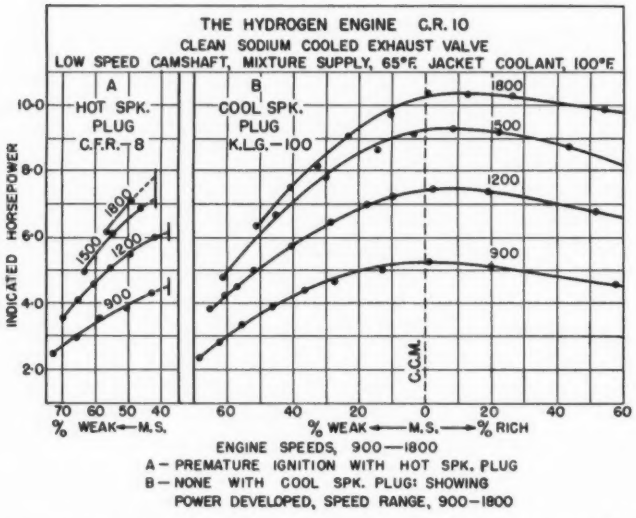

FIG. 4. Graphs *A* and *B* illustrate the effect of changing from a hot to a cool variety of spark plug; other running conditions having remained unchanged.

Cool Spark Plug Experiments

A K.L.G. 100 was used as a cool plug. The relation between I.H.P. and M.S. then obtained without otherwise changing conditions of experiment is given by the *B* graphs of Fig. 4. They show that a remarkable effect, which prevented premature ignition, had been obtained. Thus referring to the figure it will be

seen that hydrogen–air mixtures ranging from 70% weak to 80% rich were used at speeds ranging from 900 to 1800.

The values obtained for I.T.E. and I.M.E.P. when the M.S. was used for maximum power and optimum spark timing are given, in Table II, below. Maximum power was always obtained when using a mixture 5% rich. The values for I.T.E. and the corresponding values of I.M.E.P. obtained when using the M.S. for maximum I.T.E. are given in Table III.

TABLE II

MIXTURE STRENGTH FOR MAXIMUM POWER, 5% RICH
ONE COOL SPARK PLUG, LOW SPEED CAMSHAFT, C.R. 10

Speed, r.p.m.	% Vol. eff.	Spk. timing	I.H.P.	I.M.E.P.	I.T.E.
1800	77	1° adv.	10.4	123	36
1500	84	t.d.c.	9.3	132	35
1200	86	1° ret'd	7.6	134	35
900	86	1° ret'd	5.4	126	33

TABLE III

MIXTURE STRENGTH FOR MAXIMUM THERMAL EFFICIENCY, 55% WEAK
ONE COOL SPARK PLUG, LOW SPEED CAMSHAFT, C.R. 10

Speed, r.p.m.	% Vol. eff.	Spk. adv.	I.H.P.	I.M.E.P.	I.T.E.
1800	75	35°	6.1	75	43.6
1500	85	26°	6.0	85	44.0
1200	91	28°	4.9	87	42.4
900	91	22°	3.6	85	42.0

It is shown by the data of Tables II and III that a maximum value of 134 was obtained for I.M.E.P. with a speed of 1200 and the somewhat lower value of 132 on increasing speed to 1500. A maximum of 42.4% was obtained for I.T.E. with a speed of 1200 and of 44% on increasing the speed to 1500. The I.H.P. obtained with the maximum lower mixture increased from 4.9 to 6.0 on increasing the speed from 1200 to 1500 but an increase to 6.1 only was obtained on further increasing speed to 1800 and the I.M.E.P. decreased from 132 to 123.

It is evident that the valve timing provided by the low speed camshaft was suitable for use at speeds of from 1200 to 1500 but not for a speed of 1800. Comprehensive performance data were obtained for the four speeds used for the experiments and with mixtures ranging from 66% weak to 60% rich. The data are given by the graphs of Fig. 5 for a speed of 1500 only.

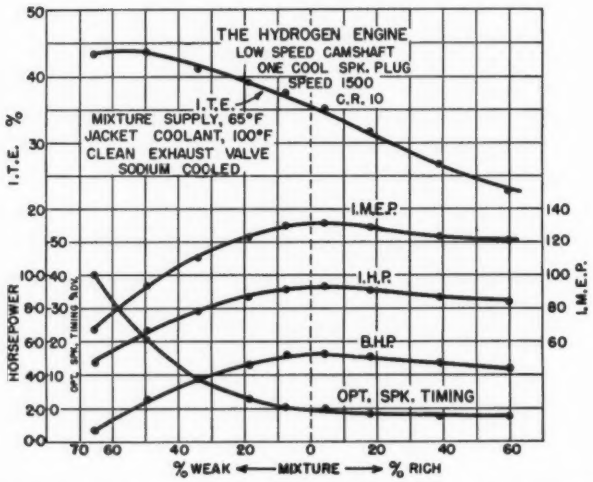

FIG. 5. Performance data, mixtures 66% weak to 60% rich, obtained when ignition is by a cool spark plug, speed 1500 r.p.m. and C.R. 10:1.

III. THE MEAN TEMPERATURES ATTAINED BY HOT AND COOL SPARK PLUG CORES, AN UNCOOLED EXHAUST VALVE, AND THE EXHAUST GAS AS AFFECTED BY MIXTURE STRENGTH

The experiments were carried out with an engine speed of 1200 r.p.m., a C.R. of 10, temperatures of jacket coolant and mixture supply 100° and 65°F. respectively. The experimental results are given by the graphs of Fig. 6.

The C.F.R.-8 Spark Plug

The spark plug with a thermocouple in the central electrode near the tip of the ceramic core was supplied by the Champion Spark Plug Company. Thus the temperature at that position could be measured while the spark plug, placed in the standard position, was used to fire the hydrogen–air mixture. The temperatures attained as M.S. was increased from 70% weak are given by the *A* graph of the figure. Preignition occurred on increasing the M.S. to 33% weak. A temperature of 1150°F. had then been attained at the position of the thermocouple.

The Uncooled Exhaust Valve

The valve was of silchrome steel, supplied as standard for the C.F.R.-A.S.T.M. motor method of knock rating. It was obtained with the stem drilled for a thermocouple to be fitted in a manner suitable for the measurement of the temperature of the exposed surface. The temperatures thus measured while ignition was provided by a cool spark plug, a K.L.G. 100, in the standard position, are given by the *B* graph of the figure. It will be seen that the temperature of the exhaust valve rose from 590° to a maximum of 1150°F. as M.S. was increased from 66% weak to 5% rich. There was no preignition.

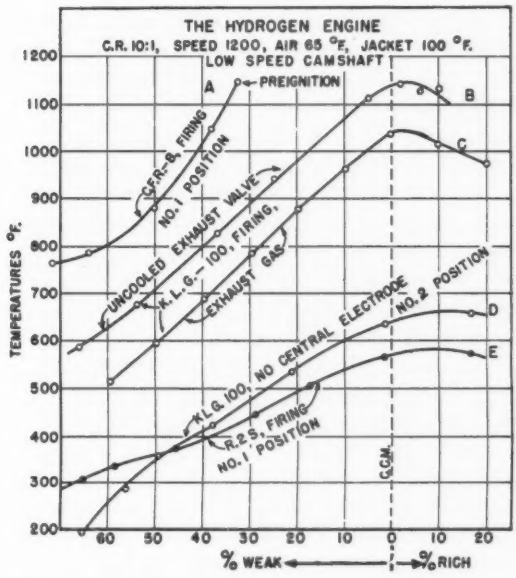

FIG. 6. Mixture strength and the corresponding temperatures of an uncooled exhaust valve, the exhaust gas, and hot and cool spark plugs.

The Exhaust Gas

The temperature was measured by using a bare thermocouple placed in the exhaust system approximately 3 in. from the valve. The temperatures thus measured, as M.S. was increased from 60% weak to 20% rich, are given by the *C* graph of the figure. They were measured at the same time as those of the uncooled exhaust valve. It will be noted that the temperature of the uncooled exhaust valve was always higher than that of the exhaust gas. The temperature of a sodium cooled valve in an air cooled cylinder was always lower than that of the exhaust gas, according to experiments by Sanders, Wilstead, and Mulcahy (17).

The Cool Spark Plugs, R2-S and K.L.G. -100

An R2-S spark plug with a thermocouple in the central electrode near the top of the ceramic core was placed in the standard position and used for firing the mixture. A K.L.G.-100 was prepared for the experiments by removing the central electrode and replacing it by a thermocouple cemented in at about 1/8 in. from the tip of the ceramic core. This plug was placed in the No. 2 position. The inlet valve was of the plain type, thus there was no swirl to influence the relative temperatures attained by the spark plugs. The K.L.G. plug in the No. 2 position was however closer to the exhaust valve than the champion plug in the standard positions. The temperatures, as measured while M.S. was increased from 70% weak to 20% rich, are given by graphs *D* and *E* of the figure. It will be seen that the temperatures attained by the two

plugs did not differ to a significant extent, allowing for their relative positions, and that the maximum temperature of 670°F., which was attained with a mixture 10% rich by the K.L.G.-100 plug, is far below that required for the ignition of any hydrogen–air mixture.

IV. THE LIMITATION OF POWER AND THERMAL EFFICIENCY BY THE ONSET OF PREIGNITION DUE TO THE EXHAUST VALVE HAVING ATTAINED AN IGNITING TEMPERATURE

The experiments described in Sections II and III demonstrated that preignition due to the ceramic core of the spark or to its central electrode did not occur when a cool type of spark plug was used. It was shown however, by the *B* graph of Fig. 6, that the temperature attained by the exhaust valve approached the value required for the ignition of a correct hydrogen–air mixture when the engine speed was 1200 r.p.m. and the C.R. 10:1. It appeared therefore that preignition by the exhaust valve might become a limiting factor in respect of power and thermal efficiency on raising the heat load.

Experiments were therefore carried out in the operating conditions used for those described in Sections II and III, except that volumetric efficiency and the consequent heat load were increased by using a "high speed" camshaft. There was then a corresponding increase in the temperature of the exhaust valve and a further increase due to the valve lift being increased from 0.238 in. to 0.312 in. and to the time the valve was off its cooling seat being increased from 145° to 155° of crank revolution. The values for I.H.P. obtained with mixtures ranging from 70% weak to 60% rich are given by the graphs of Fig. 7. The I.H.P. attained a maximum of 11.0 with a speed of 1800 r.p.m. as compared with the value of 10.4 obtained when using the low speed camshaft,

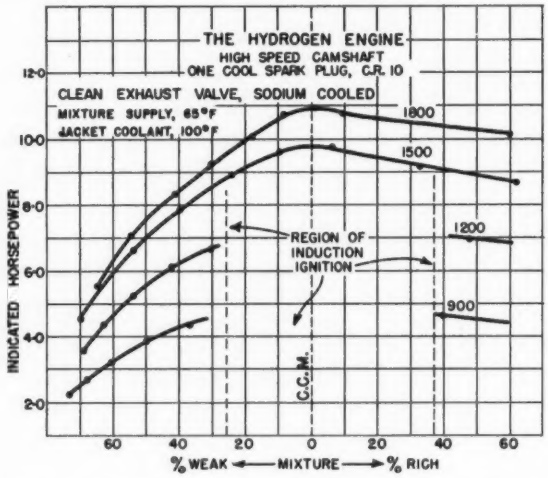

FIG. 7. Premature ignition at speeds lower than 1500 r.p.m. as obtained when changing to the high speed camshaft, other running conditions remaining unchanged.

Fig. 4. The especially noteworthy feature of the experiments was that preignition and backfiring into the induction system occurred when speed was *reduced*.

An explanation was provided by the results of the experiments with steel combustion tubes, Part XXVI (10). It was found in these experiments that the igniting effect of a clean stainless steel surface was reduced if it was aged by exposure at high temperatures to hydrogen–air mixtures for the time required for the formation of an adherent layer of oxide. Moreover it was shown that the difference in the igniting effects increased as time of exposure to hydrogen–air mixtures was increased. Thus it would be expected that in the engine an exhaust valve with a clean surface would ignite a hydrogen–air mixture at a lower temperature than would be required by one with an aged surface and that the difference in the igniting effects would increase on decreasing the engine speed.

The surface of the exhaust valve had always been cleaned with abrasive material for the experiments described earlier in this Part but in view of the results of the experiments with stainless steel combustion tubes the clean exhaust valve was replaced by a similar sodium cooled valve which had been put aside after having been used for a long period during which a coating of oxide had formed. The valve is described accordingly as "aged".

The engine then ran at speeds ranging from 900 to 1800 r.p.m. with an entire absence of preignition. No alteration other than the change of exhaust valves had been made in the operating conditions. The values obtained for I.H.P. when mixtures ranging from 70% weak to 70% rich were used are given by the graphs of Fig. 8. The experiments were of a preliminary nature made to verify that preignition would be avoided by using an aged instead of an initially clean exhaust valve.

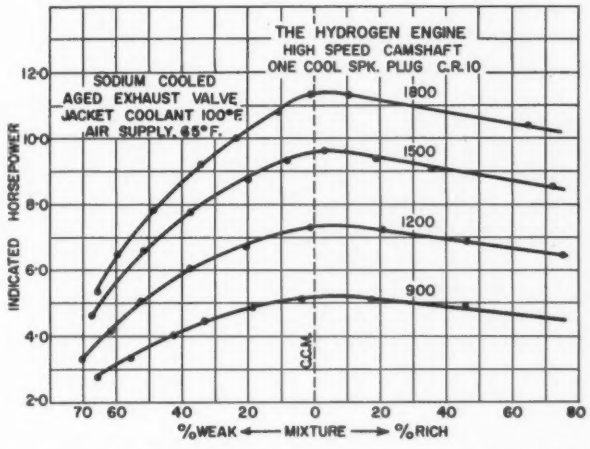

Fig. 8. Graphs showing the absence of low speed premature ignition when the exhaust valve was aged.

Performance Data for Six Engine Speeds

Further experiments were carried out to obtain complete performance data when the aged exhaust valve was used with speeds of 1100 and 1300 r.p.m. in addition to the speeds of 900, 1200, 1500, and 1800 r.p.m., while mixtures were varied from 70% weak to 70% rich. The data obtained when the mixtures required for maximum I.H.P. and maximum I.T.E. were used are tabulated in Tables IV and V, respectively.

TABLE IV

MIXTURE STRENGTH FOR MAXIMUM POWER; AGED EXHAUST VALVE
HIGH SPEED CAMSHAFT, ONE COOL SPARK PLUG, C.R. 10

Speed	% Vol. eff.	Spk. timing	M.S.	I.H.P.	I.M.E.P.	I.T.E.%
1800	81.1	2° adv.	5% rich	11.40	135	36.5
1500	89.6	t.d.c.	5% rich	9.65	139	35.0
1300	89.0	t.d.c.	7% rich	8.05	132	34.5
1200	90.6	t.d.c.	6% rich	7.40	131	34.0
1100	87.8	t.d.c.	6% rich	6.60	128	33.5
900	84.5	2° retard	5% rich	5.25	122	33.0

TABLE V

MIXTURE STRENGTH FOR MAXIMUM INDICATED THERMAL EFFICIENCY, 55% WEAK;
AGED EXHAUST VALVE
HIGH SPEED CAMSHAFT, ONE COOL SPARK PLUG, C.R. 10

Speed	% Vol. eff.	Spk. adv.	I.H.P.	I.M.E.P.	I.T.E.%
1800	83	24°	7.0	83	44.4
1500	87	27°	6.1	87	43.2
1300	84	30°	5.1	84	42.0
1200	84	31°	4.8	84	41.5
1100	82	30°	4.2	82	41.5
900	80	30°	3.3	80	40.2

It will be seen by reference to Table IV that I.H.P. was 11.4 at 1800 r.p.m., as compared with 10.4 H.P. obtained when the low speed camshaft was used, see Table II. The maximum values for I.M.E.P. and volumetric efficiency were obtained at 1500, indicating that the valve timing provided by the high speed camshaft was most suitable for that engine speed provided that preignition was avoided by using an aged exhaust valve. The I.M.E.P. was then 139 as compared with a value of 132 p.s.i. obtained when the low speed camshaft and a speed of 1500 was used, and 134 when the speed was 1200 r.p.m. It may be concluded that in so far as I.M.E.P. is concerned, the valve timing provided by the low speed camshaft is most suitable for an engine speed of 1200 and that provided by the high speed camshaft is best for an engine speed of 1500 r.p.m.

The maximum values for I.T.E. were always obtained when the mixtures were 55% weak, when either the low or the high speed camshaft was used.

The values obtained with the low speed camshaft, Table III, increased from 42% at a speed of 900 to attain a maximum of 44% at 1500 r.p.m. and a lower value of 43.6% at 1800 r.p.m. On the other hand the values obtained when the high speed camshaft was used increased with fair regularity from a low of 40.2% at 900 to a maximum of 44.4% at 1800 r.p.m., Table V. Performance data for mixtures ranging from 70% weak to 80% rich are given by the graphs of Fig. 9 for the engine speed of 1500 at which a maximum of 139 was obtained for I.M.E.P.

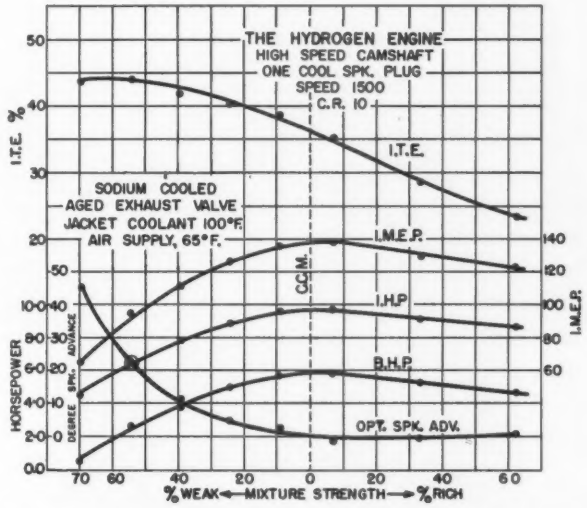

FIG. 9. Performance data, mixtures 70% weak to 64% rich, obtained when using the high speed camshaft and the aged exhaust valve. Speed 1500 r.p.m. C.R. 10:1.

Indicator Diagrams

The indicator diagrams, Fig. 10, were taken when a Draper-Li pressure pickup was used. The pressure scale is linear and maximum values in pounds per square inch are given by the calibration marks on the diagrams. The diagrams were taken when a C.R. of 10 was used and when, under the operating conditions used, the performance data given in Tables IV and V were obtained, at an engine speed of 1500 r.p.m.

The pressure waves started by the spark are most pronounced, when with mixtures nearly correct the pressure rise due to combustion began immediately after its passage, diagrams *A* and *B*. Spark timing is shown on the diagrams by small rather faint blips fed into the electronic circuit. These are marked by arrows. Similar blips marked by short vertical lines were fed into the circuit at t.d.c. and at intervals of 10° for 30° before and after.

Spark timing was always adjusted to obtain maximum power output and it will be noted that maximum combustion pressure then occurred at approxi-

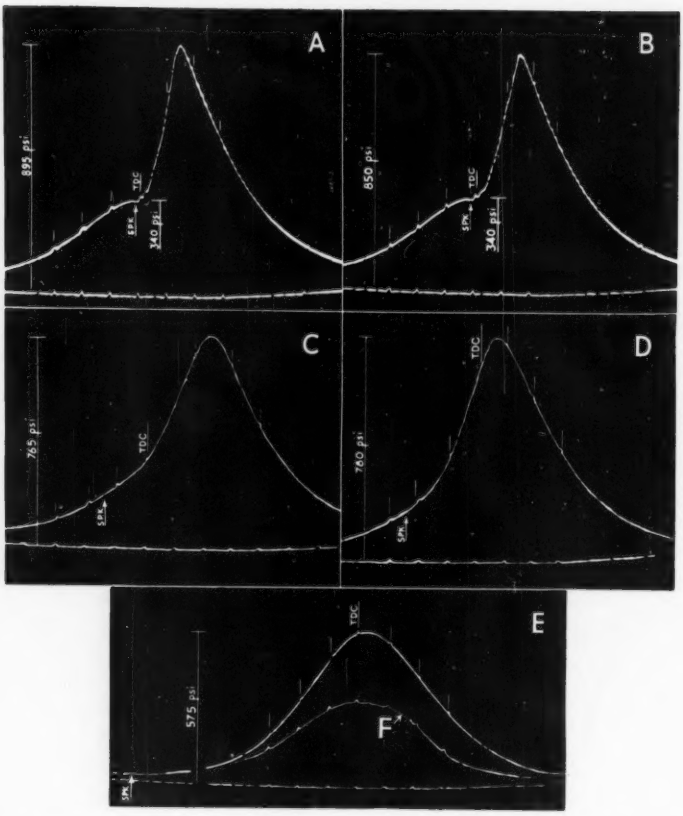

FIG. 10. Pressure–time diagrams taken with a Draper-Li pressure pickup. C.R. 10:1 speed 1500 r.p.m.
A, M.S. 3% rich, spk. 1° retard. *B*, M.S. 8% weak, spk. 1° adv.
C, M.S. 34% weak, spk. 14° adv. *D*, M.S. 50% weak, spk. 25° adv.
E, M.S. 80% weak, spk. 75° adv. *F*, air only.

mately 15° after t.d.c. when the mixture was nearly correct, diagrams *A* and *B*, but at approximately 5° after t.d.c. when mixtures 34, 50, and 80% weak were used, diagrams *C*, *D*, and *E*.

The power developed with a mixture 80% weak was insufficient to overcome friction and pumping losses and the speed of 1500 r.p.m. was maintained by partial motoring of the engine. Diagram *F*, shown below diagram *E*, was taken when air only was supplied to the engine. The pressures shown accordingly can be used for estimating the approximate combustion pressures obtained when mixtures with hydrogen were used.

The diagrams show that if lubricating oil passed into the combustion chamber at the minimum rate practicable, the rate of burning of a hydrogen–air mixture 5% rich or 8% weak was such that its combustion required a time

represented by nearly 15° of crank revolution and that *autoignition did not occur even when the compression ratio was* 10:1.

V. OPERATION OF THE ENGINE AT 12:1 COMPRESSION RATIO

The controllable operating conditions were as had been used at a C.R. of 10, as described in Section IV, except that the temperature of the jacket coolant was reduced from 100° to 65°F. An unavoidable change in conditions occurred on raising the C.R. to 12:1, in that the top piston ring then lost its bearing on the cylinder wall at the three spark plug holes. Moreover a larger pocket into which lubricating oil could leak past the piston was formed between the end of the spark plug and the top piston ring than between the ends of the two blank plugs and the piston ring.

The operation of the engine at a C.R. of 12 and a speed of 1800 r.p.m. in the conditions described was accompanied by some degree of preignition which occurred occasionally only and did not lead to backfiring. When however volumetric efficiency was increased by reducing the speed to 1500 r.p.m., preignition occurred occasionally with a mixture 5% rich, frequently with one 30% rich, and developed into backfiring with a mixture 80% rich.

The engine was then dismantled for inspection and cleaning of the combustion chamber. Patches of soot, easily wiped off, were found on the piston crown adjacent to the three spark plug holes. The patch adjacent to the spark plug hole was larger than those adjacent to the two holes occupied by blank plugs. Similar patches of soot were not found when the engine was dismantled after running at a C.R. of 10.

Method of Avoiding Preignition by Lubricating Oil Soot and the Consequent Improvement in Engine Performance

The extent of the deposits of soot on surfaces in the combustion chamber was found to depend on the time of running required for the accumulation of a quantity of lubricating oil in the pockets provided by the spark plug holes. Thus starting with a weak mixture and taking the observations required for performance data as rapidly as possible, it was found that preignition did not occur until a mixture richer than correct was used. When a mixture 10% weak was again used and the engine run for 10 to 15 min., the excess soot on the piston crown burned off and observations for performance data for the richer mixture without interruption by preignition were obtained. With this procedure, performance data were obtained for mixtures ranging from 70% weak to 80% rich and, in the absence of preignition, higher values for power and thermal efficiency were obtained than when experiments had been interrupted by preignition and backfiring.

Values for I.H.P. obtained at speeds of 1200, 1500, and 1800 r.p.m. and with hydrogen–air mixtures ranging from 70% weak to 80% rich are given by the graphs of Fig. 11.

Values for I.H.P., B.H.P., I.M.E.P., I.T.E., and opt. spark timing are given for a speed of 1500 with mixtures ranging from 70% weak to 80% rich, by the graphs of Fig. 12.

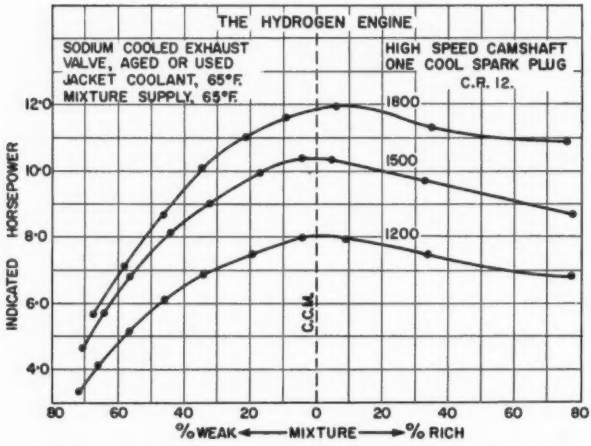

FIG. 11. Power developed at 12:1 C.R. on reducing the concentration of soot derived from pyrolysis of the vapor of excess lubricating oil and thus avoiding nuclear ignition.

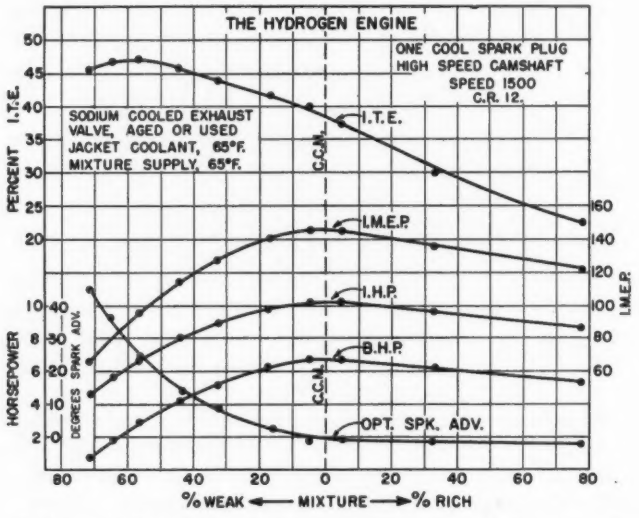

FIG. 12. Performance data obtained in the absence of nuclear ignition when using mixtures 70% weak to 80% rich at 1500 r.p.m. and a C.R. of 12:1.

Performance data obtained when the mixture strength was that required for maximum power and that required for maximum indicated thermal efficiency are of especial interest and are given in Tables VI and VII respectively. Values of opt. spark timing and volumetric efficiency are also given.

It will be seen by references to the tables that a maximum of 146 p.s.i. was obtained for I.M.E.P. when the engine was operated at 1500 r.p.m. and

TABLE VI

MIXTURE STRENGTH FOR MAXIMUM POWER; AGED OR CLEAN EXHAUST VALVE
HIGH SPEED CAMSHAFT, ONE COOL SPARK PLUG, COMPRESSION RATIO 12:1

Speed, r.p.m.	% Vol. eff.	Spark timing	I.H.P.	I.M.E.P.	I.T.E.%
1800	85.4	1° retard	11.9	140	37
1500	89	1° retard	10.3	146	37
1200	87.3	2° retard	8.0	141	36

TABLE VII

MIXTURE STRENGTH FOR MAXIMUM INDICATED THERMAL EFFICIENCY;
AGED OR CLEAN EXHAUST VALVE
HIGH SPEED CAMSHAFT, ONE COOL SPARK PLUG, COMPRESSION RATIO 12:1

Speed, r.p.m.	% Vol. eff.	Spark timing	I.H.P.	I.M.E.P.	I.T.E.%
1800	83.7	25° adv.	7.6	90	47
1500	91.5	25° adv.	6.9	96	47
1200	91	27° adv.	5.3	91	44

that a maximum of 47% was obtained for I.T.E. when the engine was operated at 1800 r.p.m. Values of 47½% were not uncommon but are not shown on the relevant graph of Fig. 12.

Lubricating oil always passed the piston at an abnormal rate when the C.R. was raised to 12. There was therefore always an appreciable concentration of lubricating oil vapor in the compressed hydrogen–air mixture. The pyrolysis of this vapor produced the finely divided carbon which remained in part as soot on the piston crown and required removal by the method described in order to avoid preignition. In these circumstances the difference in the igniting effect due to the exhaust valve being aged or initially clean was masked by the nuclear igniting effect.

The procedure adopted to obtain performance data with a hydrogen–air mixture at a C.R. of 12 was made necessary by the particular design of the C.F.R. cylinder and piston. It could therefore be changed in a manner such that experiments could be carried out at compression ratios higher than 12:1. Thus we have, by limiting the time during which oil passed the piston, been able to operate for a short period at a C.R. of 16:1 with a maximum power mixture.

DISCUSSION

Hydrogen either free or in combination with carbon is a constituent of the gases or liquids commonly used as engine fuels. The characteristics of the combustion of hydrogen only should therefore be of fundamental significance. It seems however to have long been accepted that hydrogen cannot be used as the sole fuel, because of the occurrence of premature ignition, in the operating conditions required to obtain optimum values for power output and the corresponding thermal efficiency.

Lucke (14, 1906) states that "Gases rich in hydrogen *preignite easily* and that approximately one atmosphere should be deducted from the compression pressure allowable with no hydrogen for each 5% of hydrogen present". Tizard (19, p. 22, 1921) states that "Hydrogen *detonates easily* in an internal combustion engine, at quite low compression ratios, but nevertheless it has a high ignition temperature". Ricardo (16, pp. 334–337, 1922), with the E35 engine operated at 1500 r.p.m., found that it was possible to use a nearly correct hydrogen–air mixture at a compression ratio of 5.45:1, but "if an attempt was made to use a rich mixture, violent *preignition* occurred, accompanied by firing back into the carburetor, which rendered further running impossible. Even with the compression ratio lowered to 3.8:1, the same thing occurred". Burstall (2, 1927) operating another E35 engine, at 1000 r.p.m. and compression ratios of 5 and 7:1, found that "The experimental range (of mixture strength) which can be used with hydrogen is strictly limited by its readiness to *detonate*, both at high compression ratios and with rich mixtures, and even more by its tendency to backfire with mixtures richer than 20% weak at a compression ratio of 5:1". Premature ignition, described as *detonation*, was obtained by Egerton, Smith, and Ubbelohde when they were using an ethyl knock testing engine (5, 1935). The effect was attributed at the time to nitrogen peroxide formed from the nitrogen of the air, but some years later to *preignition* (4, p. 917, 1949).

Downs, Walsh, and Wheeler (3, p. 517, 1951), as a result of experiments with hydrogen as the fuel for a Ricardo E6 engine, state that "In most cases, owing to the *extreme ease with which it ignites*, a mixture richer than about 25 to 30% weaker than chemically correct cannot be used. If the attempt is made to run with a richer mixture, *self-ignition* occurs so early in the compression stroke that the mixture is eventually ignited in the induction manifold". The statement that hydrogen–air mixtures "ignite with extreme ease" cannot be accepted as fact. Reference was made to the finding of King, Wallace, and Mahapatra that, by keeping the combustion chamber as clean as possible, the engine could be operated over the whole mixture range without backfiring (12). It was not mentioned that this occurred at a compression ratio of 10:1 and a speed of 900 r.p.m. The reference is also misleading in that it should have been to fluffy carbon that accumulated in an initially clean combustion chamber as described on page 269 of reference (12). Moreover it was not mentioned that preignition and backfiring occurred when charcoal dust was added to the mixture supplied to the engine. Although Ricardo's early statement regarding the impossibility of using rich mixtures is echoed, they describe the premature ignition as "*self-ignition*" instead of by the term *preignition* used by Ricardo. Self-ignition was treated as detonation and attributed to a chain reaction mechanism to be described in a subsequent publication.

Anzilotti and associates (1, 1954) describe experiments with a C.F.R. engine operated at 900 r.p.m. with a jacket coolant temperature of 212°F. and an inlet mixture temperature of 100°F. The results obtained were similar to those of Downs, Walsh, and Wheeler (3) in that, when the mixture strength re-

quired for maximum power was used, the highest compression ratio usable without knock was approximately 8:1. It is stated that the "knock" was similar to that obtained with paraffinic fuels and was attributed to the chain reaction mechanism devised by Lewis and Von Elbe to explain the autoignition of *hydrogen–oxygen* mixtures. In our preliminary experiments also carried out with a similar engine and operating conditions but with a combustion chamber initially clean, the knock limited compression ratio was 10:1 when a nearly correct mixture was used (see Fig. 1, this Part) and it was shown by subsequent experiments described in Section I to have been due at 900 r.p.m. to the ceramic core of the spark plug having attained an igniting temperature.

Livengood and Leary (13) obtained what appeared to be autoignition of a correct hydrogen–air mixture when using the compression ignition machine developed by C. F. Taylor and associates (18). The compression ratio was 12:1 and after nearly adiabatic compression the mixture was held against the thick plate glass window which formed the cylinder head until ignition occurred after a few milliseconds. The window was used for photographic recording of the process of ignition and therefore was not cooled. In view of the experiments described in Section III in which a mixture 33% weak was ignited by the surface of the ceramic core of a spark plug at a compression ratio of 10:1, it may safely be assumed that the ignition observed by Livengood and Leary occurred because a layer of molecules on the surface of the uncooled plate glass window attained the required temperature. Thus it was observed by them that "all mixtures give off a bright yellow light during autoignition. When specimen inflammations were examined with a spectrograph, the presence of a strong sodium-D line was revealed in each instance". Efforts were made to find and eliminate the source of the sodium but apparently it was not realized that it could be provided by the plate glass. In spite of their efforts, "all fuels including hydrogen, continued to emit the characteristic yellow light".

The experiments described in this Part show clearly that optimum performance in terms of power and economy is limited only by preignition arising from the temperature attained by the ceramic core of the spark plug or by the exhaust valve or from nuclei formed by pyrolysis of lubricating oil vapor. It was shown by indicator diagrams that detonation, defined as auto or self ignition, did not occur in the absence of nuclei of ignition.

On reducing the magnitude of the igniting effects mentioned it became possible to operate the engine at speeds rising to 1800 r.p.m., with the compression ratio fixed at 12:1. Values of 146 p.s.i. for I.M.E.P. and of 37% for I.T.E. were obtained when the maximum power mixture strength was used. The values obtained with a mixture 55% weak were 90 p.s.i. for I.M.E.P. and 47% for I.T.E. These values exceed those recorded in the literature of the subject, by a wide margin.

ACKNOWLEDGMENTS

The experiments described in this Part were carried out in the Department of Mechanical Engineering, University of Toronto, with the co-operation of

Professor E. A. Allcut, Head of the Department, the assistance of Mr. S. V. Hayes, Scientific Officer Defence Research Board, and that of Joseph Thurner, Technician. Acknowledgment is also made of the assistance with preliminary experiments given by Professor Bernard D. Wood, Department of Mechanical Engineering, University of Manitoba.

The Consumers Gas Company, Toronto, contributed to the experimental work by providing facilities under the direction of Mr. J. Alex Morrison for the calibration of hydrogen metering orifices; the Champion Spark Plug Company, by supplying spark plugs with thermocouples in the central electrodes; The Eaton Manufacturing Company, Detroit, by supplying a silchrome valve with the stem drilled for leads to a thermocouple in the head.

The Authors are indebted to the Chairman of the Defence Research Board for permission to publish this paper.

REFERENCES

1. Anzilotti, W. F., Rogers, J. D., Scott, G. W., and Tomsic, V. J. Ind. Eng. Chem. 46: 1314–1318. 1954.
2. Burstall, A. F. Proc. Inst. Automobile Engrs. 22: 358–392. 1927.
3. Downs, D., Walsh, A. D., and Wheeler, R. W. Trans. Roy. Soc. (London), A, 243: 463–524. 1951.
4. Egerton, A. and Moore, N. W. P. Nature, 163: 917. 1949.
5. Egerton, A., Smith, F. L., and Ubbelohde, A. R. Trans. Roy. Soc. (London) A, 234: 433–521. 1935.
6. Hundere, A. and Bert, J. A. S.A.E. Quart Trans. 546–562. Oct. 1948.
7. King, R. O. Can. J. Research, F, 26: 228–240. 1948.
8. King, R. O., Durand, E. J., and Morrison, J. A. Can. J. Research, F, 27: 435–449. 1949.
9. King, R. O., Durand, E. J., Wood, B. D., and Allan, A. B. Can. J. Research, F, 28: 134–155. 1950.
10. King, R. O., Sandler, S., and Strom, R. Can. J. Technol. 33: 388–407. 1955.
11. King, R. O., Wallace, W. A., and Durand, E. J. Nature, 163: 729. 1949.
12. King, R. O., Wallace, W. A., and Mahapatra, B. Can. J. Research, F, 26: 264–276. 1948.
13. Livengood, J. C. and Leary, W. A. Ind. Eng. Chem. 43: 2797–2805. 1951.
14. Lucke, C. E. Gas engine design. D. Van Nostrand Company, Inc., New York. 1905.
15. Pye, D. R. The internal combustion engine. 2nd ed. Oxford University Press, London. 1937.
16. Ricardo, H. R. Proc. Inst. Automobile Engrs. Vol. 18. 1923–1924.
17. Sanders, J. C., Wilstead, H. D., and Mulcahy, B. A. Natl. Advisory Comm. Aeronaut. Rept. No. 754. 1943.
18. Taylor, C. F., Taylor, E. S., Livengood, J. C., Russell, W. A., and Leary, W. A. S.A.E. Quart. Trans. Apr. 1950.
19. Tizard, H. T. North East Coast Inst. Engrs. & Shipbuilders, May 1921.

APPENDIX

Metering of Hydrogen Supply

Accurate measurement of rate of hydrogen supply to the engine is of prime importance in respect of determinations of thermal efficiency. The novel method used for the experiments was based on the use of two calibrated square edged orifices in thin plates. One was 0.1286 in. and the other 0.0784 in. diameter. The plates were 0.013 in. thick. The orifices were mounted midway in brass tubes 4 in. diameter and 4 ft. long provided with baffles and wire mesh screens for the elimination of pressure pulsations from the induction system of the engine. The double system of hydrogen supply to the engine through

small orifices of different diameters, which could be used singly or in parallel, was such that hydrogen could be supplied at rates required for the experiments while the velocity of flow through a metering orifice was never less than 750 ft. per sec. This feature in conjunction with the means taken to eliminate pressure fluctuations made possible the use of orifice calibrations determined in steady flow conditions.

The orifices, in position in the tube mountings, were calibrated in the Meter Testing Department of the Consumer's Gas Company, Toronto, under the direction of Mr. J. Alex Morrison, Supervisor of the Appliance Laboratory. A special gasometer which had been calibrated by the Ontario Department of Weights and Measures was used. A graph obtained accordingly for the relation between pressure difference and rate of hydrogen flow through the 0.1286 in. diameter orifice as plotted on a logarithmic scale is given by Fig. 13. The values given for rates of hydrogen flow are for a temperature of 60°F. and a pressure of 30 in. Hg.

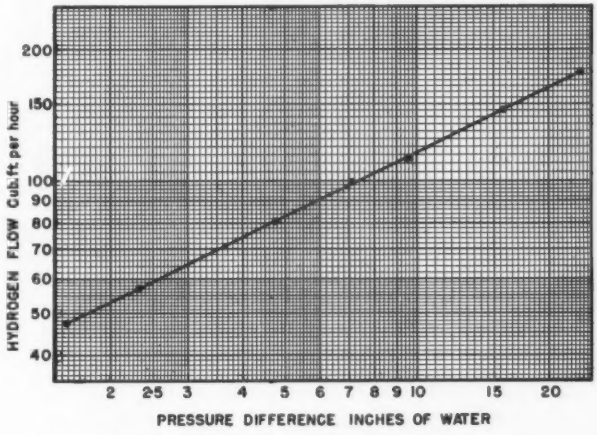

FIG. 13. Calibration graph for orifice 0.1286 in. diameter.

Accuracy of Measurement of Thermal Efficiency

The accuracy of measurement of I.H.P. by the motoring method, which is in general use, is not regarded as better than $\pm\frac{1}{2}$ of 1%. It is considered that the rate of hydrogen consumption was made with an accuracy of $\pm\frac{1}{4}$ of 1%. The values for I.T.E. given in this part are comparable with those obtained by Ricardo (16) and Burstall (2) when they used the motoring method of measuring I.H.P. Values for power and thermal efficiency are not given in more recent publications by others (1, 3).

The Spark Plugs

The spark plugs used for the experiments are illustrated by Fig. 14. Champion C.F.R.-8 is near the top of the commercial heat scale and was used as a

hot variety with a spark gap of 0.025 in. Spark plugs K.L.G. 100 and R2-S, rated at the bottom of a commercial heat scale, were used as cool varieties. The spark gaps of these plugs are not readily adjustable. They were used as supplied with gaps of 0.018 in. approximately. It would be expected according

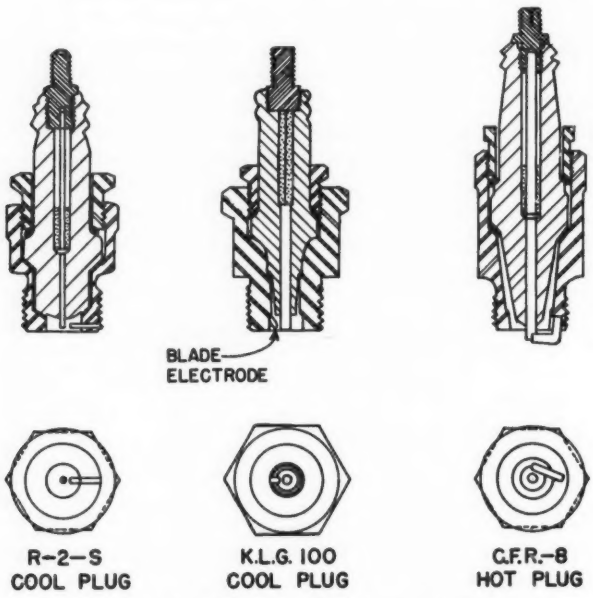

FIG. 14. Spark plugs used for the experiments.

to the designs that the K.L.G. plug would run hotter than the R2-S but it was shown by experiments, Section III, that neither attained the temperature required for the preignition of hydrogen–air mixtures in the conditions of the experiments of this Part.

Valve Timing

The low and high speed camshafts were designed to provide valve timings as tabulated below, according to the C.F.R. handbook. The given values were found to be correct within 1°.

	Low speed camshaft	High speed camshaft
Inlet valve opens	10° after t.d.c.	15° before t.d.c.
Inlet valve closes	34° after b.d.c.	50° after b.d.c.
Exhaust valve opens	40° before b.d.c.	50° before b.d.c.
Exhaust valve closes	15° after t.d.c.	15° after t.d.c.
Valve lift	0.238 in.	0.312 in.
Valve overlap	5°	30°

When the high speed camshaft was used, the exhaust valve with a lift of 0.312 in. was off its cooling seat for 155° of crank revolution. When the low

speed camshaft was used, the exhaust valve with a lift of 0.238 in. was off its cooling seat for 145° of crank revolution.

Exhaust Valves

The types of sodium cooled and uncooled silchrome exhaust valves used for the experiments described in this Part are illustrated by Fig. 15.

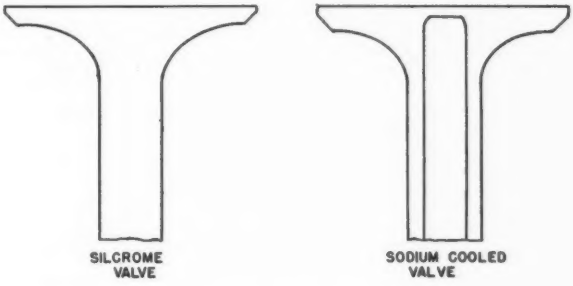

FIG. 15. Types of exhaust valves used for the experiments.

FLUID TURBULENCE AND SUSPENDED SEDIMENT[1]

By A. W. Marris[2]

ABSTRACT

A formula is derived for the concentration of fine sediment, "wash load", for a stream of infinite width flowing turbulently over a smooth bed. The theory is analogous to that currently employed in the problem of turbulent heat transfer. Sensibly exact formulae and then simple close approximations are derived for the total sediment load borne by the stream.

PRINCIPAL SYMBOLS

C_y = concentration at distance y above bed of stream.
C_z = concentration at non-dimensional depth z.
C_1 = concentration at bed.
C_m = mean concentration.
h = depth of stream.
y = reference distance above stream-bed.
u = flow velocity at position y.
u_m = mean flow velocity for stream.
τ = shear at position y.
τ_0 = shear at bed.
$u_\tau = \sqrt{(\tau_0/\rho)}$ = shear velocity.
ρ = mass density of water.
w = settling velocity of sediment in still water.
$M = u_{\max}/\sqrt{(\tau_0/\rho)}$ = constant in velocity distribution law.
N = von Karman's constant in turbulent velocity distribution law.
$\theta = Nw/u_\tau$ = exponent in concentration law.
ϵ_s = eddy diffusivity for sediment.
ϵ_M = eddy diffusivity for momentum.
$k = \epsilon_s/\epsilon_M$.
μ = viscosity of water.
$\nu = \mu/\rho$ = kinematic viscosity of water.
P = pressure at point y.
x = distance measured in direction of mean flow.
$z = 1-(y/h)$ = non-dimensional depth below surface.
z_m = value of z at which concentration is at its mean value.
$U = u/u_\tau$ = non-dimensional velocity.
$Q = u_\tau h/\nu$ = Reynolds number for shear velocity.
d = boundary of laminar layer and turbulent core assuming no intermediate "buffer layer".
$\delta = 1-(d/h)$.

[1]*Manuscript received April 7, 1955.*
Contribution from the Department of Civil Engineering, University of British Columbia, Vancouver, British Columbia.
[2]*Instructor in the Department of Civil Engineering.*

ϵ_V = eddy diffusivity for vorticity.
u_s = sediment velocity in direction of mean flow at P.
v_s = sediment velocity in direction of y.
j, j' = constants of slip of water over sediment.
a_s = molecular diffusivity of sediment.
Sc = ν/a_s = Schmidt number for molecular diffusion of sediment.
$S = k$ Sc.
α = non-dimensional boundary of laminar boundary layer.
β = non-dimensional boundary of "semiturbulent" buffer layer.
L = width of stream.
W_Q = total sediment load carried by stream.
$W_Q' = W_Q/L$ = sediment load per unit width of stream.

INTRODUCTION

For the theoretical prediction of the concentration depth distribution of suspended sediment in a turbulently flowing body of water it has been customary to employ the formula (1, 22)

$$[1] \qquad \frac{C_y}{C_d} = \left(\frac{h-y}{y} \times \frac{d}{h-d}\right)^{\theta} = H^{\theta}$$

which expresses the ratio of the concentrations and heights y and d above the bed of a river of depth h in terms of these heights. The exponent θ is equal to Nw/u_τ where $u_\tau = \sqrt{(\tau_0/\rho)}$, τ_0 being the shear at the stream-bed, ρ being the mass density of the water, N von Karman's constant occurring in the turbulent velocity law (11, 13)

$$[2] \qquad \frac{u-u_{\max}}{\sqrt{(\tau_0/\rho)}} = N \log_e \frac{y}{h},$$

and w the settling velocity of the sediment in still water.

The formula [1] is derived on the assumption that under steady conditions the upward transport of the sediment by the turbulence balances the settling due to gravity. One may write

$$[3] \qquad wC = -\epsilon_s \, dC/dy$$

where C is the concentration of that portion of the sediment with a settling velocity w, and ϵ_s is the eddy diffusivity for the sediment due to the turbulence. ϵ_s is directly analogous to the diffusion coefficient of Fick's law in which the quantity mass is transferred by microscopic molecular fluctuations, or again to the thermal diffusivity for gaseous heat transfer.

Integration of equation [2] yields the relation

$$[4] \qquad \log_e \frac{C}{C_d} = -w \int_d^y \frac{dy}{\epsilon_s}$$

in which C_d is the concentration at the datum level $y = d$.

The velocity of flow being a function of y, ϵ_s must also be.

On the statistical theory of Reynolds, Prandtl, von Karman (4, 5, 6, 12, 13, 15) the equation for horizontal turbulent flow in the x direction may be written

$$[5] \qquad \frac{1}{\rho}\frac{dP}{dz} = \frac{d}{dy}\left(\epsilon_M \frac{du}{dy}\right) + \nu \frac{d^2u}{dy^2} = \frac{d}{dy}\left[(\epsilon_M + \nu) \frac{du}{dy}\right]$$

where dP/dx is the mean pressure gradient and du/dy is the velocity gradient perpendicular to the mean flow direction. ν is the kinematic viscosity μ/ρ, μ being the viscosity, and ϵ_M is the eddy diffusivity for momentum. ϵ_M, which is a function of depth, is effectively an additional kinematic viscosity caused by the turbulence. Equation [5] is derived on the assumption that momentum is transferred by the velocity fluctuations to increase the pressure gradient. Implicit in equation [5] is the assumption that the turbulent pressure fluctuations play no part in the over-all transfer of momentum (18, 19).

Expressing the equations for the steady motion as

$$[6] \qquad \tau = \tau_0 \frac{h-y}{h} = \tau_0 z,$$

where τ is the shear stress at the point y, $z = 1-(y/h)$ is the depth below the free surface in non-dimensional form, and

$$[7] \qquad -\frac{dP}{dz} = \frac{\tau_0}{h} = \frac{\tau}{h-y} = \frac{\tau}{hz},$$

and defining a non-dimensional velocity

$$[8] \qquad U = u/u_\tau \text{ where } u_\tau = \sqrt{(\tau_0/\rho)}$$

and a Reynolds number for friction velocity

$$[9] \qquad Q = hu_\tau/\nu$$

one has, from equation [5],

$$\frac{\tau_0}{h\rho} = \frac{d}{dy}\left[(\epsilon_M + \nu) \frac{du}{dy}\right] = \frac{u_\tau}{h^2}\frac{d}{dz}\left[(\epsilon_M + \nu) \frac{dU}{dz}\right],$$

i.e.

$$Q = \frac{u_\tau h}{\nu} = \frac{d}{dz}\left[\left(\frac{\epsilon_M}{\nu}+1\right)\frac{dU}{dz}\right]$$

or

$$[10] \qquad \frac{\epsilon_M}{\nu} = -\frac{Qz+dU/dz}{dU/dz}.$$

If the velocity distribution law is given by

$$[11] \qquad U = U_{\max} + N \log_e(1-z)$$

equation [10] gives

$$[12] \qquad \epsilon_M/\nu = (Q/N)z(1-z)-1.$$

It is seen that the graph of ϵ_M/ν is a parabola and that ϵ_M/ν is negative throughout intervals of length $O(1/Q)$ at $z = 0$ and $z = 1$. The latter interval,

for the case of flow over a smooth bed, would be of the order of the width of the laminar flow boundary layer for which, of course, equation [4] does not hold.

Writing $\epsilon_M/\nu = (Q/N)z(1-z)$ and proposing equality between ϵ_M and ϵ_s one obtains from [3]

$$\log_e \frac{C}{C_\delta} = \frac{Nwh}{Q\nu} \int_\delta^z \frac{dz}{z(1-z)} = \frac{Nw}{u_\tau} \int_\delta^z \frac{dz}{z(1-z)}$$

where $\delta = 1-(d/h)$, which on integration yields

$$[1] \qquad \frac{C}{C_\delta} = \left(\frac{z}{1-z} \times \frac{1-\delta}{\delta}\right)^\theta = H^\theta.$$

Experiments (1, 22) have shown that [1] yields results of sensibly the correct form provided the exponent is 20%–50% less than the value Nw/u_τ, so that the concentration distribution is more uniform than anticipated theoretically. This is particularly the case for small values of θ corresponding to the very fine sediment. It would be expected that such would obey the law better, as the finer the sediment the more capable it should be of following the turbulence. It is also found that there is a tendency for the sediment content near the surface to exceed that indicated by the distribution law, a phenomenon attributed to random turbulence caused by the sides of the stream. Such random turbulence would increase ϵ_s.

It has been stated that a statistical theory of turbulence in which momentum is considered conserved and regarded as the property transferred by the eddies requires that the fluctuating pressures that certainly exist in the turbulent field do not influence the mean transport of momentum. This was first pointed out by Taylor (18, 19), who simultaneously proved that for this reason the momentum transfer theory cannot hold if, for example, the motion is wholly two dimensional. This was verified experimentally for the case of turbulent flow in the annulus between rotating coaxial cylinders. He further showed that the only configuration under which the conditions for the momentum transfer theory are met is for momentum in a given direction x, say, to be transferred in the plane perpendicular to x by turbulent motion in which the flow lines parallel to x are not interfered with but remain in that direction throughout the motion. Such seems to be the case for flow through a straight tube of circular section. The theory of heat transfer, for example, based on an analogy with a momentum transfer theory of turbulence has been reasonably well ratified by experiment for this particular case.

To overcome the difficulty for purely two-dimensional motion, Taylor (18, 19) suggested that if the whole motion is confined to a plane yz say, then as in the case of two-dimensional motion of an ideal fluid, vorticity in the x direction is conserved, and could be taken as the property transferred by the turbulence to cause the pressure gradient. The theory was subsequently generalized to three dimensions, and a modified vorticity transfer theory set up, one of the main assumptions of which was that each of the components of vorticity was conserved and transferable in the sense of say mass in a kinetic theory of molecular diffusion (20, 21).

This modified vorticity transfer theory yields a turbulent velocity distribution for pipe flow in as good agreement with experiment as the logarithmic decrement law derived from the momentum theory. The theory gives good results for wakes (where the turbulence may be approximately two dimensional in the form of a von Karman vortex street) but it breaks down in the neighborhood of solid boundaries.

The vorticity vector being the curl of the velocity vector, the eddy diffusivity for vorticity involves the second differential of the velocity. It may be shown that on this theory the equation analogous to [5] is

$$\frac{1}{\rho}\frac{dP}{dz} = \epsilon_V \frac{d^2u}{dy^2} + \nu \frac{d^2u}{dy^2} = (\epsilon_V + \nu)\frac{d^2u}{dy^2} \tag{13}$$

which yields, as before, by equations [6], [7], [8], [9]

$$\frac{\epsilon_V}{\nu} = -\frac{Q}{d^2U/dz^2} - 1 \tag{14}$$

$$= (Q/N)(1-z)^2 - 1 \tag{15}$$

for the velocity distribution law [11].

It is seen that ϵ_V/ν is negative throughout an interval adjacent to the boundary defined by $1-(N/Q)^{\frac{1}{2}} < z < 1$, an interval of width $O(1/Q^{\frac{1}{2}})$ and so of higher order than either the corresponding interval on the momentum transfer theory or the laminar boundary layer, the latter for a smooth boundary being of thickness $O(1/Q)$.

It is seen that $\epsilon_V = (Q/N) - 1$ at the free surface $z = 0$ instead of zero as is ϵ_M.

The assumption of equality between ϵ_s and ϵ_V and the insertion of [15] in [3] now yields

$$\log_e \frac{C}{C_\delta} = \frac{Nw}{u_\tau} \int_\delta^z \frac{dz}{(1-z)^2}$$

so that

$$\frac{C}{C_\delta} = A_\delta \exp \frac{\theta}{1-z} \qquad \text{where } A_\delta = \exp\left(-\frac{\theta}{1-\delta}\right). \tag{16}$$

Here it is assumed that $\delta \gg O(1/Q^{\frac{1}{2}})$. Writing $(Q/N)(1-z)^2 - 1 = (Q/N)(1-z)^2$ is an approximation equivalent to neglecting ν in comparison with ϵ_V.

Whereas equation [16] certainly yields the experimentally observed finite concentration at the surface $z = 0$ (taking $\delta = 0.5, \theta = 0.5, C_0/C_{\frac{1}{2}} = \exp(-\frac{1}{2})$), the formula gives an infinite concentration near the wall and wholly too steep a concentration gradient.

It appears then that the observed sediment distribution cannot reasonably be predicted on the basis of the vorticity transfer theory and one returns to the momentum transfer analogy.

The author attempts to produce a more accurate result than equation [1] by considering, instead of a general vertical equilibrium, the transport of sediment through an infinitesimal fluid element and integrating the "equation

of continuity" thus obtained. The work is roughly analogous to that of Boelter (2), Martinelli (10), Lion (7), Reichardt (14), and the author (8, 9) for the problem of turbulent heat transfer. The theory is applicable to the case of rectilinear flow over a smooth bed; it assumes that the river is sufficiently wide for the effect of the banks to be ignored. It also assumes that the sediment is sufficiently minute to exhibit no gravitational acceleration and to form a denser continuum within the continuum of the water. As in the case of radial heat transfer from a pipe wall to a fluid flowing turbulently through the pipe it is necessary to assume a linear longitudinal concentration gradient at the bed whereas in fact the concentration will be constant along the bed. In this work an uncorrected result is obtained under the assumption of the linear gradient and this is then used to obtain the appropriate correction. The method employed is that described by Seban and Shimazaki (16) for the heat transfer problem.

DERIVATION OF UNCORRECTED FORMULA ON BASIS OF ANALOGY BETWEEN TURBULENT MOMENTUM TRANSFER AND SEDIMENT TRANSFER

Consider a body of water flowing in steady turbulent motion in the horizontal direction x as shown in Fig. 1. The equation of motion of the water is given by equation [5]

$$[5] \qquad \frac{1}{\rho}\frac{dP}{dx} = \frac{d}{dy}\left[(\epsilon_M+\nu)\frac{du}{dy}\right].$$

Here u is the horizontal velocity at height y above the bed.

As has been seen, equation [5] serves as a definition for ϵ_M in terms of the transverse velocity gradient

$$[10] \qquad \frac{\epsilon_M}{\nu} = -\frac{Qz+dU/dz}{dU/dz}$$

where $U = u/\sqrt{(\tau_0/\rho)} = u/u_\tau$ and $z = 1-(y/h)$.

Consider now the sediment passing through a rectangular prism of section $ABCD$ as shown in Fig. 1. If u_s and v_s are the sediment velocities the equation

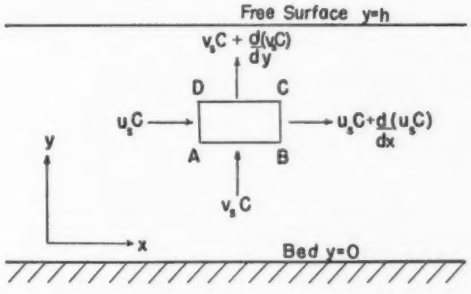

FIG. 1.

expressing no accumulation of sediment within the element is

$$\frac{d(u_s C)}{dx}+\frac{d(v_s C)}{dy} = 0 \qquad [17]$$

where

$$v_s C = (\epsilon_s+a_s)\, dC/dy. \qquad [18]$$

Here ϵ_s is the eddy diffusivity for the sediment, and a_s is the molecular diffusivity, independent of depth.

By [17] and [18]

$$\frac{d(u_s C)}{dx} = -\frac{d}{dy}\left[(\epsilon_s+a_s)\frac{dC}{dy}\right], \qquad [19]$$

and the similarity between equations [5] and [19] is at once apparent.

Before proceeding further a relation must be assumed between the longitudinal velocity u_s of the sediment and the velocity of the stream u. It will be assumed that there is a slip velocity between the sediment and the stream proportional to the stream velocity.

Writing $u-u_s = j'u$, one has on this assumption $u_s = ju$ where $j = 1-j'$. The motion being rectilinear and steady, $du/dx = 0$ and equation [19] becomes

$$ju\frac{dC}{dx} = -\frac{d}{dy}\left[(\epsilon_s+a_s)\frac{dC}{dy}\right]. \qquad [20]$$

In terms of the non-dimensional velocity and distance $U = u/u_\tau = u/\sqrt{(\tau_0/\rho)}$, $z = 1-(y/h)$, equation [19] may be written

$$jQhU\frac{dC}{dx} = -\frac{d}{dz}\left[\frac{\epsilon_s+a_s}{\nu}\frac{dC}{dz}\right] \qquad [21]$$

where $Q = hu_\tau/\nu$.

It is necessary to assume now that dC/dx is independent of z; i.e. that the longitudinal concentration gradient is the same for all strata parallel to the bed. This will not be the case in practice when the water flows over a bed of constant concentration. In this case dC/dx is zero for $x = 1$. However it is believed that the error introduced will only influence a small region adjacent to the bed. The magnitude of the correction for this will be investigated in the next section.

Under this assumption equation [21] can be written

$$\frac{dC}{dz} = -jQh\frac{dC}{dx}\frac{\nu}{\epsilon_s+a_s}\int_0^z U\, dz, \qquad [22]$$

as $dC/dz = 0$ when $z = 0$.

The quantity dC/dz is now eliminated from equation [22] in favor of the quantity $(v_s C)_1$, the value of $(v_s C)$ at the bed, by means of equation [17].

Since adjacent to the bed there exists a boundary region of laminar flow, $(v_s C)_1$ may be taken as $-wC_1$ where w is the fall velocity of the sediment in still water.

By equation [17]

$$j\frac{d(uC)}{dx}-\frac{1}{h}\frac{d}{dz}(v_sC)=0$$

or
$$(v_sC)_1 = hj\int_0^1\frac{d(uC)}{dx}dz = hj\int_0^1 u\frac{dC}{dx}dz$$

[23]
$$= hj\frac{dC}{dx}\int_0^1 udz,$$

the surface value of (v_sC) being zero.

Again if the mean flow velocity u_m is defined by

$$u_m = \int_0^1 udz \Big/ \int_0^1 dz,$$

one has
$$(v_sC)_1 = -wC_1 = hju_m\,dC/dx$$

or

[24]
$$dC/dx = -wC_1/hju_m$$

and substituting in equation [22] one obtains

[25]
$$\frac{dC}{dz} = \frac{wC_1Q}{u_m}\left(\frac{\nu}{\epsilon_s+a_s}\right)\int_0^z Udz,$$

from which it is seen that slip in the assumed form has no effect on the concentration gradient. Assuming a relationship $\epsilon_s = k\epsilon_M$ between the eddy diffusivities it is now possible to express dC/dz in terms of the fluid velocity and velocity gradient.

One has

$$\frac{\nu}{\epsilon_s+a_s} = \left(\frac{\epsilon_s}{\nu}+\frac{1}{\mathrm{Sc}}\right)^{-1} = \left(\frac{k\epsilon_M}{\nu}+\frac{1}{\mathrm{Sc}}\right)^{-1}$$
$$= \left(-\frac{k(Qz+dU/dz)}{dU/dz}+\frac{1}{\mathrm{Sc}}\right)^{-1}$$
$$= \mathrm{Sc}\left((1-S)-\frac{SQz}{dU/dz}\right)^{-1}$$

where $\mathrm{Sc} = \nu/a_s$, the Schmidt number for the molecular diffusion of the sediment, and $S = k\mathrm{Sc}$.

For the case to be considered, $S \gg 1/Q$ and we may write without introducing error (8)

[26]
$$\frac{\nu}{\epsilon_s+a_s} = -\mathrm{Sc}\left(\frac{SQz}{dU/dz}\right)^{-1} = -\frac{1}{kQz}\left(\frac{dU}{dz}\right).$$

Equation [22] now becomes

[27]
$$\frac{dC}{dz} = -\frac{wC_1}{ku_m}\left(\frac{1}{z}\frac{dU}{dz}\right)\int_0^z Udz,$$

so that

[28]
$$C_1-C_z = -\frac{wC_1}{ku_m}\int_z^1\frac{1}{z_2}\frac{dU}{dz_2}\int_0^{z_2} Udz_1\,dz_2,$$

the suffixes being inserted to indicate the order of integration. Equation [25] can be integrated once the appropriate velocity function is inserted in it.

For a fully developed turbulent region the velocity law

$$[2] \qquad \frac{u}{u_\tau} = \frac{u_{\max}}{u_\tau} + N \log_e \frac{y}{h}$$

holds, i.e.

$$[11] \qquad U = U_{\max} + N \log_e (1-z).$$

The constant N has the value 2.5 for sediment-free water, but because of the effect of sediment in damping the turbulence, N increases with sediment concentration up to about 3. $U_{\max}$ depends on the Reynolds number for friction velocity according to

$$U_{\max} = M + N \log_e Q$$

where for a smooth boundary $M = 5.5$.

Thus the law may be written

$$[11a] \qquad U = M + N \log_e Q(1-z).$$

From equation [11a] it is seen that

$$U_{\max} - U_{\text{mean}} = -N \int_0^{1-(\beta/Q)} \log_e (1-z)\, dz \Big/ \int_0^{1-(\beta/Q)} dz,$$

assuming that the region of fully developed turbulence extends from $z = 0$ to $z = 1-(\beta/Q)$, i.e. to within $O(1/Q)$ of the boundary. One thus has

$$[29] \qquad U_{\text{mean}} = (M-N) + N \log_e Q,$$

$$[30] \qquad U_{\max} - U_{\text{mean}} = N.$$

The corresponding formula for flow through a tube of circular section is $U_{\max} - U_{\text{mean}} = 3N/2$.

Following von Karman the non-dimensional velocity will be taken as $U = M + N \log_e Q(1-z)$ for the fully developed turbulent region defined by the interval $0 < z < 1-(\beta/Q)$; as $U = K + J \log_e Q(1-z)$ for the buffer region defined by $1-(\beta/Q) < z < 1-(\alpha/Q)$; and as $U = Q(1-z)$, the "straight" portion of the Poiseauille parabolic law, for the laminar adjacent-to-the-wall region defined by $1-(\alpha/Q) < z < 1$. See Fig. 2. Between the several constants α, β, K, J, M hold the boundary relations

$$[31] \quad J = \alpha, \qquad K = \alpha(1-\log_e \alpha), \qquad M + N \log_e \beta = \alpha\,[1-\log_e(\alpha/\beta)] = \gamma$$

expressing continuity of U and dU/dz at $z = 1-(\alpha/Q)$, the boundary between laminar and buffer layers, and continuity of U only at $z = 1-(\beta/Q)$. The relations [31] used in connection with the experimental results of Nikuradse (11) and Stanton and Pannell (17) yield the numerical values $\alpha = J = 5$, $\beta = 30$, $K = 3.05$, $M = 5.5$, $N = 2.5$, $\gamma = 14$, for the case of a smooth boundary.

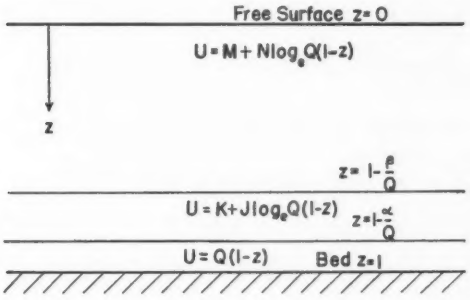

FIG. 2.

Since the molecular diffusivity a_z has been neglected, there is no means by which the sediment can be transported across the laminar boundary layer. It will be considered that the sediment at the bed has extended at least to the lower boundary of the buffer layer and as far as the integration is concerned the value $z = 1-(\alpha/Q)$ will be taken as the upper limit of z.

It follows from equation [28] that for $0 < z < 1-(\beta/Q)$, i.e. for points in the region of fully developed turbulence,

$$[32]\quad C_1-C_z = \frac{wC_1}{ku_m}\Bigg\{N\int_z^{1-(\beta/Q)}\frac{1}{z_2(1-z_2)}\int_0^{z_2}[M+N\log_e Q(1-z_1)]\,dz_1dz_2$$
$$+J\int_{1-(\beta/Q)}^{1-(\alpha/Q)}\frac{1}{z_2(1-z_2)}\Bigg[\int_0^{1-(\beta/Q)}[M+N\log_e Q(1-z_1)]\,dz_1$$
$$+\int_{1-(\beta/Q)}^{z_2}[K+J\log_e Q(1-z_1)]\,dz_1\Bigg]dz_2\Bigg\}.$$

Considering these integrals in turn,

$$\int_z^{1-(\beta/Q)}\frac{1}{z_2(1-z_2)}\int_0^{z_2}[M+N\log_e Q(1-z_1)]\,dz_1dz_2$$
$$=\int_z^{1-(\beta/Q)}\frac{1}{z_2(1-z_2)}[(M-N+N\log_e Q)z_2-N(1-z_2)\log_e(1-z_2)]\,dz_2$$
$$=\int_z^{1-(\beta/Q)}\left[(M-N+N\log_e Q)\frac{1}{1-z_2}-\frac{N\log_e(1-z_2)}{z_2}\right]dz_2$$
$$=\left[(M-N+N\log_e Q)\left(\log_e(1-z)-\log_e\frac{\beta}{Q}\right)\right.$$
$$\left.+N\left(\sum_1^\infty\frac{[1-(\beta/Q)]^n}{n^2}-\sum_1^\infty\frac{z^n}{n^2}\right)\right]$$
$$[33]\quad=\left[(M-N+N\log_e Q)\left(\log_e(1-z)-\log_e\frac{\beta}{Q}\right)+N\left(\frac{\pi^2}{6}-\sum_1^\infty\frac{z^n}{n^2}\right)\right]$$
$$+O\left(\frac{1}{Q}\right).$$

It follows similarly that

$$[34]\quad \int_{1-(\beta/Q)}^{1-(\alpha/Q)} \frac{1}{z_2(1-z_2)} \int_0^{1-(\beta/Q)} [M+N\log_e Q(1-z_1)]\,dz_1dz_2 = (M-N+N\log_e Q)\log_e\frac{\beta}{\alpha}+O\left(\frac{1}{Q}\right),$$

and that

$$[35]\quad \int_{1-(\beta/Q)}^{1-(\alpha/Q)} \frac{1}{z_2(1-z_2)} \int_{1-(\beta/Q)}^{z_2} [K+J\log_e Q(1-z_1)]\,dz_1dz_2 = O\left(\frac{1}{Q}\right).$$

Substituting the results [33], [34], [35] in equation [32], we have

$$[36]\quad C_1-C_z = \frac{wC_1}{ku_m}\Bigg[(M-N+N\log_eQ)\left(N\log_e(1-z)+N\log_e\frac{Q}{\beta}+\alpha\log_e\frac{\beta}{\alpha}\right) +N^2\left(\frac{\pi^2}{6}-\sum_1^\infty\frac{z^n}{n^2}\right)\Bigg]+O\left(\frac{1}{Q}\right).$$

By [31] $$-N\log_e\beta+\alpha\log_e\frac{\alpha}{\beta} = M-J = M-\alpha$$

so that

$$[37]\quad C_1-C_z = \frac{wC_1}{ku_m}\Bigg[(M-N+N\log_eQ)(N\log_e(1-z)+N\log_eQ+M-\alpha) +N^2\left(\frac{\pi^2}{6}-\sum_1^\infty\frac{z^n}{n^2}\right)\Bigg],$$

i.e.

$$[38]\quad 1-\frac{C_z}{C_1} = \frac{w}{ku_m}\Bigg[N^2(\log_eQ)^2+N(2M-\alpha-N)\log_eQ+(M-\alpha)(M-N)+N^2\frac{\pi^2}{6} -N((M-N)+N\log_eQ)\log_e\frac{1}{1-z}-N^2\sum_1^\infty\frac{z^n}{n^2}\Bigg].$$

Assuming that $C_0 = 0$, i.e. zero concentration at the surface of the water, equation [38] gives

$$[39]\quad \frac{w}{ku_m} = [N^2(\log_eQ)^2+N(2M-\alpha-N)\log_eQ+(M-\alpha)(M-N)+\tfrac{1}{6}N^2\pi^2]^{-1}$$

so that

$$[40]\quad \frac{C_z}{C_1} = \frac{N[(M-N)+N\log_eQ]\log_e\frac{1}{1-z}+N^2\sum_1^\infty\frac{z^n}{n^2}}{N^2(\log_eQ)^2+N(2M-\alpha-N)\log_eQ+(M-\alpha)(M-N)+\frac{1}{6}N^2\pi^2}.$$

Again since

$$\frac{C_m}{C_1} = \int_0^{1-(\alpha/Q)}\frac{C_z}{C_1}\,dz \Big/ \int_0^{1-(\alpha/Q)} dz = \int_0^{1-(\alpha/Q)}\frac{C_z}{C_1}\,dz+O\left(\frac{1}{Q}\right),$$

it follows from [40] that

$$[41]\quad \frac{C_m}{C_1} = \frac{N^2\log_eQ+N(M-2N)+\frac{1}{6}N^2\pi^2}{N^2(\log_eQ)^2+N(2M-\alpha-N)\log_eQ+(M-\alpha)(M-N)+\frac{1}{6}N^2\pi^2}$$

in which are used the integrals

$$\int \log_e(1-z)\,dz = -(1-z)\log_e(1-z)+C,$$

$$\int \sum_1^\infty \frac{z^n}{n^2}\,dz = z\sum_1^\infty \frac{z^n}{n^2} - (1-z)\log_e(1-z)-z+C.$$

Inserting the numerical values $\alpha = 5$, $N = 2.5$, $M = 5.5$ appropriate to turbulent flow along a smooth bed one obtains

$$[40a] \qquad \frac{C_z}{C_1} = \frac{[17.3+33.1\log_{10}Q]\log_{10}\frac{1}{1-z}+6.25\sum_1^\infty \frac{z^n}{n^2}}{33.1(\log_{10}Q)^2+20.0\log_{10}Q+11.8},$$

$$[41a] \qquad \frac{C_m}{C_1} = \frac{14.4\log_{10}Q+11.5}{33.1(\log_{10}Q)^2+20.0(\log_{10}Q)+11.8}.$$

It has been shown by Vanoni (22) and others that sediment in the water has the effect of damping out the turbulence, that is of increasing N.

With $N = 3$ instead of 2.5 equations [40] and [41] yield

$$[40b] \qquad \frac{C_z}{C_1} = \frac{[17.3+47.7\log_{10}Q]\log_{10}\frac{1}{1-z}+9\sum_1^\infty \frac{z^n}{n^2}}{47.7(\log_{10}Q)^2+20.7(\log_{10}Q)+16.3},$$

$$[41b] \qquad \frac{C_m}{C_1} = \frac{20.7\log_{10}Q+13.3}{47.7(\log_{10}Q)^2+20.7(\log_{10}Q)+16.3}.$$

Writing

$$[42] \qquad \Phi(z) = \sum_1^\infty \frac{z^n}{n^2} = -\int_0^z \frac{\log_e(1-z)}{z}\,dz,$$

it may be shown (3) that

$$[43] \qquad \begin{aligned} \Phi(1) &= \frac{\pi^2}{6}, \\ \Phi\left(2\sin\frac{\pi}{10}\right) &= \frac{\pi^2}{10}-\left[\log_e\left(2\sin\frac{\pi}{10}\right)\right]^2, \\ \Phi\left[\left(2\sin\frac{\pi}{10}\right)^2\right] &= \frac{\pi^2}{15}-\left[\log_e\left(2\sin\frac{\pi}{10}\right)\right]^2, \\ \Phi(\tfrac{1}{2}) &= \frac{\pi^2}{12}-\tfrac{1}{2}[\log_e 2]^2, \end{aligned}$$

and Tables I and II are computed for these values from equations [40] and [41]. Table IV gives values of $\log[z/(1-z)]$ and $\log(C_z/C_\delta)$ appropriate for the formula

$$\frac{C_z}{C_\delta} = \left(\frac{z}{1-z}\times\frac{1-\delta}{\delta}\right)^\theta$$

for the case $\delta = \frac{1}{2}$. It is seen that the distribution ratio C_z/C_δ and therefore θ is pretty well independent of Q and that the quantities are not appreciably

affected by variations in N caused by the damping of the turbulence by the sediment load.

The graph in Fig. 3 shows, however, that $\log(C_z/C_{\frac{1}{2}})$ is not proportional to $\log[z/(1-z)]$ as is required by the distribution law [1] but that θ decreases with z as shown in Fig. 4 for the case $Q = 10^5$. This is in agreement with the findings of Vanoni that the experimental value of the exponent for fine sediment was from 20% to 40% less than predicted by the simple power law [1].

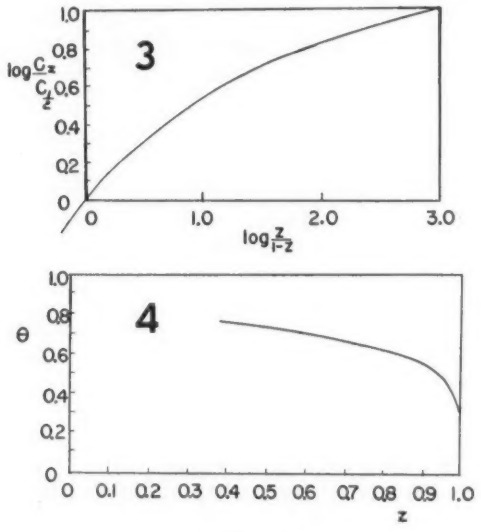

FIGS. 3 and 4.

It is also in general agreement with the results of Anderson (1) who found that the exponent would have to be decreased 50%–60% in order to fit the results. Sediment distribution in practice being so subject to extraneous disturbances, the results are naturally scattered so that it is extremely difficult to extract from them any conclusive information concerning the depth variation of the exponent θ. What can be said, however, is that the distributions are generally more uniform than predicted by [1], and that this could well correspond to an "annulment" caused by θ decreasing with depth below surface (increasing z). The highest values of θ occur just below the surface and Vanoni (22) repeatedly finds that the concentration is unduly high in this region.

From equations [41*a*], [41*b*] it is seen that as Q becomes large

$$[41c] \qquad \frac{C_m}{C_1} = \frac{1}{\log_e Q} = \frac{1}{2.3026 \log_{10} Q}.$$

This approximation gives results about 3% low throughout the range $Q = 10^3$ to $Q = 2\times10^5$. See Table III.

TABLE I

CASE $N = 2.5$

z	C_z/C_1							
	$Q=10^3$	$Q=5\times10^3$	$Q=10^4$	$Q=2\times10^4$	$Q=5\times10^4$	$Q=7.5\times10^4$	$Q=10^5$	$Q=2\times10^5$
0	0	0	0	0	0	0	0	0
0.382	0.073	0.060	0.055	0.051	0.047	0.045	0.043(5)	0.041
0.50	0.105	0.086	0.079	0.073	0.067	0.064	0.062(5)	0.059
0.618	0.145	0.119	0.109(5)	0.101	0.092	0.089	0.086(5)	0.081(5)
0.90	0.335	0.276	0.253	0.236	0.215	0.208	0.202	0.191
0.95	0.433	0.356	0.327	0.303	0.278	0.269	0.262	0.249
0.99	0.657	0.544	0.497	0.463	0.424	0.409	0.400	0.377
0.999	0.975	0.808	0.741	0.690	0.631	0.609	0.595	0.562
1.00	1.0	1.0	1.0	1.0	1.0	1.0	1.0	1.0
	C_m/C_1							
	$Q=10^3$	$Q=5\times10^3$	$Q=10^4$	$Q=2\times10^4$	$Q=5\times10^4$	$Q=7.5\times10^4$	$Q=10^5$	$Q=2\times10^5$
	0.148	0.120	0.110	0.103	0.095	0.091	0.089	0.084

TABLE II

CASE $N = 3$

z	C_z/C_1			
	$Q = 10^3$	$Q = 10^4$	$Q = 10^5$	$Q = 2\times10^5$
0	0	0	0	0
0.382	0.074	0.055	0.043(5)	0.041
0.50	0.106	0.079	0.062(5)	0.059
0.618	0.146	0.109	0.086(5)	0.082
0.90	0.336	0.254	0.202	0.191
0.95	0.434	0.327	0.262	0.249
0.99	0.658	0.497	0.400	0.378
0.999	0.976	0.740	0.595	0.562
1.000	1.0	1.0	1.0	1.0
	C_m/C_1			
	$Q = 10^3$	$Q = 10^4$	$Q = 10^5$	$Q = 2\times10^5$
	0.149	0.110	0.089	0.084

TABLE III

COMPARISON OF EXACT VALUES OF C_m/C_1 FOR $N=2.5$ WITH VALUES OF $1/\log_e Q$

Q	10^3	5×10^3	10^4	5×10^4	10^5	2×10^5
$\frac{C_m}{C_1}$	0.148	0.120	0.110	0.095	0.089	0.084
$\frac{1}{\log_e Q}$	0.145	0.118	0.108	0.092	0.087	0.082

TABLE IV

z	$\log \frac{z}{1-z}$	$\log \frac{C_z}{C_a}$			
		$Q = 10^3$	$Q = 10^4$	$Q = 10^5$	$Q = 2\times10^5$
Case $N = 2.5$					
0.382	−0.209	−0.158	−0.157	−0.157	−0.158
0.500	0	0	0	0	0
0.618	+0.209	0.140	0.142	0.141	0.140
0.900	+0.954	0.504	0.506	0.510	0.510
0.950	1.279	0.615	0.617	0.622	0.625
0.990	1.996	0.796	0.799	0.806	0.805
0.999	3.000	0.968	0.972	0.979	0.979
Case $N = 3$					
0.382	−0.209	−0.155	−0.157	−0.157	−0.158
0.500	0	0	0	0	0
0.618	+0.209	0.140	0.142	0.141	0.140
0.900	+0.954	0.501	0.507	0.510	0.510
0.950	1.279	0.613	0.617	0.622	0.625
0.990	1.996	0.794	0.799	0.806	0.807
0.999	3.000	—	0.971	0.979	0.979

CORRECTION FOR UNIFORM LONGITUDINAL SEDIMENT DISTRIBUTION AT BED

For a linear longitudinal concentration gradient at the boundary, by equations [38] and [41],

$$[44] \qquad \frac{C_1-C_z}{C_1-C_m} = R_1 - R_2 \log_e \frac{1}{1-z} - R_3 \sum_1^\infty \frac{z^n}{n^2}.$$

This result will now be approximately corrected so as to apply to the case of constant longitudinal concentration at the boundary. The method is that suggested by Seban and Shimazaki (16) for the heat transfer problem but used by these authors to obtain results appropriate for a computer rather than to obtain an explicit equation.

It will be assumed that the concentration $(C_1-C_z)/(C_1-C_m)$ is invariable in the direction of flow, that is, a function of z only, so that

$$[45] \qquad \frac{d}{dx}\frac{C_1-C_z}{C_1-C_m} = \frac{1}{C_1-C_m}\left(\frac{dC_1}{dx}-\frac{dC_z}{dx}\right) - \frac{C_1-C_z}{(C_1-C_m)^2}\left(\frac{dC_1}{dx}-\frac{dC_m}{dx}\right) = 0.$$

If the wall concentration is constant so that $dC_1/dx = 0$, equation [45] gives

$$[46] \qquad \frac{dC_z}{dx} = \frac{C_1-C_z}{C_1-C_m}\frac{dC_m}{dx},$$

so that in place of [22] one has

$$[47] \qquad \frac{dC}{dz} = -kQh\frac{\nu}{\epsilon_s+a_s}\int_0^z \frac{C_1-C_z}{C_1-C_m}\frac{dC_m}{dx}\,U dz,$$

[48] $$= -kQh\frac{\nu}{\epsilon_s+a_s}\frac{dC_m}{dx}\int_0^z U\frac{C_1-C_z}{C_1-C_m}\,dz,$$

and in place of [23]

$$(v_sC)_1 = -wC_1 = hk\int_0^1 u\frac{dC}{dx}\,dz$$

[49] $$= hk\frac{dC_m}{dx}\int_0^1 u\frac{C_1-C_z}{C_1-C_m}\,dz.$$

Now $(C_1-C_z)/(C_1-C_m)$ is near unity for $z < 0.9$ say, i.e. through a large proportion of the range of integration, so that $[u(C_1-C_z)/(C_1-C_m)]_{\text{mean}}$ may be taken as $u_m[(C_1-C_z)/(C_1-C_m)]_{\text{mean}}$ or u_m,

i.e. $$u_m = \int_0^1 u\frac{C_1-C_z}{C_1-C_m}\,dz \Big/ \int_0^1 dz = \int_0^1 u\frac{C_1-C_z}{C_1-C_m}\,dz,$$

so that in place of equation [24]

[50] $$dC_m/dx = -wC_1/hku_m.$$

By equations [48] and [50] as before,

[51] $$C_1-C_z = -\frac{wC_1}{ku_m}\int_z^1\frac{1}{z_2}\frac{dU}{dz_2}\int_0^{z_2} U\frac{C_1-C_z}{C_1-C_m}\,dz$$

so that finally, substituting from equation [44] and approximating as before,

[52] $$C_1-C_z = \frac{wC_1}{ku_m}\Bigg\{N\int_z^{1-(\beta/Q)}\frac{1}{z_2(1-z_2)}\int_0^{z_2}[M+N\log_e Q(1-z)] \times\left[R_1-R_2\log_e\frac{1}{1-z}-R_3\sum_1^\infty\frac{z^n}{n^2}\right]dz_1dz_2$$
$$+J\int_{1-(\beta/Q)}^{1-(\alpha/Q)}\frac{1}{z_2(1-z_2)}\int_0^{z_2}[M+N\log_e Q(1-z)] \times\left[R_1-R_2\log_e\frac{1}{1-z}-R_3\sum_1^\infty\frac{z^n}{n^2}\right]dz_1dz_2\Bigg\}.$$

Whereas the integral

$$\int\log_e(1-z)\sum_1^\infty\frac{z^n}{n^2}\,dz$$

can be evaluated in terms of logs and the series $\sum_1^\infty\frac{z^n}{n^2}$, $\sum_1^\infty\frac{z^n}{n^3}$, the result is very cumbersome; accordingly an approximation will be made using instead of $\sum_1^\infty\frac{z^n}{n^2}$, the value of this series at $z = \frac{1}{2}$.

Since $$\Theta(z) = \sum_1^\infty\frac{z^n}{n^2}+\sum_1^\infty\frac{(1-z)^n}{n^2}+\log_e z\log_e(1-z) = \Theta(1) = \frac{\pi^2}{6},$$

$$\sum_1^\infty\frac{(\frac{1}{2})^n}{n^2} = \frac{\pi^2}{12}-\tfrac{1}{2}(\log_e 2)^2,$$

so that writing $$R_1 - R_3 \sum_1^\infty \frac{(\frac{1}{2})^2}{n^2} = R_1'$$

one has

$$\int_z^{1-(\beta/Q)} \frac{1}{z_2(1-z_2)} \int_0^{z_2} (M+N\log_e Q(1-z_1))\left(R_1 - R_2 \log_e \frac{1}{1-z} - R_3 \sum_1^\infty \frac{z_1^n}{n^2}\right) dz_1$$

$$= \int_z^{1-(\beta/Q)} \frac{1}{z_2(1-z_2)} \int_0^{z_2} (M+N\log_e Q(1-z_1))\left(R_1' - R_2 \log_e \frac{1}{1-z_1}\right) dz_1$$

[53] $$= S_1\left[\log_e(1-z) - \log_e \frac{\beta}{Q}\right] - S_2\left[\sum_1^\infty \frac{z^n}{n^2} - \frac{\pi^2}{6}\right]$$

$$+ S_3\left[[\log_e(1-z)]^2 \log_e z + 2\log_e(1-z) \sum_1^\infty \frac{(1-z)^n}{n^2} - 2\sum_1^\infty \frac{(1-z)^n}{n^3}\right] + O\left(\frac{1}{Q}\right)$$

where

[54] $$\begin{cases} S_1 = (M-N+N\log_e Q)R_1' - (M-2N+N\log_e Q)R_2, \\ S_2 = NR_1' + (M-2N+N\log_e Q)R_2, \\ S_3 = NR_2. \end{cases}$$

Putting $\beta = \alpha$ and $z = 1-(\beta/Q)$, the second integral in equation [52] becomes simply

[55] $$\alpha \log_e \frac{\beta}{\alpha} + O\left(\frac{1}{Q}\right)$$

so that by [50]

[56] $$C_1 - C_z = \frac{wC_1}{ku_m}\left\{S_1[N\log_e Q + M - \alpha] + NS_2\frac{\pi^2}{6} - NS_1\log_e\frac{1}{1-z} - NS_2\sum_1^\infty \frac{z^n}{n^2}\right.$$

$$\left. + NS_3\left[[\log_e(1-z)]^2\log_e z + 2\log_e(1-z)\sum_1^\infty \frac{(1-z)^n}{n^2} - 2\sum_1^\infty \frac{(1-z)^n}{n^3}\right]\right\}$$

in which is used the boundary relation

$$-N\log_e \beta + \alpha \log_e \frac{\beta}{\alpha} = M - \alpha.$$

By equation [36]

[57] $$R_1 = \frac{wC_1}{ku_m}\frac{1}{C_1 - C_m}[(M-N+N\log_e Q)(N\log_e Q + M - \alpha) + \tfrac{1}{6}N^2\pi^2],$$

[58] $$R_2 = \frac{wC_1}{ku_m}\frac{N}{C_1 - C_m}(M-N+N\log_e Q),$$

[59] $$R_3 = \frac{wC_1}{ku_m}\frac{N^2}{C_1 - C_m},$$

so that

$$R_1' = R_1 - \left[\frac{\pi^2}{12} - \frac{1}{2}(\log_e 2)^2\right] R_3$$

$$= \frac{wC_1}{ku_m}\frac{1}{C_1 - C_m}\Big[(M - N + N\log_e Q)(N\log_e Q + M - \alpha) + N^2\left(\frac{\pi^2}{12} + \frac{1}{2}(\log_e 2)^2\right)\Big]$$

$$[60] \qquad = 1 + \frac{wC_1}{ku_m}\frac{1}{C_1 - C_m}\Big[N^2\left(\frac{\pi^2}{12} + \frac{1}{2}(\log_e 2)^2\right) + N(M - 2N + N\log_e Q)\Big]$$

by equations [39] and [41].

It follows that

$$S_1 = (M - N + N\log_e Q)\, R_1' - (M - 2N + N\log_e Q)\, R_2$$

$$[61] \qquad = (M - N + N\log_e Q)\left[1 + \frac{wC_1}{ku_m}\frac{1}{C_1 - C_m} N^2\left(\frac{\pi^2}{12} + \frac{1}{2}(\log_e 2)^2\right)\right],$$

$$S_2 = NR_1' + (M - 2N + N\log_e Q)\, R_2$$

$$[62] \qquad = N\left\{1 + \frac{wC_1}{ku_m}\frac{1}{C_1 - C_m}\Big[N^2\left(\frac{\pi^2}{12} + \frac{1}{2}(\log_e 2)^2\right) + (M + N\log_e Q)(M - 2N + N\log_e Q)\Big]\right\},$$

and $S_3 = NR_2$

$$[63] \qquad = \frac{wC_1}{ku_m}\frac{N^2}{C_1 - C_m}(M - N + N\log_e Q).$$

Substituting the results [61], [62], and [63] in equation [56] and writing from [36]

$$(C_1 - C_z)_{\text{unc}} = \frac{wC_1}{ku_m}\Big[(M - N + N\log_e Q)(N\log_e(1 - z) + N\log_e Q + M - \alpha) + N^2\left(\frac{\pi^2}{6} - \sum_1^\infty \frac{z^n}{n^2}\right)\Big],$$

one has finally

$$[64] \quad (C_1 - C_z)_{\text{cor}} = (C_1 - C_z)_{\text{unc}} + a_1\frac{wC_1}{ku_m}\left(\frac{C_1 - C_z}{C_1 - C_m}\right)_{\text{unc}} + a_2\left(\frac{wC_1}{ku_m}\right)^2\frac{1}{(C_1 - C_m)_{\text{unc}}}\left(\frac{\pi^2}{6} - \sum_1^\infty \frac{z^n}{n^2}\right)$$

where

$$[65] \qquad a_1 = N^2\left(\frac{\pi^2}{12} + \frac{1}{2}(\log_e 2)^2\right),$$

$$[66] \qquad a_2 = (M + N\log_e Q)(M - 2N + N\log_e Q)N^2.$$

Taking $M = 5.5$, $N = 2.5$, the correction factors [65] and [66] become

[65a] $$a_1 = 9.475,$$

[66a] $$a_2 = 17.2+216 \log_{10}Q+207(\log_{10}Q)^2,$$

and equation [64] may be written

[67] $$\left(\frac{C_z}{C_1}\right)_{cor} = \left(\frac{C_z}{C_1}\right)_{unc} - a_1\left(\frac{w}{ku_m}\right)\left(\frac{1-C_z/C_1}{1-C_m/C_1}\right)_{unc} - a_2\left(\frac{w}{ku_m}\right)^2 \frac{1}{(1-C_m/C_1)_{unc}}\left(\frac{\pi^2}{6} - \sum_1^\infty \frac{z^n}{n^2}\right)$$

where $(C_1)_{cor} = (C_1)_{unc}$, i.e. the same boundary concentration is considered in both cases, and where by [39] and [41]

[68] $$\frac{w}{ku_m} = \frac{C_m}{C_1}\left(N^2\log_e Q+N(M-2N)+N^2\frac{\pi^2}{6}\right)^{-1}$$

[68a] $$= \frac{C_m}{C_1}(14.4\log_{10}Q+11.5)^{-1}$$

for the values of M and N considered.

Tables V, VI, and VII now give the corrected values of the concentration ratio C_z/C_1.

It is seen that the boundary condition $C_0 = 0$ has had to be abandoned because of the approximation so that the calculated value of the correction must be too large near the surface. For values of $Q > 10^4$ the correction is entirely insignificant. The change in concentration between the bed and the fluid is localized in the laminar adjacent-to-bed region to leave the concentration gradient throughout the turbulent core sensibly unchanged from its almost constant value.

TABLE V

CASE $N = 2.5$, $Q = 10^3$,

$$\frac{C_m}{C_1} = 0.148, \frac{W}{ku_m} = 2.71\times10^{-3}, a_2 = 1286,$$

$$\left(\frac{C_z}{C_1}\right)_{cor} = \left(\frac{C_z}{C_1}\right)_{unc} - 0.30\times10^{-2}\left(1-\frac{C_z}{C_1}\right)_{unc} - 1.11\times10^{-2}\left(\frac{\pi^2}{6}-\sum_1^\infty\frac{z^n}{n^2}\right)$$

z	$\left(\frac{\pi^2}{6}-\sum_1^\infty\frac{z^n}{n^2}\right)$	$\left(\frac{C_z}{C_1}\right)_{unc}$	$1-\left(\frac{C_z}{C_1}\right)_{unc}$	$\left(\frac{C_z}{C_1}\right)_{cor}$
0	1.645	0	1	−0.021
0.382	1.219	0.073	0.927	0.057
0.500	1.062	0.105	0.895	0.091
0.618	0.890	0.145	0.855	0.132
0.900	0.5	0.335	0.665	0.327
0.950	—	0.433	0.567	0.427
0.990	—	0.657	0.343	0.653
0.999	—	0.975	0.025	0.975
1.000	—	1.000	0	1.000

TABLE VI

CASE $N = 2.5$, $Q = 10^4$

$$\frac{C_m}{C_1} = 0.110, \quad \frac{W}{ku_m} = 1.59\times10^{-3}, \quad a_2 = 3312,$$

$$\left(\frac{C_z}{C_1}\right)_{cor} = \left(\frac{C_z}{C_1}\right)_{unc} - 0.17\times10^{-2}\left(1-\frac{C_z}{C_1}\right)_{unc} - 0.94\times10^{-2}\left(\frac{\pi^2}{6}-\sum_1^\infty \frac{z^n}{n^2}\right)$$

z	$\left(\frac{\pi^2}{6}-\sum_1^\infty \frac{z^n}{n^2}\right)$	$\left(\frac{C_z}{C_1}\right)_{unc}$	$1-\left(\frac{C_z}{C_1}\right)_{unc}$	$\left(\frac{C_z}{C_1}\right)_{cor}$
0	1.645	0	1	−0.017
0.382	1.219	0.055	0.945	0.042
0.500	1.062	0.079	0.921	0.067
0.618	0.890	0.109(5)	0.890(5)	0.099
0.900	0.5	0.253	0.747	0.247
0.950	—	0.327	0.673	0.326
0.990	—	0.497	0.503	0.496
0.999	—	0.741	0.259	0.741
1.000	0	1.000	0	1.000

TABLE VII

CASE $N = 2.5$, $Q = 10^5$,

$$\frac{C_m}{C_1} = 0.089, \frac{W}{ku_m} = 1.065\times10^{-3}, \quad a_2 = 5175,$$

$$\left(\frac{C_z}{C_1}\right)_{cor} = \left(\frac{C_z}{C_1}\right)_{unc} - 0.11\times10^{-2}\left(1-\frac{C_z}{C_1}\right)_{unc} - 0.60(5)\times10^{-2}\left(\frac{\pi^2}{6}-\sum_1^\infty \frac{z^n}{n^2}\right)$$

z	$\left(\frac{\pi^2}{6}-\sum_1^\infty \frac{z^n}{n^2}\right)$	$\left(\frac{C_z}{C_1}\right)_{unc}$	$1-\left(\frac{C_z}{C_1}\right)_{unc}$	$\left(\frac{C_z}{C_1}\right)_{cor}$
0	1.645	0	1.000	−0.011
0.382	1.219	0.043(5)	0.956(5)	0.035
0.500	1.062	0.062(5)	0.937(5)	0.055
0.618	0.890	0.086(5)	0.913(5)	0.080
0.900	0.500	0.202	0.798	0.198
0.950	—	0.262	0.738	0.261
0.990	—	0.400	0.600	0.399
0.999	—	0.595	0.405	0.595
1.000	0.000	1.000	0.000	1.000

TOTAL LOAD CARRIED BY TURBULENT STREAM

It remains to consider the total wash load carried by the stream, i.e. to obtain a maximum value for the sediment deposited if the turbulence were to be stopped by flow into a reservoir for example.

Consider a sheet of the stream contained between the planes z and $z+dz$. Then if L (assumed large in comparison with the depth) is the width of the stream, the weight of sediment crossing a given section of the sheet per unit time is $u_s C_z L dz$. This is the weight of sediment that in one second would be set free to fall back to the bed if the turbulence between the planes were to be suddenly stopped.

Assuming $u_s = ju$ where u is the velocity of the stream at z, one has for the total weight of sediment transported in unit time across a plane x = const. perpendicular to the mean flow direction

$$[69] \qquad W_Q = \int_0^{1-(\alpha/Q)} u_s C_z L dz = \int_0^{1-(\alpha/Q)} ju_\tau U C_z L dz$$

$$[70] \qquad = ju_\tau L \int_0^{1-(\beta/Q)} U C_z dz + O\left(\frac{1}{Q}\right)$$

$$[71] \qquad = ju_\tau L C_1 \int_0^{1-(\beta/Q)} (M + N \log_e Q(1-z)) \left(\frac{C_z}{C_1}\right) dz + O\left(\frac{1}{Q}\right)$$

where C_z/C_1 is given by equation [40].

This integral again requires the integral

$$\int \log_e(1-z) \sum_1^\infty \frac{z^n}{n^2} dz,$$

but as the term involved is small the analysis is once again simplified by taking $\sum_1^\infty \frac{z^n}{n^2}$ at the constant value $\sum_1^\infty \frac{(\frac{1}{2})^n}{n^2} = \frac{\pi^2}{12} - \frac{1}{2}(\log_e 2)^2$.

With this approximation the integral [71] gives

$$[72] \quad W_Q = ju_\tau L C_1 \left\{ \frac{N^3(\log_e Q)^2 + N^2[2M - 3N + N(\frac{1}{12}\pi^2 - \frac{1}{2}(\log_e 2)^2)] \log_e Q}{N^2(\log_e Q)^2 + N(2M - \alpha - N)\log_e Q + (M-\alpha)(M-N) + \frac{1}{6}N^2\pi^2} + \frac{N(M-N)[M - 2N + N(\frac{1}{12}\pi^2 - \frac{1}{2}(\log_e 2)^2)]}{N^2(\log_e Q)^2 + N(2M - \alpha - N)\log_e Q + (M-\alpha)(M-N) + \frac{1}{6}N^2\pi^2} \right\},$$

and inserting the numerical values $N = 2.5$, $M = 5.5$, $\alpha = 5$,

$$[72a] \qquad \frac{W_Q}{ju_\tau L C_1} = \frac{82.8(\log_{10} Q)^2 + 71.4 \log_{10} Q + 14.7}{33.1(\log_{10} Q)^2 + 20.0 \log_{10} Q + 11.8}$$

and for the higher value of N, $N = 3$,

$$[72b] \qquad \frac{W_Q}{ju_\tau L C_1} = \frac{143.2(\log_{10} Q)^2 + 77.7 \log_{10} Q + 9.37}{47.7(\log_{10} Q)^2 + 20.7 \log_{10} Q + 16.3}.$$

For large values of Q, $W_Q/ju_\tau L C_1$ tends simply to the value N, and is independent of Q. The alteration of N due to the damping of the turbulence by the sediment load now becomes an important factor.

The formulae [72a], [72b] give the load set free per second on stopping the turbulence in terms of the concentration C_1 at the bed.

Assuming no slip between the sediment and the water, $j = 1$, so that if $W_Q' = W_Q/L$ the mass deposited per unit width of stream

$$[73a] \qquad \frac{W_Q'}{C_1 u_\tau} = \frac{82.8(\log_{10} Q)^2 + 71.4 \log_{10} Q + 14.7}{33.1(\log_{10} Q)^2 + 20.0 \log_{10} Q + 11.8} \qquad \text{for } N = 2.5$$

and

$$[73b] \qquad \frac{W_Q'}{C_1 u_\tau} = \frac{143.2(\log_{10} Q)^2 + 77.7 \log_{10} Q + 9.37}{47.7(\log_{10} Q)^2 + 20.7 \log_{10} Q + 16.3} \qquad \text{for } N = 3.$$

In terms of the mean concentration for the case of no slip, equations [72] and [41] give

$$[74] \quad \frac{W_Q'}{u_\tau C_m} = \left\{ \frac{N^3(\log_e Q)^2 + N^2[2M-3N+(\frac{1}{12}\pi^2-\frac{1}{2}(\log_e 2)^2)N]\log_e Q}{N^2\log_e Q + N(M-2N)+\frac{1}{6}N^2\pi^2} + \frac{N(M-N)[M-2N+(\frac{1}{12}\pi^2-\frac{1}{2}(\log_e 2)^2)N]}{N^2\log_e Q+N(M-2N)+\frac{1}{6}N^2\pi^2} \right\},$$

i.e.

$$[74a] \quad \frac{W_Q'}{C_m u_\tau} = \frac{82.8(\log_{10} Q)^2+71.4\log_{10} Q+14.7}{14.4\log_{10} Q+11.5} \qquad \text{for } N = 2.5,$$

$$[74b] \quad \frac{W_Q'}{C_m u_\tau} = \frac{143.2(\log_{10} Q)^2+77.7\log_{10} Q+9.37}{20.7\log_{10} Q+13.3} \qquad \text{for } N = 3.$$

It is seen that $W_Q'/u_\tau C_m$ approaches the value $N \log_e Q$ when Q becomes large.

C_m can be determined from readings across the flow profile, or taken as the concentration at a point z_m, where, by equations [37] and [38],

$$[75] \quad z_m = 1-\exp\left[-\frac{N^2\log_e Q+N(M-2N)+\frac{1}{6}N^2\pi^2}{N^2\log_e Q+N(M-N)}\right]$$

$$[75a] \quad = 1-\exp\left[-\frac{14.4\log_{10} Q+11.5}{14.4\log_{10} Q+7.5}\right] \qquad \text{for } N = 2.5,$$

$$[75b] \quad = 1-\exp\left[-\frac{20.7\log_{10} Q+13.3}{20.7\log_{10} Q+7.5}\right] \qquad \text{for } N = 3.$$

Table VIII gives values of $W_Q'/C_1 u_\tau$ and $W_Q'/C_m u_\tau$ and also z_m, the value of z at which the concentration is at its mean, for values of Q from 10^3 to 10^6.

It is seen that throughout the range of Q a satisfactory approximation is obtained by setting

$$[76] \quad W_Q'/C_1 u_\tau = N$$

TABLE VIII

Q	$\frac{W_Q'}{C_1 u}$	$\frac{W_Q'}{C_m u}$	$N\log_e Q$	z_m
Case $N = 2.5$				
10^3	2.63	17.8	17.3	0.660
10^4	2.62	23.5	23.0	0.654
10^5	2.60	29.2	28.8	0.650
10^6	2.58	34.9	34.6	0.647
Case $N = 3$				
10^3	3.02	20.3	20.7	0.662
10^4	3.03	27.3	27.6	0.655
10^5	3.03	34.0	34.5	0.651
10^6	3.03	41.0	41.4	0.648

where N is von Karman's constant occurring in the original turbulent velocity distribution law.

More apparent still is the closeness of $W_Q'/C_m u_\tau$ to $N \log_e Q$ throughout this extended range of Q.

Also apparent is the invariance of z_m, the point at which the concentration takes on its mean value. The value $z_m = 0.65$ will give results accurate to 1% over the range of Q.

The concentration varying slowly over the region about $z = 0.65$, this seems a satisfactory method of determining C_m.

Once C_m is determined experimentally the formula

$$W_Q' = C_m u_\tau \log_e Q \tag{77}$$

is a simple expression for determining the deposit rate per unit stream width on stopping the turbulence. The friction velocity u_τ is directly obtainable from the hydraulic grade line and Q is merely the Reynolds number constructed with friction velocity u_τ.

SUMMARY

An equation has been derived for the sediment concentration ratio as a function of depth on the momentum transfer analogy for the case of infinitely fine sediment suspended in a river flowing turbulently over a smooth bed. The equation is of the form

$$\frac{C_z}{C_1} = \frac{(a+b \log_e Q) \log_e \dfrac{1}{1-z} + C \sum_1^\infty \dfrac{z^n}{n^2}}{d(\log_e Q)^2 + e \log_e Q + f} \tag{78}$$

where the constants a, b, c, d, e, f are given by the constants defining the velocity distribution. The velocity distribution considered consists of a laminar flow layer adjacent to the river bed, a semiturbulent buffer layer, and the major body of the fluid throughout which the turbulence is fully developed and in which the flow velocity is given by the von Karman velocity defect law.

Results from the above formula are compared with those from the power law

$$\frac{C_z}{C_1} = \left(\frac{z}{1-z} \times \frac{1-\delta}{\delta} \right)^\theta \tag{1}$$

obtained on the simple assumption of equilibrium between the upward transport of sediment by turbulence and its settling due to gravity.

Full agreement between the two equations can only be obtained by allowing the exponent θ of equation [1] to vary, but approximate over-all agreement is obtained by taking θ at about half its value Nw/u_τ. Both the author's equation [78] and equation [1] with the lower index imply the more uniform concentration–depth distribution that has been found experimentally by Vanoni (22) and Anderson (1).

The equation yields a simple closely approximate formula for the ratio of the mean concentration to the concentration at the bed,

$$[41c] \qquad \frac{C_m}{C_1} = \frac{1}{\log_e Q} = \frac{1}{2.3026 \log_{10} Q}.$$

In the author's original derivation it was necessary to assume that near the boundary, the sediment concentration, instead of being constant in the flow direction, had to vary linearly with distance. Using this result a first correction was obtained towards the constant boundary concentration case. The correction was found to be entirely negligible; the longitudinal concentration distribution in the adjacent-to-bed region does not appear to affect the distribution in the main body of the water.

It was found possible to obtain an expression for the total sediment load carried by the flow, that is, the sediment that would be freed to fall on stopping the turbulence. Without knowledge of the mechanism of "pick up" from the bed (and of the transport through the laminar boundary layer) it is possible only to express this quantity in terms of either the concentration at the bed or the mean concentration. However, the simple result

$$[77] \qquad W_Q' = C_m u_\tau \log_e Q$$

for the load per unit stream width would seem to be satisfactory for practical application, particularly as the mean concentration is shown to occur at the sensibly invariable depth $0.65h$, where h is the total depth of the river.

REFERENCES

1. ANDERSON, A. G. Trans. Am. Geophys. Union, 23: 678. 1942.
2. BOELTER, L. M. K., MARTINELLI, R. C., and JONASSEN, F. Trans. A.S.M.E. 63: 447. 1941.
3. EDWARDS, J. Integral calculus. Vol. II. The MacMillan Co., New York. 1922. p. 286.
4. KARMAN, T. VON. Proc. 3rd Intern. Congr. Appl. Mech. Stockholm, 85. 1930.
5. KARMAN, T. VON. Natl. Advisory Comm. Aeronaut. Tech. Mem. No. 611. Washington. 1931.
6. KARMAN, T. VON. Trans. A.S.M.E. 61: 705. 1939.
7. LION, R. N. Oak Ridge Natl. Lab., A.E.C.D. 1992. 1948.
8. MARRIS, A. W. Can. J. Phys. 32: 167. 1954.
9. MARRIS, A. W. Can. J. Phys. 32: 419. 1954.
10. MARTINELLI, R. C. Trans. A.S.M.E. 69: 947. 1947.
11. NIKURADSE, J. Ver. deut. Ing. Forschungsheft, 356: 36. 1932.
12. PRANDTL, L. Z. angew. Math. u. Mech. 5: 137, 138. 1925.
13. PRANDTL, L. Z. Ver. deut. Ing. 77: 107, 108. 1933.
14. REICHARDT, H. Z. angew. Math. u. Mech. 20: 297. 1940.
15. REYNOLDS, O. Trans. Roy. Soc. (London), A, 186: 123. 1894.
16. SEBAN, R. A. and SHIMAZAKI, T. T. Trans. A.S.M.E. 73: 803. 1951.
17. STANTON, T. E. and PANNELL, J. R. Trans. Roy. Soc. (London), A, 214: 199. 1914.
18. TAYLOR, G. I. Trans. Roy. Soc. (London), A, 215: 1. 1915.
19. TAYLOR, G. I. Proc. Roy. Soc. (London), A, 135: 685. 1932.
20. TAYLOR, G. I. Proc. Roy. Soc. (London), A, 151: 494. 1935.
21. TAYLOR, G. I. Proc. Roy. Soc. (London), A, 159: 499. 1937.
22. VANONI, V. A. Trans. Am. Soc. Civil Engrs. 111: 67. 1946.

CONTENTS OF VOLUME 33

Allan, A. B. See King, R. O., 335.

Bannard, R. A. B. and **Ross, J. H.** Aminomethionate salts. II. Optimum conditions for formation of monopotassium aminomethionate by the von Pechmann and Manck process, 317.

Bartlet, J. C. and **Farmilo, C. G.** The determination of the origin of opium. Part I. By means of the composition of the ash, 134.

Bartlet, J. C., Kavanagh, D., and **Chapman, R. A.** The determination of the fluoride content of edible bone meal, 348.

Barton, B. C. See Doak, K. W., 98.

Beeckmans, J. M. L. See Johnson, A. I., 434.

Berkowitz, N. Physicochemical studies on Alberta coals. I. Surface area measurements, 169.

Physicochemical studies on Alberta coals. II. On the physical behavior of coal in ultrasonic fields, 378.

Bleakney, H. H. An evaluation of the recovery theory of creep, 56.

Braid, P. E. and **Langille, R. C.** A new type of impact machine for evaluating sensitiveness of explosives, 228.

Butters, R. G. and **Myers, H. P.** A low temperature attachment for an X-ray goniometer, 356.

Butters, R. G. and **Parr, J. G.** A high-temperature X-ray goniometer, 117.

Campbell, J. E. and **Heaps, H. S.** Transmission of stress through a thick slab supported by a yielding foundation, 324.

Caule, E. J. and **McCully, G.** An automatic recording analytical balance, 1.

Chapman, R. A. See Bartlet, J. C., 348.

Clarke, R. M. and **Wright, G. F.** The explosibility of wet ammonia–air mixtures, 161.

Cole, D. G. See Handegord, G. O., 303.

Doak, K. W., Ganzhorn, G. H., and **Barton, B. C.** Promoters for the reaction of rubber with carbon black, 98.

Edwards, W. D. A frequency stable transistor audio oscillator of very simple design, 413.

Eng, J., Govier, G. W., and **Quon, D.** The air blowing of Redwater asphalt base stock. The use of phosphorus pentoxide as an addition agent, 360.

Farmilo, C. G. See Bartlet, J. C., 134.

Farnand, J. R., McIlhinney, A. E., Peterson, W. S., Gishler, P. E., and **Puddington, I. E.** The chemical bleaching of hydrocarbon oils, 426.

Fensom, D. S. A comparison of the flow of high polymers in the cavity of a Mooney plastometer, 194.

Ganzhorn, G. H. See Doak, K. W., 98.

Gevantman, L. H. and **Sam, D.** The penetration of concrete by radionuclides in solution, 122.

Gishler, P. E. See Farnand, J. R., 426.

Govier, G. W. See Eng, J., 360.

Green, B. C. and **Spinks, J. W. T.** Automatic plotting of the position of a moving radioactively tagged object, 307.

Handegord, G. O. and **Cole, D. G.** An operation-time controller for a recording potentiometer, 303.

Heaps, H. S. See Campbell, J. E., 324.

Hodgins, J. W. and **Hoffman, T. W.** The storage and transfer of low potential heat. I. Glauber's salt as a heat storage material, 293.

Hoffman, T. W. See Hodgins, J. W., 293.

Huang, C.-J. See Johnson, A. I., 421.

Johnson, A. I. and **Beeckmans, J. M. L.** Statistical factors in tower packing, 434.

Johnson, A. I. and **Huang, C.-J.** Estimation of the heat capacities of organic liquids, 421.

Kahana, S. See Wait, J. R., 77.

Kase, S. Nomographs for evaluation of tensile data of rubber, 409.

Kavanagh, D. See Bartlet, J. C., 348.

King, R. O. and **Allan, A. B.** The oxidation, decomposition, ignition, and detonation of fuel vapors and gases. XXV. The transition from spark to nuclear ignition as compression ratio is raised, 335.

King, R. O. and **Rand, M.** The oxidation, decomposition, ignition, and detonation of fuel vapors and gases. XXVII. The hydrogen engine, 445.

King, R. O., Sandler, S., and **Strom, R.** The oxidation, decomposition, ignition, and detonation of fuel vapors and gases. XXVI. The effect of flow configuration on the oxidation and ignition of hydrogen in mixtures with air supplied to vertical combustion tubes of various materials, 388.

Kuzmak, J. M. and **Sereda, P. J.** The blistering of paint in the presence of water, 67.

Langille, R. C. See Braid, P. E., 228.

Lentz, C. P. Humidification of cold storages: The jacket system, 265.

McConnell, W. B. Some characteristics of spray-dried wheat gluten, 256.

McCully, G. See Caule, E. J., 1.

McIlhinney, A. E. See Farnand, J. R., 426.

Makow, D. Fractional frequency generation by regenerative modulation, 41.

Marris, A. W. Fluid turbulence and suspended sediment, 470.

Marshall, H. B. See Newcombe, A. G., 152.

Mateer, C. L. Average insolation in Canada during cloudless days, 12.

Mentel, T. J. Plastic deformations due to dynamic loading of a beam with an attached mass, 237.

Meredith, C. C. and **Wright, G. F.** An apparatus for the determination of dipole moments, 182.

Myers, H. P. See Butters, R. G., 356.

Newcombe, A. G. and **Marshall, H. B.** The effect of chlorination and subsequent dechlorination on the tanning properties of ligninsulphonates, 152.

Niven, C. D. On the friction of rubber covered wheels on ice, 204.

Parr, J. G. See Butters, R. G., 117.

Peterson, W. S. See Farnand, J. R., 426.

Puddington, I. E. See Farnand, J. R., 426.

Quon, D. See Eng, J., 360.

Raciszewski, Z. M., Spencer, E. Y., and **Trevoy, L. W.** Chemical studies of a goitrogenic factor in rapeseed oilmeal, 129.

Rand, M. See King, R. O., 445.

Ross, J. H. See Bannard, R. A. B., 317.

Sam, D. See Gevantman, L. H., 122.

Sandler, S. See King, R. O., 388.

Sereda, P. J. See Kuzmak, J. M., 67.

Shu, P. Automatic translation of aeration data between different fermentors, 279.

Simpson, F. J. Separation of starch and gluten. VII. The application of bacterial pentosanases to the recovery of starch from wheat flours, 33.

Spencer, E. Y. See Raciszewski, Z. M., 129.

Spinks, J. W. T. See Green, B. C., 307.

Strom, R. See King, R. O., 388.

Trevoy, L. W. See Raciszewski, Z. M., 129.

Wait, J. R. and **Kahana, S.** Calculated patterns of circumferential slots on a circular conducting cylinder, 77.

Wait, J. R. and **Walpole, R. E.** Calculated radiation characteristics of slots cut in metal sheets, 211.

Walpole, R. E. See Wait, J. R., 211.

Whalley, E. Thermodynamic properties of argon in the temperature range −100 to +600°C. and pressure range 0 to 80 atmospheres, 111.

Wright, G. F. See Clarke, R. M., 161; Meredith, C. C., 182.

CORRECTION

Vol. 33, p. 353. In the first line of Item 4 under Procedure (Reagents) "0.75 gm. salicylic acid" should read "0.075 gm. salicylic acid".